Chapter 1

Introduction

1.1 Background to the Study

Energy demand is increasing rapidly all over the world. Due to the population increment as well as the development in various sectors like industry, agriculture, and trading, the need for energy has become a mandatory request in those sectors [1, 2]. This demand is facing a lot of problems related to the scarcity of conventional energy resources that are to be eliminated, as well as the bad effects of those resources represented by crude oil, natural gas, coal, etc. on the environment as an increase in CO_2 emissions and greenhouse gases [2, 3]. Those gases harm agriculture, people, and animal health. Due to the effects mentioned above, countries around the world have started adopting other resources described as clean and renewable, like hydropower, solar energy, wind energy, etc.

Two-thirds of the energy needs all over the world could be met by renewable resources energy, which would also significantly reduce CO_2 emissions during the next 30 years [4]. Building photovoltaic power plants has gained importance due to rising energy demands, environmental concerns, and the need for sustainable power sources. These solar energy facilities use the sun's energy to create electricity and provide many other advantages in addition to energy generation. In 2017, photovoltaic (PV) was the leading source of new renewable energy (RE) capacity for power generation due to the significant rapid growth in China; as a result, the market's growth can be linked to the market's greater competitiveness to the tune of 402 GWp [5].

In addition to importing 87% of its required power, Palestine imports all of its fossil fuels [5]. Moreover, recent developments in high living standards, rapid industrial development, and significant population growth have increased Palestine's need for energy. Palestinian citizens use the least amount of energy overall in the MENA region—roughly 0.79 MWh per person, but at a higher cost than in any other nation. The Palestinian energy sector has a number of difficulties, including political unpredictability and dependence on Israeli electricity, which makes it challenging to import energy from other nations and transfer it. Energy demand is another difficulty in addition to the high cost of electricity. It is challenging to strengthen the

energy industry in Palestine because of bad management, weak infrastructure, and a lack of plans to cope with supply and demand for energy [6]. To remedy this risky condition, it is therefore vital to generate electricity from alternative sources, such as renewable energy sources [7].

Some of the variables control the use of one renewable resource than others, represented by country location, topography, climate, and the availability of those resources at a low cost and competitive prices. One of the most renewable energy resources used is photovoltaic solar energy because it is simple, low-cost, more accessible, has a range of capabilities, and has an appropriate efficiency. Due to the high radiation intensity and availability of full sunlight throughout the day and most of the year's seasons, PV systems are one of the most effective renewable energy sources in Palestine, with 5.4 $kWh/m^2/day$ of solar radiation potential and around 3000 hours of sunshine per year [8].

Most efforts in this field in Palestine are limited to the installation of PV panels on the roofs of homes and some small-scale ground-based PV plants. The installation of a land-based PV power plant offers a free and clean energy source that decreases the dependency on conventional sources, which harm the environment and affect human health. Additionally, the use of land-based solar photovoltaic power plants reduces the amount of money municipalities spend on their electricity bills, allowing them to use the money they save to build new projects and raise the quality of services they provide to the public.

A lot of measures have been adopted to evaluate PV systems. One of those measures is the techno-economic assessment. This evaluation deals with different parameters related to economics, like net present value, simple payback period, and levelized cost of electricity, as well as technical issues like system yields, system efficiency, capacity utilization factor, and performance ratio. Those measures give a clear view of the investment in this field and evaluate the overall long-term performance by highlighting the problems that may face this sector and the proposed solutions.

The goal of artificial intelligence (AI), a branch of computer science, is to develop software that will enable computers to act in ways that are usually regarded as intelligent [9]. Electric network control and operation have used AI approaches [10]. For at least two decades, artificial intelligence has been applied to the field of energy systems. Many practitioners,

academics, and researchers in the field appear to view the systems based on artificial inelegance as a "black box," which could cause them to ignore numerous significant and affecting elements in their modeling border [11].

One of the most well-known artificial intelligence techniques is particle swarm optimization (PSO), which Kennedy and Eberhart (1995) first proposed. The PSO imitates birds' social behavior when it searches for food sources, sharing information about each bird's location and the closest food particle with the other birds [12]. This method has a lot of applications in the assessment of renewable energy systems, such as giving the optimum solution for a specific property, like the application for the technical and economic evaluation of photovoltaic systems.

1.2 Research objective

The thesis's main objective is to analyze the technical and economic parameters of a 1.5 MW PV power plant in Al Dhahriya town in order to determine the long-term effectiveness and performance of land-based on-grid photovoltaic power plants in Palestine. As well as utilizing artificial intelligence by applying the PSO method in order to achieve the optimal connection point location to the grid for energy generation in Al Dhahriya.

Specific objectives:

- discussing the Palestinian energy situation and emphasizing the usage of RE resources.
- studying the problems facing the PV plant and finding an appropriate solution.
- studying the importance of using techno-economic indicators for on-grid PV power plants through a review of sustainable development.
- Listing recommendations and results that the researchers can use in different locations and various climate zones, as well as on a larger scale in the long run,.

1.3 Statement of the Problem

According to previous studies on the techno-economic evaluation of PV power plants, most of those studies have analyzed rooftop PV systems, while a low number of those studies have discussed the energy parameters for a MW-scale power plant. The current study fills this gap

by evaluating and assessing the techno-economic parameters for a connected PV power plant with a capacity of 1.5 MW by applying the energy parameters. As well, this study will utilize artificial intelligence to ensure that the plant location is optimal for energy generation in Al Dhahriya. Therefore, this study will reflect all related issues of the on-grid photovoltaic system in this plant, to be documented and controlled after analyzing the needed issues.

1.4 Motivation

The installation of a PV power plant offers a free and clean energy source that decreases dependency on conventional sources, which harm the environment and affect human health. Additionally, the use of land-based solar photovoltaic power plants reduces the amount of money municipalities spend on their electricity bills, allowing them to use the money they save to build new projects and raise the quality of services they provide to the public.

The technical and economic evaluation of a PV power plant gives a clear vision of the long-term plant performance and overall system efficiency and indicates the feasibility of constructing new power plants, taking into consideration the results and recommendations that were achieved from the techno-economic assessment of the existing PV power plant. By utilizing artificial intelligence, it became easy to determine the optimum location for PV plant installation, taking into consideration the future plan for investment in this field.

Finally, Al Dhahriya was selected as a case study because of its semi-desert environment and position in the southern region of the West Bank in order to examine the effectiveness of applying solar power systems in this region since it has a large land area with an appropriate topography for installing large PV power plants as well as being far away from the center of accommodation, buildings, and forests, which proposed to increase project lifecycle and overall power plant efficiency.

1.5 Thesis Structure

The thesis includes six chapters, which are:

Chapter 1: Introduction.

This chapter contains an introduction to the thesis subject, RE and why it's important to humans and the environment, the energy situation in Palestine, electro-economic assessment for PV systems, and the particle swarm optimization method. This chapter also lists the thesis objectives, statement of problem, and motivation to do this research.

Chapter 2: Literature Review.

The literature for the thesis has been reviewed, which contains previous studies of the electro-economic assessment of PV systems and the applications of artificial intelligence to renewable energy resources.

Chapter 3: Modeling of PV Systems.

The theories adopted in this field have been listed and reviewed. This chapter also discusses PV system modeling, which covers system design analysis and feasibility studies.

Chapter 4: Methodology.

It includes the needed plant data for analysis, the study area, and the methods that were adopted to do this research, including both sectors: techno-economic assessment and particle swarm optimization theory.

Chapter 5: Results and Discussions.

This chapter includes the results of applying the techno-economic parameters to the photovoltaic power plant and the results of applying PSO theory to the plant. As well as discussing the results.

Chapter 6: Conclusions and Recommendations.

This chapter illustrates the conclusions of this research and highlights the proposed recommendations based on this study.

Chapter 2

Literature review

2.1 Introduction

According to the swift progress in various sectors and the considerable growth in population around the world, besides the shortage of traditional energy resources supply along with their harmful effects on humans, animals, and the environment, the countries have started adopting clean and free resources of energy. Those renewable resources are sustainable, environment-friendly, and relatively cheaper than traditional resources.

Six percent of the region's total energy is generated by renewable sources in the Arab countries, namely 4.7% from hydropower, 0.9% from wind energy, and 0.4% from solar energy. Unfortunately, the usage of renewable energy is limited in these nations. Increasingly more effective methods and new energy (biomass, wind, and solar) are underway [13].

In Palestine, over 66% of families heat the water with renewable energy sources, including solar and biomass. Several studies have, however, outlined the potential of wind. The creation of internationally authorized national workplaces for renewable energy knowledge and research, the development of RE needs, and the expansion of appropriate professional skills in the RE sector [13].

Employing PV systems for electrifying the countryside in Palestine is more cost-effective and advantageous than using generators or expanding the high-voltage electrical infrastructure. Less reliance on conventional energy sources, which contribute to numerous environmental issues, is one benefit of the widespread usage of PV and its connectivity to the grid. PV generation is becoming more common in electrical distribution, but quality issues have been found that could impact network performance, which is a very difficult challenge [14].

2.2 Photovoltaic (PV) systems

One of the finest methods for supplying enough clean energy is renewable energy. Solar, wind, fuel cells (FC), hydro, and other renewable energy sources are readily available. Solar energy stands out among them as a clean, pollution-free, and dependable green source to fulfill the rising need [15, 16, 17].

One of the most popular RE sources is solar energy, which has been utilized to produce energy for extended periods of time. Using a photovoltaic (PV) system, solar radiation can be converted into power [18]. The PV system uses the photovoltaic effect as a principle to turn sunlight into electrical power. Whenever light enters a photovoltaic cell, photon energy is transferred to the charge carriers. The charge carriers split into electrons with a negative charge and positive charge holes at that moment due to the electric field present throughout the junction. Current will flow through the circuit if a load is attached, creating a closed channel [19, 20].

The solar energy system is one of the best RE resources that Palestine may use. With an average daily solar radiation intensity of 5.4 kWh/m2/day, Palestine is regarded as a country with significant solar energy potential. Its value serves as a strong motivator to fully utilize this energy [21].

Palestinians began employing photovoltaic systems in the previous decade as a result of increased awareness of the financial benefits of PV systems brought on by the recent sharp decline in PV prices, which fell from 2 to 0.5 US dollars per watt. Also, the use of photovoltaic plants has been promoted by the introduction of advantageous governmental laws like Net Metering and Feed-in Tariff (FiT) [22].

Most of the efforts in Palestine are concentrated on installing rooftop grid-connected PV systems for buildings, homes, and public institutions. The construction of mega-scale land-based solar PV power plants has recently increased, which highlights the importance of evaluating those plants from different points of view related to performance, technical, economic, feasibility study, and other assessment parameters in order to give a clear vision on the investment in this field and to illustrate the recommendations to the plant's clients, the public sector, and other stakeholders.

2.3 Techno-economic assessment of PV systems

A lot of studies have discussed the evaluation of power plants through different scales and tools, and they have linked energy production to the economy and environment. These tools aim to measure the impact of power plant design on the surrounding environment and economic wisdom in order to have a clear vision of investment in this field.

The techno-economic parameters of a centralized 10 MW grid-connected PV power plant in Uganda have been assessed, and the data on energy production has been taken over 3-year period. They found that the average generation of annual energy is 16,702 MWh, the daily final yield is around 4.58 h/d, the annual performance ratio is 75.84%, the annual capacity factor is 19.07%, and the estimated payback period is 9.28 years. They have concluded that the plant is economically viable [23].

The Benin Republic's utility-scale grid-tied solar photovoltaic system's techno-economic analysis has been examined. The authors found that the photovoltaic plant generates roughly 13,222 MWh of electricity per year on average that can be exported to the grid. This results in a performance ratio of roughly 67.3% and a capacity factor of 15.1%. The project's levelized cost of energy (LCOE) is between 0.110 and 0.125 dollars per kWh in the absence of income and capital subsidies. Additionally, the PV project is appealing to investors when the feed-in tariff exceeds 0.10 USD/kWh [24].

Five climate zones in Pakistan have been chosen in order to analyze the techno-economic parameters of mega-scale on-grid photovoltaic plants in the industrial sector. They concluded that all five locations are feasible with regard to the technical, environmental, and economical aspects. Zone "C," which has the highest solar insolation, is the most optimal placement due to the high value of the capacity utilization factor (20.3%), highest annual generation (4,441 MWh), lowest payback period (3.2 years), and lowest cost of energy (0.026 USD/kWh) [25].

The economic performance has been checked through applying an economic parameter for a 1 MW on-grid photovoltaic power plant in Bahrain, they have analyzed the levelized cost of

electricity (LCOE), payback period, energy payback time, and net present value. The analysis shows a positive impact of using photovoltaic power plants in electricity generation [26].

Also, the feasibility of constructing a 1 MW PV power plant at University Malaysia Pahang was analyzed. The researchers concluded that the studied system could produce about 1,390 MWh of electricity per year with a reduction of 818.71 tons of CO_2 per year [27].

The technical and economic performance of on-grid photovoltaic rooftop plants for five climate zones in China have been evaluated. The study concluded that Kunming zone is the most economically feasible with the least NPC ($113,382) and COE ($0.073kWh). The lowest GHG emissions of Kunming zone also make it the best zone for on-grid PV power generation with regard to the environmental perspective [28].

The technical and economic feasibility assessment of an on-grid photovoltaic system installed on a residential building's rooftop in Jeddah, Saudi Arabia, has been studied. Yield factor, capacity factor, standardized cost of energy, performance ratio, internal rate of return, net present value, and payback period have been evaluated. The study concluded that the installation of PV panels in residential buildings is an effective path for the energy management sector [29].

Nine locations in Turkey have been selected for the economic analysis of five KW on-grid residential rooftop PV systems. The researchers have used HOMER software for system simulation. Profitability Index (PI), Internal Rate of Return (IRR), and Disconnected Payback Period (DPBP) are parameters that have been evaluated in order to ensure the system's viability. The results showed that the systems are viable only in the southern part of Turkey and in the northern part [30].

The life cycle sustainability evaluation of grid-connected PV systems in northeast England has been studied. Five parameters were adapted in the proposed model to evaluate the techno-economic performance of three types of PV systems: monocrystalline, cadmium telluride thin film, and polycrystalline. The results showed that the multi-silicon photovoltaic model is the most sustainable system due to its high performance in techno-economic assessment [31].

A feasibility assessment of 25.4 MW grid-connected rooftop PV systems for 3 industries with a total appropriate rooftop area for photovoltaic application of 164,594.56 m^2 in Uganda has been implemented. The economic indicators represented by the LCOE of 5.75 US cents per kWh, the BCR of 1.27, and the internal rate of return of seven percent showed a feasible investment with a short loan period of five years when the investment cost equals 75% of the loan share [32].

5MW on-grid photovoltaic plants in 8 selected cities on Iran's southern coast have been assessed from the perspective of techno-economic indicators. Fixed tilt, 1-axis, and 2-axis systems have been evaluated; the results showed that the 1-axis tracking system is the most preferable choice of tracking system for investment in all cities with regard to the economic aspect. The study also showed that Iran's southern coast has a high potential for investment in on-grid PV projects [33].

The techno-economic parameters on 12 panels of 250W on-grid photovoltaic plants for a real case of a residential building in Nottingham, UK, have been applied. The performance parameters of net present value, payback period, standardized cost of energy, and return on investment have been considered and evaluated in this study. There are few studies that have been conducted in Palestine to study the technical and economical evaluation of on-grid photovoltaic plants [34].

The analysis obtained from continuous data obtained for 3-years of 41KW rooftop PV panels of medicine building faculty at An-Najah National University in Nablus has been presented. Final yield, reference yield, performance ratio, and capacity utilization factor are the techno-economic indicators that have been studied for system assessment. The author highlights the importance of using these results for individuals to study the feasibility of investment in grid-connected photovoltaic plants [35].

In 2023, a lot of studies have recently studied rooftop PV plants in terms of techno-economic parameters. The technical and economic parameters for different building usages have been evaluated in order to check the impact of the PV systems on the building's energy demand, monthly electricity invoice, energy yields, system losses, payback period, and other techno-economic parameters. All those studies highlight the importance of installing photovoltaic

plants on the rooftops of utilities in order to improve the energy situation in those countries [36], [37], [38], and [39].

2.4 Artificial Intelligence Techniques:

Artificial intelligence are becoming useful as a different way of using traditional technologies. They have been utilized to solve complex practical problems in different fields and are becoming more and more popular nowadays [40]. They can be applied for a wide range of various applications, including medicine, transportation, knowledge management, education, engineering, business, power electronics, and other wide applications. In the field of power systems, a lot of applications can be analyzed and optimized using artificial intelligence.

In the literature of this field, considerable studies and research have been implemented to gain deeper knowledge and a more precise evaluation of the studied topics. Artificial intelligence along with wavelet transform have been used to forecast the generated power of a solar PV system. Artificial intelligence has been utilized in this study in order to capture the nonlinear photovoltaic fluctuation in a better way [41].

Maximum power point tracking (MPPT) in PV systems has been verified and compared by applying various artificial intelligence techniques. The study has illustrated the validity of each MPPT technique and compared it with other artificial intelligence techniques. With regard to the artificial intelligence that is used in techno-economic assessment, there are a lot of papers that have discussed this issue [42].

Artificial intelligence model has been proposed for RE forecasting and the impact of energy efficiency on the economy [43]. An effective deep learning-based forecasting algorithm has been developed for techno-economic analysis of potential solutions involving the use of differently rated residential and commercial PV systems in Estonia [44].

Artificial intelligence techniques cover a wide range of optimization methods. Several engineering applications, like signal processing and electrical power systems, call for an efficient and effective algorithm that can address their specific optimization challenges. Particle swarm optimization (PSO), also known as Ant Colony Optimization (ACO), as well

as other meta-heuristic algorithms like Genetic Algorithm (GA) and Differential Evolution (DE), have all been used to solve real-world optimization problems [45].

2.4.1 Particle Swarm Optimization (PSO):

The flocking habit of birds in nature is the source of inspiration for the Particle Swarm Optimization (PSO) method. Each particle in this method is viewed as a potential solution to a certain optimization issue. Position and velocity are the two vectors that make it up. The values for each of the parameters in the issue are included in the position vector. The particles will have two-dimensional position vectors if the problem, for example, has two parameters. Then, every particle will have a range of motion in an *n*-dimensional search space, where *n* is the total number of variables. The second vector (velocity) is taken into account while updating the position of the particles. For each dimension and particle separately, this vector specifies the size and direction of the step [46].

Particle Swarm Optimization is effective at managing the ratio of exploration to exploitation. Whereas the exploitation phase concentrates on favorable regions, the exploration phase involves vast space exploration. The particle swarm optimization performs better when there is a better balance between exploration and exploitation [45]. PSO has achieved widespread popularity among academics due to its simplicity, and as a result, it has been widely recognized as offering effective performance in a range of application domains. This method is frequently used because of its capacity for hybridization, specialization, and emergent behavior in high-dimensional search spaces for the identification of workable regions. [47,48].

With fewer changing parameters than other optimization approaches like genetic algorithms (GA), it has a higher computational efficiency. As a result, PSO has caught the interest of numerous researchers working on various engineering applications [49]. By using various metaheuristic techniques, including particle swarm optimization, several researchers have tried to increase the efficiency of solar energy systems. A PV system under partial shading has been studied, focusing to get the maximum power point tracking utilizing modified PSO. In order to analyze the optimal selection, technical, and economic evaluation of a hybrid power-generating system [50].

Particle Swarm Optimization code in MATLAB has been programmed. This code was used to confirm the validity of results acquired through the analytical hierarchy process technique [51]. Three renewable micro grid arrangements for Shiraz climate in Iran were used to test the optimization of the techno-economic assessment utilizing a multi-objective particle swarm optimization system [52].

PSO has been utilized in order to compare and verify the obtained results of the proposed strategy for effective energy management for the economics of both on-grid and off-grid photovoltaic systems [53]. Photovoltaic systems, dispatchable diesel generators, wind energy conversion models, and battery energy storage models are used as micro grid components, technical and economic evaluation has been conducted for two various scenarios with optimal sizing, and the outcomes are contrasted utilizing the nature-inspired Firefly Algorithm (FA) and PSO [54].

The overall maximum power point (MPP) of PV generation has been tracked using an accelerated particle swarm optimization algorithm [55]. In order to find the best placement for a base biomass power plant, the particle swarm optimization methodology has been applied [56]. The problem of nonlinear optimization has been applied to the optimal site. Distribution network system losses have been significantly impacted by the locations and capacity of distributed generation sources. Both the genetic algorithm and the PSO method have been utilized for locating and scaling dispersed generation on distribution grids in a study done by [57].

In radial distribution systems, the goal is to reduce grid power losses while improving voltage regulation, voltage stability, and voltage stability within the restrictions of system operation and security. Particle swarm optimization theory has been applied for the optimization of a wind farm layout in Manjil, Iran. The goal of the optimization process is to determine the optimal parameters for the hubs of the wind turbines in this wind farm as well as their best configuration [58].

In order to achieve the best placement and size for photovoltaic on-grid plants for distributed power generation, the Particle Swarm Optimization approach has been proposed. The suggested technique achieves a superior result than genetic algorithms while taking into account similar processing costs, according to the authors [59]. One of the biggest challenges

in designing the on-grid PV system is finding the best site. In order to address the mentioned issue, a novel strategy based on particle swarm optimization has been introduced. The distribution network operator's maximum installed peak power is the primary limitation, and the net present value (NPV) has been chosen as the objective function [60].

2.4.2 Optimal Placement and Sizing of Renewable Distributed Generation (DG)

A lot of studies in the literature have reviewed the optimal location and size of renewable distributed generation (DG) utilizing artificial intelligence techniques. In order to decrease power loss, distributed generation is placed in radial distribution systems using PSO, which leads to determining the ideal distributed generation position and size that correspond to the greatest loss reduction [61].

An efficient biogeography-based optimization (BBO) has been used in order to achieve the best placement and sizing of distributed solar PV generation units, aiming to minimize power losses while keeping voltage profile and voltage harmonic distortion within limitations [62]. The optimal size and placement of the DGs at any bus in the distribution grid have been determined using the algorithm presented in the study done by [63].

The usage of the Salp Swarm Algorithm (SSA) for handling grid reconfiguration and the DG allocation problem has been suggested. The reduction of power loss and voltage deviation is the main goal of this work [64]. In the radial distribution network, an ideal size and placement of distribution generation (DG) units has been proposed based on a renewable energy resource with gravitational energy storage. The approach for optimization minimizes the overall energy loss using the coefficient particle swarm optimization method, which is constrained by equality and inequality [65].

A novel hybrid genetic PSO method has been put forth to choose the best placement for distributed generators with the goal of reducing the network's overall active and reactive losses as well as its voltage regulation. The technique combines the advantages of both the genetic algorithm and PSO techniques on the same population [66]. In order to address the issue of DG unit placement and size optimization in radial distribution networks, a newly developed adaptable PSO algorithm known as phasor particle swarm optimization has been suggested [67].

The goal of a study done by [68] is to determine where and how many DGs should be placed in a radial distribution network before and after reconfiguration. To decide where and how big to put the DGs before and after reconfiguring the radial network, a multi-objective PSO technique has been used. The optimal distribution of distributed generations was achieved using a hybrid approach, a fuzzy logic controller, and a radial distribution system. In this study, an improved concept is put forth for resolving optimal load flow problems with uncertainties using a combination of the Fuzzy Logic Controller (FLC) technique, Ant-Lion Optimization Algorithms (ALOA), and Particle Swarm Optimization (PSO)-based algorithms [69].

In 2023, a lot of studies have recently studied the optimal location and size of DG in case of power loss minimization in distribution networks utilizing the PSO method. They have utilized the PSP method in the case of determining the least real power losses at the electricity grid in order to achieve the optimal placement of the studied PV power plants. Those studies have concluded that the PSO is an effective method for the selection of optimal plant locations and sizing of distributed generation [70], [71], [72], [73], and [74].

Chapter 3

Modeling of PV systems

3.1 Introduction

With the continued development of industries and the growth of population all around the world, the energy demand has been raised. Contributing to this high demand for conventional energy, a lot of negative impacts will be achieved regarding the huge usage of those resources. Because of the previously mentioned reasons, researchers and decision-makers started adapting renewable energy resources to produce clean energy with minimal production costs. Those resources include solar energy, hydro energy, tidal energy, wind energy, fuel cells, geothermal energy, etc.

One of the most popular and effective RE systems is solar energy. This type of energy harvests sunlight in order to generate different types of energy. By utilizing the thermal energy of the sun, a solar collector system can provide hot water or other hot liquids to convert the thermal energy into mechanical energy, like moving turbine blades. Another effect of the sun's light is to harvest the sun's insolation in the form of photovoltaic irradiance, and then, by utilizing a photovoltaic module, the stored energy in the sunlight will be converted into electrical energy by using the semiconductor effect that is included in the module structure. After oxygen, silicon is thought to be the second most plentiful element in the earth's crust and is extensively utilized in the production of PV modules. Also, its cost and availability had a big impact on how much energy was converted. Photovoltaics (PV), which converts solar energy directly into electricity in a solid-state device, is a direct technique for producing power from solar radiation.

Photovoltaic systems are mainly categorized into two major categories: on-grid PV systems and off-grid PV systems (standalone PV systems). In the case of grid-connected PV systems, the main electrical distribution panel of a house receives the alternative current (AC) output of a grid-connected PV system, where it can either supply electricity to the house or send power back to the grid. While in off-grid PV systems the generated electricity is stored in batteries since this system is not connected to the grid, usually this kind is used in remote areas that are far away from the grid, off-grid PV systems have a higher cost for energy production due to the high cost of batteries.

The construction of PV systems requires continuous monitoring and evaluation in order to develop the system and increase efficiency by minimizing the costs of energy production and increasing the generated electricity. One of the main processes that are adapted for the evaluation of PV systems is the techno-economic assessment, which evaluates the technical issues as well as the economic aspects through selected parameters, aiming to achieve more stable and develop systems with higher efficiencies.

In PV systems, the selection of connection points to the grid is an important issue, such that some connection points cause electricity losses in the grid while others cause less losses, which leads to more efficient generation with a lower cost of production. Because of the previously mentioned reasons, it is mandatory to choose the PV power plant location. In order to achieve this objective, artificial intelligence techniques are used. The particle swarm optimization method is usually used for those optimizations because it's simple, accurate, and effective for power plant location selection.

3.2 Modeling of grid-connected PV systems

Every time sunlight strikes solar cells, the PV solar modules produce direct current (DC) electricity. The solar panels should face straight south, be angled at the best angle for that area, and never be shaded throughout the day. To achieve the required voltage and current output, the PV cells of a PV module can be linked in both series and parallel. The grid-connected PV systems, as indicated in Figure 3.1, consist of a series of photovoltaic modules, a combiner box, an array disconnect, an inverter, a breaker, a utility meter, and wiring connections. In rooftop PV systems, the main electrical distribution panel of a house receives the alternative current (AC) output of the on-grid photovoltaic system, which can either supply electricity to the house or send power back to the grid.

The electric meter often runs backwards anytime the photovoltaic system supplies more electricity than the home currently requires, accumulating a credit with the utility. At times, the grid supplies extra electricity when demand is greater than what the PVs can supply. While at the land-based solar photovoltaic power plant, all of the generated electricity will be fed to the grid since no storage batteries are available.

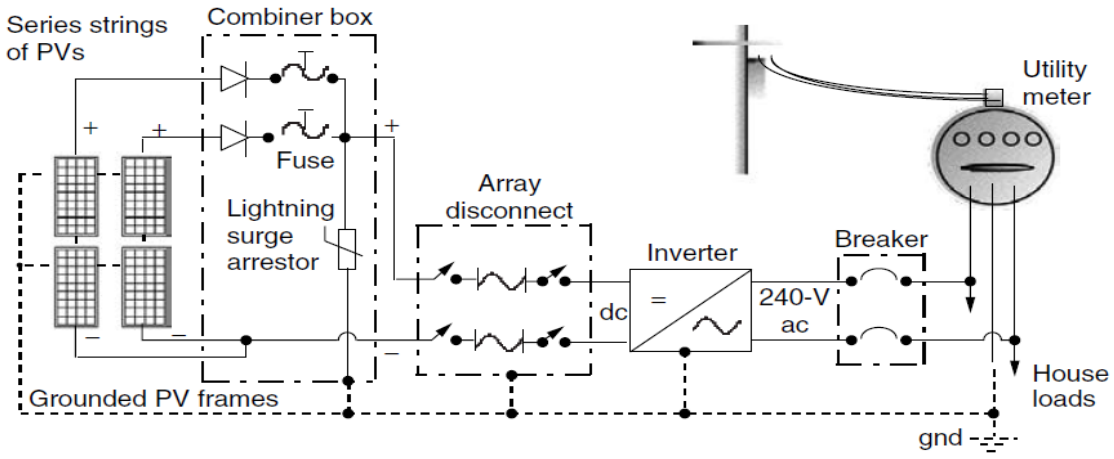

Figure 3.1 Schematic of grid-connected PV generation system [75]

While large on-grid systems may utilize a separate inverter for each string, AC modules each have their own inverters located on the backside of the collector, making it simple to expand the system at any moment.

3.3 Modeling of energy techno-economics

In order to evaluate PV systems, many different methods have been developed. One of these methods is the techno-economic assessment, which deals with various economic parameters like net present value (NPV), simple payback period (SPBP), and levelized cost of electricity (LCOE), as well as technical parameters like system yields, capacity utilization factor (CUF), system efficiency, and performance ratio (PR). By identifying the issues presented in this area and the suggested solutions, those indicators provide a clear image for the investment in this area and the evaluation of the overall long-term success.

3.3.1 Modeling of energy techniques

3.3.1.1 The system yields

Three categories—array, final, and reference yields—can be used to categorize system yields. The yields represent how well the array is actually operating compared to its rated capacity. The DC energy output from the photovoltaic panels during a specific time period, normalized by the PV-rated power, is referred to as the array yield (Y_A). It shows how many hours the photovoltaic array must run at its rated PV capacity to generate the same quantity of energy as was measured [76]. It can be given as indicated in equation (1).

$$Y_A = \frac{E_{DC}}{Ppv.rated} \qquad (kWh\ /\ kWp) \tag{1}$$

where E_{DC} is the DC energy output (kWh) from the photovoltaic array. And Ppv. rated is the rated capacity of photovoltaic array power.

Final yield (Y_F) is calculated as the sum of all AC energy produced by the photovoltaic system during a specified time frame (day, month, or year), divided by the connected photovoltaic system's rated output power [77], and is given by equation (2):

$$Y_{F} = \frac{E_{AC}}{Ppv.rated} \qquad (kWh\ /\ kWp) \tag{2}$$

Where E_{AC} is the AC energy output in kWh.

Reference yield (Y_R) [78,79] is known as the total in plane Solar Insolation H_T (kWh/m^2 divided by the Reference Irradiance H_R (1 kW/ m^2) and The value of this parameter is the same amount of hours at the reference irradiance. as indicated in equation (3).

$$Y_R = \frac{H_T}{H_R} \qquad (kWh\ /\ kWp) \tag{3}$$

where H_T is the plane solar insolation, and H_R is the reference irradiance.

3.3.1.2 Energy losses

The array Capture Losses (L_C) emphasize the array's incapacity to completely exploit the available irradiance by representing losses brought on by array operation. It is the variation between the array yield and the reference yield [80] , as indicated in equation (4):

$$L_C = Y_R - Y_A \quad (kWh / kWp) \tag{4}$$

The energy lost during the inverters' conversion of DC power to AC power is reflected in the System Loss (LS), which is represented by losses in system components. The difference between the final yield and the array yield is what it is [80], as represented in equation (5):

$$L_S = Y_A - Y_F \quad (KWh / KWp) \tag{5}$$

3.3.1.3 PV system's efficiencies

The photovoltaic array efficiency is the DC energy produced by the photovoltaic array system in accordance with the available irradiance on the whole photovoltaic module surface. A PV system's efficiency is a cascading function of the PV array efficiency, system installation efficiency, and inverter efficiency [81], the equation (6) below gives the array efficiency PV:

$$\eta_{pv} = \frac{100\ x\ E_{DC}}{H_T\ x\ A_M}\ (\%) \tag{6}$$

where A_M is the PV module total area (m^2).

The system installation efficiency is computed using Equation (7) and reflects the performance of all system arrays:

$$\eta_{sys} = \frac{100\ x\ E_{AC}}{H_T\ x\ A_M}\ (\%) \tag{7}$$

The inverter efficiency can be represented as listed in equation (8):

$$\eta_{Inv} = \frac{100\ x\ E_{AC}}{E_{DC}}\ (\%) \tag{8}$$

3.3.1.4 Performance ratio

The performance ratio (PR), which depends on array temperature, inadequate absorption of incident solar radiation, and system component inefficiencies or malfunctions, shows the overall impact of losses on a PV array's normal power output. A PV system's PR, which is independent of orientation, location, tilt angle, and nominal rated power capacity [82, 83], reveals how closely it performs to optimum performance in actual operation. Under standardized test settings, the nominal efficiency of the photovoltaic generator is compared to the efficiency of the PV system. The performance ratio is computed using Equation (9), as the ratio of the photovoltaic system's final energy yield (Y_F) to its reference yield (Y_R).

$$PR = 100\ x\ \frac{Y_F}{Y_R}\ (\%) \quad (9)$$

3.3.1.5 Capacity utilization factor

The Capacity Utilization Factor (CUF) is computed as the ratio of the PV system's actual yearly energy output (E_{AC}) to how much energy it would produce if it were run at full rated power every day for a year [84]. as listed in equation (10):

$$CF = \frac{E_{AC}}{P_{PV\ rated}\ x\ 8760} \quad (10)$$

3.3.1.6 Cell temperature effect

Cell temperature is the measured temperature of the surface of the PV panel which is directly affected by the ambient temperature, as the ambient temperature increased, the cell temperature is increased. The cell temperature is affecting the energy generation of the PV module. Equation (11) shows the cell temperature calculation.

$$T_{Cell} = T_{Amb} + \left(\frac{NOCT - 20^{\circ}}{0.8}\right) * H_T \quad (11)$$

Where Tcell is Cell Temperature (°C), Tamb is Ambient Temperature, and HT is solar insolation (kW/m²). NOCT is the Nominal Operating Cell Temperature. The NOCT is cell temperature in a module when ambient is 20◦C, solar irradiation is 0.8 kW/m², and wind speed is 1 m/s.

3.3.2 Modeling of Energy Economics

3.3.2.1 Net present value

The net present value (NPV) of an investment or project is used in capital budgeting to assess its profitability. This approach is dependent on how certain future cash inflows from a project or investment will be. NPV evaluates the present value of money received and the future value of the same amount by taking inflation and the rate of return into account.

NPV is based on three basic steps in discounted cash flow (DCF) approaches. First step: find the present value of each cash flow, including all outgoing and incoming funds discounted at the project's capital cost. To find the project's net present value (NPV), secondly, sum up all of these cash flows. Selecting which project to work on is the decision. The last stage is deciding which project to select. If the net present value (NPV) is positive, the project should be approved; if it is negative, it should be denied. The project with the higher net present value (NPV) between the two should be selected [85]. Equation (12) represents this expression.

$$P_V = F_V / (1 + r)^n \quad (12)$$

Where:

(P_V) is Present Value, (F_V) is Future Value, *r* is the Interest Rate, and *n* is the Number of years.

$$NPV = \text{Income cash flow} - \text{Outcome cash flow} \quad (13)$$

3.3.2.2 Simple payback period

The payback time is the estimated number of years required to recover the initial investment. If all other factors stay the same, projects with shorter payback periods are thought to be better since investors can get their money back more quickly. Additionally, a project's liquidity is increased by a shorter payback period.

Because cash flows projected for the far future are usually riskier than those anticipated for the near future, payback is commonly used as a gauge of a project's riskiness. But there are serious disadvantages to using payback time as a metric for evaluating how effective an investment is in a project. The payback period's primary flaw is that it does not compute profitability and does not take into consideration any benefits that extend past the payback period. Payback time emphasizes capital recovery over profitability more than other factors. Earnings from the project beyond its payback period are not factored in [86]. Equation (13) represents the Simple Payback Period (SPBP) expression.

SPBP = Investment / saving cost per year (14)

3.4 Modeling of location optimization for PV systems

The determination of the optimum location for the PV power plant could be achieved through applying various measures and methods. One of the most effective methods is the use of PSO theory, which considers a lot of particles in order to achieve the most appropriate objective that has been specified previously. The best location of the power plant in this case is the location on the grid with the minimum power losses while keeping the voltage profile and voltage harmonic distortion within limitations. which will be defined as the objective function. This model has been represented by a set of equations that were analyzed in MATLAB software.

Power losses are a waste of resources and are caused by inefficient power supplies. The distribution networks' radial structure and the cables' high resistance are the primary causes of

these power losses. While non-optimal placements of distribution generation (DG) might increase power losses in the grid, appropriate placement minimizes these power losses. The total active power losses in the distribution systems can be computed using equations (15), (16), (17), and (18), which correspond to the lines joining buses i and j in Figure 3. Those equations have been developed through a practical model applied by MATLAB in a study done by [87] that aims to determine the total active power losses in specific distribution systems.

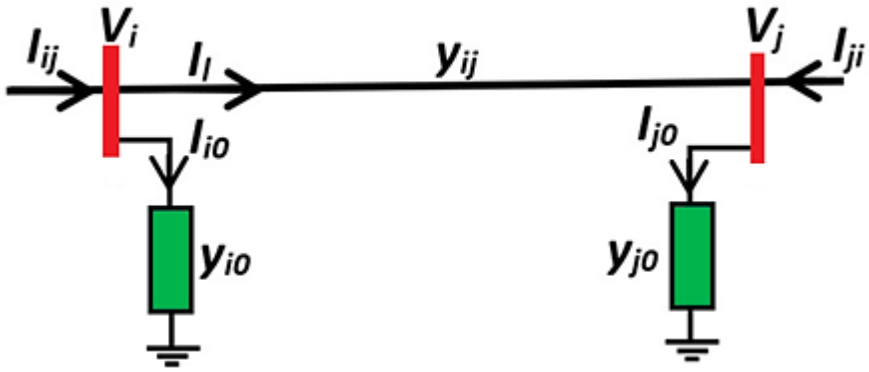

Figure 3.2: Line model to calculate Line flow [87]

The power loss in line ij can be achieved by plying the following equations:

$$S_{Loss,ij} = V_i I_{ij} + V_j I_{ji} \quad (15)$$

$$S_{Loss,ij} = P_{Loss,ij} + jQ_{Loss,ij} \quad (16)$$

where the voltage at buses *i* and *j* is denoted by V_i and V_j, respectively. The measured currents at busses *i* and *j* are denoted by I_{ij} and I_{ji}, respectively. In line *ij*, the active power losses are denoted by $P_{Loss,ij}$, while the reactive power losses are denoted by $Q_{Loss,ij}$.

One of the objective functions is to minimize the system's Total Active Power Losses (TAPL), which may be computed by adding up all of the grid's branches' active power losses. This can be stated as follows in the equation:

$$\mathrm{TAPL} = \sum_{k=1}^{N} \left(P_{loss,ij}\right)_k \quad (17)$$

where N stands for the grid's line number.

It is significant to highlight that the DG is a negative power load model in this study because it is simply defined as a constant active power supply. Therefore, when the DG unit is employed, the load on a considered bus m should be adjusted as follows:

$$P_m = P_{Load,m} - P_{DG,m} \quad (18)$$

3.4.1 Particle Swarm Optimization (PSO)

The Particle Swarm Optimization (PSO) technique draws inspiration from the flocking behavior of birds in the natural world. With this approach, every particle is seen as a possible resolution to a particular optimization problem. It is composed of two vectors: position and velocity. The position vector contains the values for every parameter in the problem. In the event that the problem, for instance, contains two parameters, the particles will have two-dimensional position vectors. Next, in an n-dimensional search space, where n is the total number of variables, each particle will have a range of motion. The particles' position is updated while accounting for the second vector, velocity.

Based on the previous equations, the real power losses will be calculated by applying the PSO algorithm method. The following steps are used to achieve the minimum real power losses [87]:

Step 1: Create n particles at random and set the time counter to t = 0.

Step 2: Update the time counter to t = t+1.

Step 3: Revise the weight of inertia, w(t) = α w(t-1). where the decrement constant, α, is less than or near 1.

Step 4: The jth particle velocity in the kth dimension is updated in accordance with

$$v_{j,k}(t) = w(t)v_{j,k}(t-1) + c_1 r_1 (x_{j,k}{}^{*}(t-1) - x_{j,k}(t-1)) + c_2 r_2 (x_{j,k}{}^{**}(t-1) - x_{j,k}(t-1)) \quad (19)$$

using the global best ($x_{j,k}{}^{**}$) and individual best ($x_{j,k}{}^{*}$) of each particle.

Step 5: Each particle modifies its position based on the updated velocities in accordance with

$$x_{j,k}(t) = v_{j,k}(t) + x_{j,k}(t-1) \quad (20)$$

Using the above listed equations (19), and (20), the updated particle velocity, and particle position will be obtained, a continuous iterations will be adapted in order to achieve the

power flow for updated particles taking into consideration the P_{best}, and $G_{best.}$ Figure 3.3 represents the flowchart of the used PSO technique.

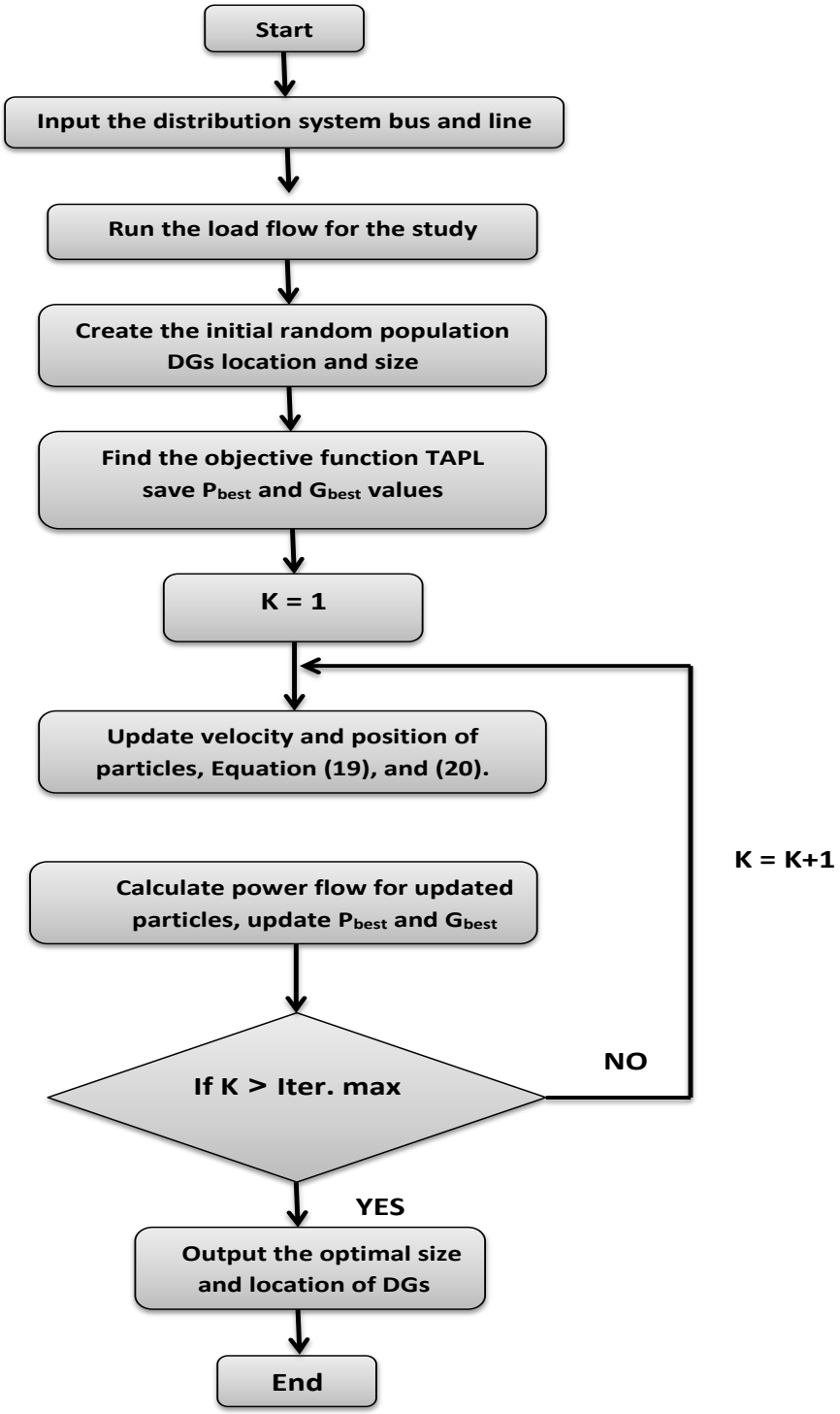

Figure 3.3: flowchart of the used PSO technique.

Chapter 4

Methodology

4.1 Introduction

This study will be implemented for a 1.5 MW photovoltaic power plant located in the southern part of the west bank at Al Dhahriya city in Hebron district. Data related to location, area, topography of solar photovoltaic power plants, climate data, and irradiation intensity have been collected. For the assessment of the land-based solar PV system, a lot of mathematical expressions and formulas will be used to indicate the techno-economic parameters by connecting technical and cost factors into the solar PV system.

To conduct the study, the monthly and annual output of the PV power plant will be provided by plant management, which will study the investment surplus as well as the PV panel specifications. Accurate information about average solar radiation data, percentage of radiation, angle of inclination of cells from the surface, and annual system loss rate will be used in order to calculate the performance parameters. PV system software ($PV_{syst.}$) is a PC software package used globally for the study, scaling, simulation, and data analysis of complete solar PV systems. This software will be used to calculate the output theoretically and compare it with actual values derived from a continuous monitoring of plants for two years.

The techno-economic performance parameters: array yield (Y_A), final yield (F_Y), reference yield (R_Y), capacity utilization factor (CUF), net present value (NPV), simple payback period (SPBP), and the annual average monthly performance ratio (PR) will be calculated through related mathematical expressions, and the system performance of long-term operations will be assessed. And finally, artificial intelligence will be utilized in this study by building an appropriate mathematical model in order to ensure whether the current plant location is optimal for energy generation in Al Dhahriya.

4.2 Study area

Wahaj Al Ghuzlan PV power plant is located in Al Dhahirya town in Hebron district, at the southern part of the west bank, at latitude 31.40° N and longitude 34.98° E. Figure 4.1 represents the Al Dhahriya location map. Al Dhahriya has been selected as a case study because of its semi-desert climate and southern location on the West Bank, which make it one of the most suggested locations for the application of solar power systems as a successful component of renewable energy resources. The large land area with an appropriate topography for installing large PV power plants is also a reason for studying this effect on the energy parameters for this power plant.

The location is far away from the center of accommodation, buildings, and forests, which has the potential to increase the lifecycle of the project and the power plant's overall efficiency. The existing factories in the region and the huge population in the adjacent town have a high demand for electricity, so it is recommended to connect them with this plant rather than connecting them from distant electricity sources, which minimizes the losses in the electricity network.

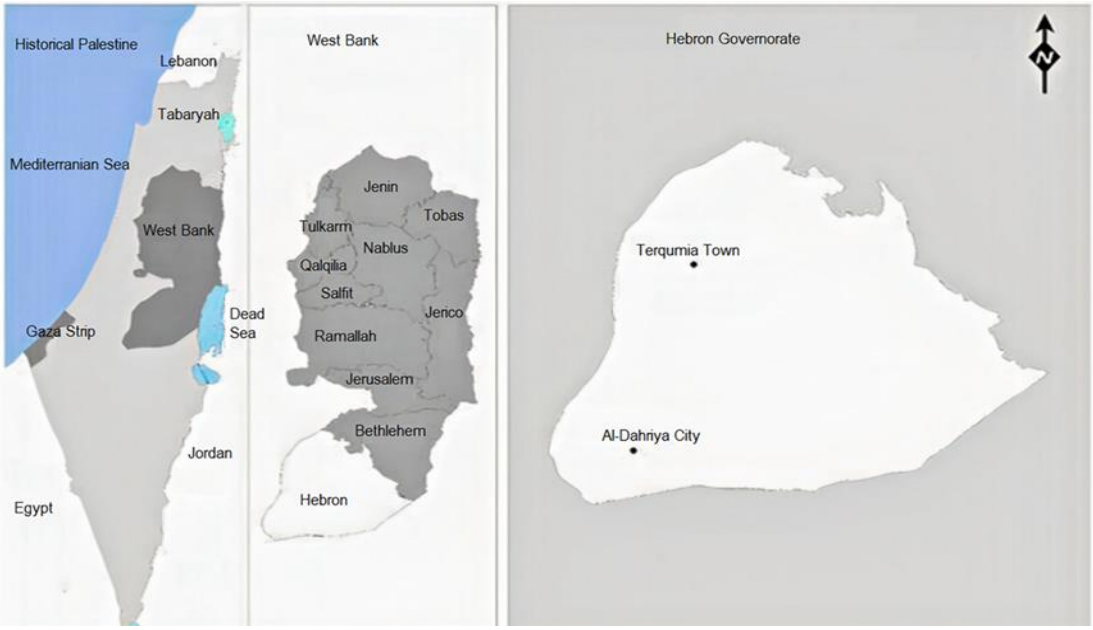

Figure 4.1: site location (Al Dhahriya map) [88]

The PV power plant located in suitable topography since no shading from buildings or trees or any objectives that may make shading on the modules, Figure 4.2 represents the actual photo of Wahaj Al Ghuzlan PV power plant at Al Dhahriya.

Figure 4.2: Wahaj Al Ghuzlan PV power plant location.

4.3 Weather Data

The Wahaj Al Ghuzlan power plant's hourly records of solar radiation, temperature, and wind speed have been obtained. The plant is located at latitude 31.40° N and longitude 34.98° E. The observation data used in this thesis came from a weather land station that was continuously monitored from January 2021 to December 2022.

Stats include temperature, wind speed, and daily and hourly solar radiation. Figure 4.3 depicts the annual Plane of Array (POA) solar irradiance in hours, for 8760 hours per year in 2021. The term

"plane of array irradiance" (POA) is widely used to describe how much incoming irradiance is received by a specific solar array. It is frequently utilized in PV performance research and modeling of PV arrays since it is the parameter most closely related to the power production of a PV module.

The total of the direct normal irradiance (DNI) and diffuse horizontal irradiance (DHI) components incident on a surface with a specified tilt and angle of incidence is known as POA irradiance. The graphic provides POA solar irradiance for the site in W/m^2 for each hour throughout the year.

Beginning in January, the value rises until it reaches its peak in the summer, then falls in the autumn until it reaches December. Evidently, the maximum amount of total POA solar irradiance is approximately 1340 W/m^2 at noon in August. The average POA solar irradiance for all the seasons in the year 2021 was around 573 W/m^2. Figure 4.4 depicts the annual POA solar irradiance in hours, for 8760 hours per year in 2022. The recorded values of POA solar irradiance in the year 2022 represent a nonhomogeneous reading since a lot of days in different months and seasons have a peak value of more than 1400 W/m^2, the maximum amount of total POA solar irradiance, which is 1784 W/m^2 at 06:00 in the morning on September 19. The average POA solar irradiance for all the seasons in the year 2022 was around 666 W/m^2.

As a comparison between the years 2021 and 2022, although the maximum and average POA irradiance values in 2021 are higher than the values in 2021, it shows a nonhomogeneous reading since most of the second part of the year 2022 shows a value of less than 1000 W/m^2 compared with the first part of the same year. While the values for the year 2021 show a normal curve with symmetrical data along the summer axis.

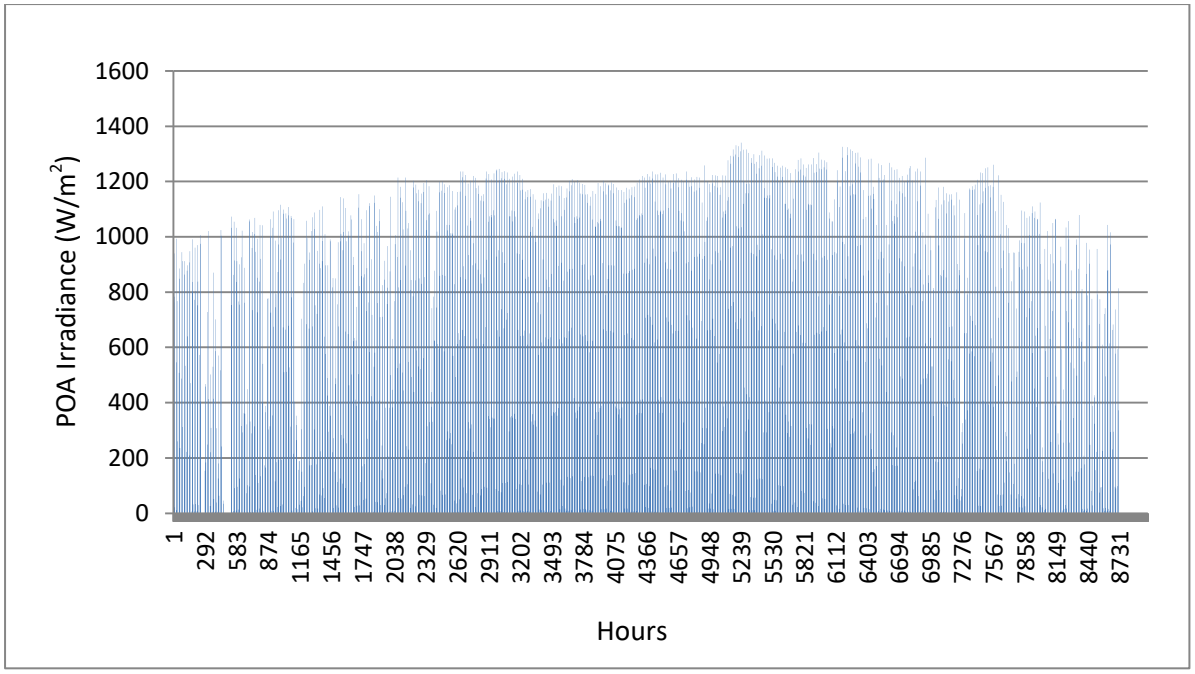

Figure 4.3: Hourly POA solar irradiance (W/m^2) for the year 2021.

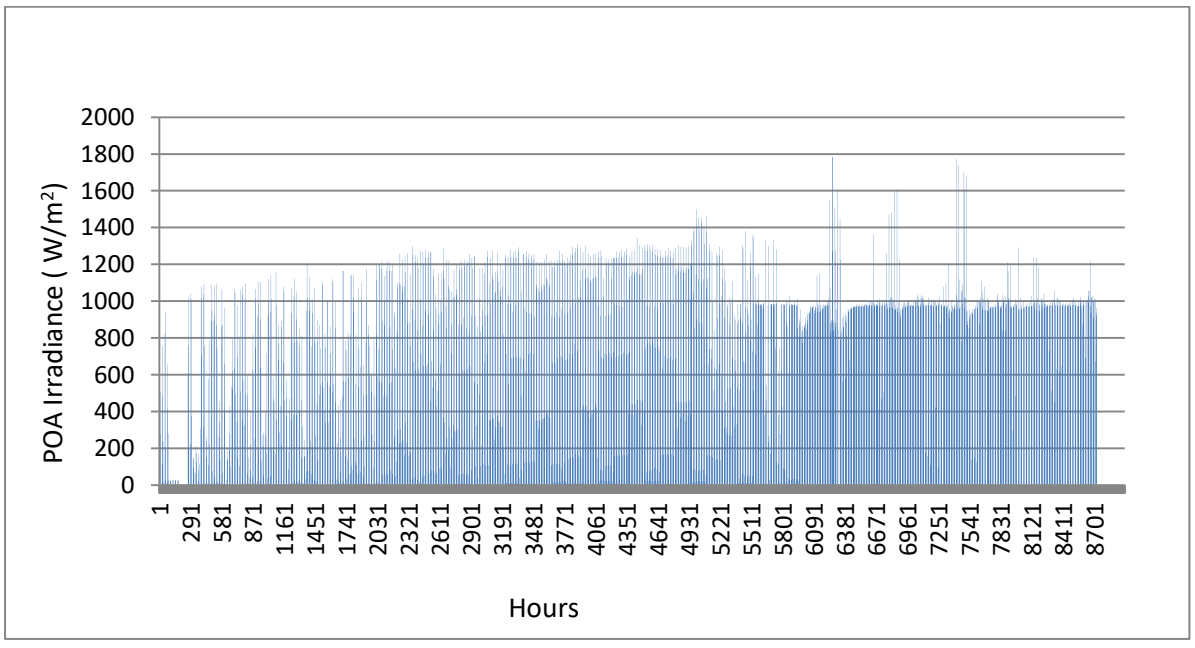

Figure 4.4: Hourly POA solar irradiance (W/m^2) for the year 2022.

Irradiance is, in the end, an instantaneous measurement of how much solar energy is passing through a specific surface per unit area and per unit time. Because of this, it is expressed in watts per square meter. It's worth it depending on how intense the sun is at a given time. Whereas insolation contains units of energy per unit area and is essentially irradiance that has

been accumulated over a period of time, The standard unit of measurement in solar insolation is kWh/m2, or more commonly, sun-hour. Figures 4.5 and 4.6 indicate the hourly solar insolation for the years 2021 and 2022, respectively.

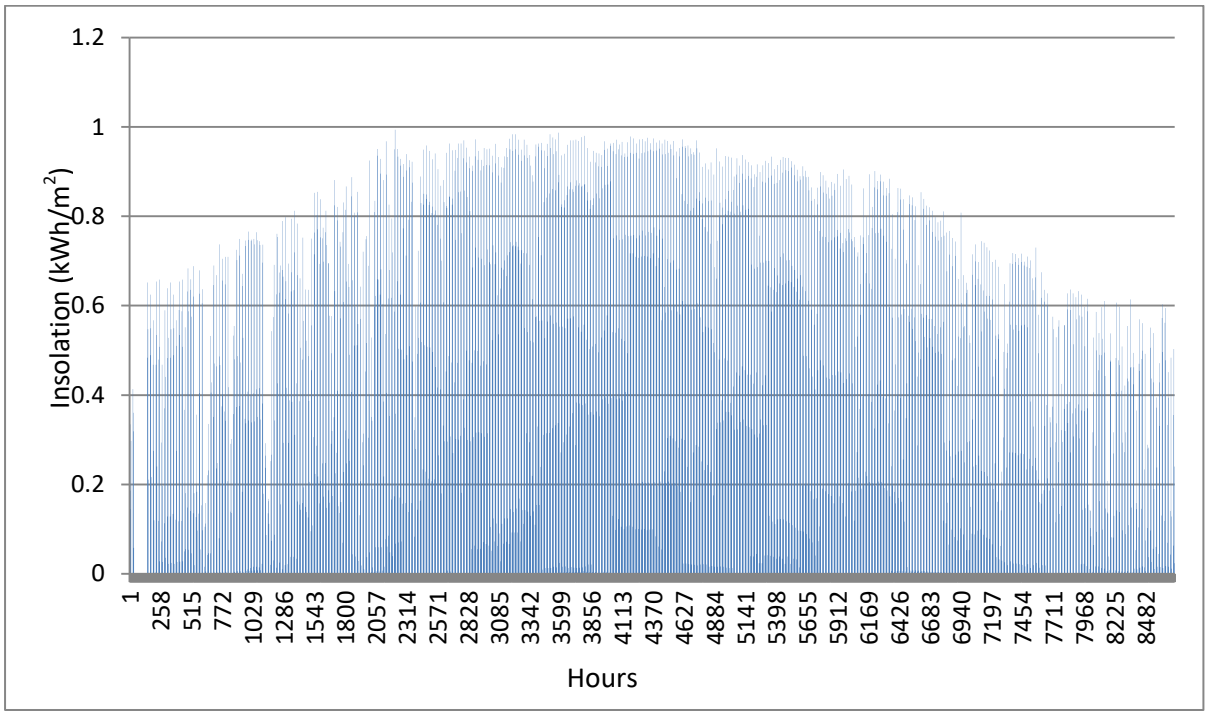

Figure 4.5: Hourly solar insolation (kWh/m^2) for the year 2021.

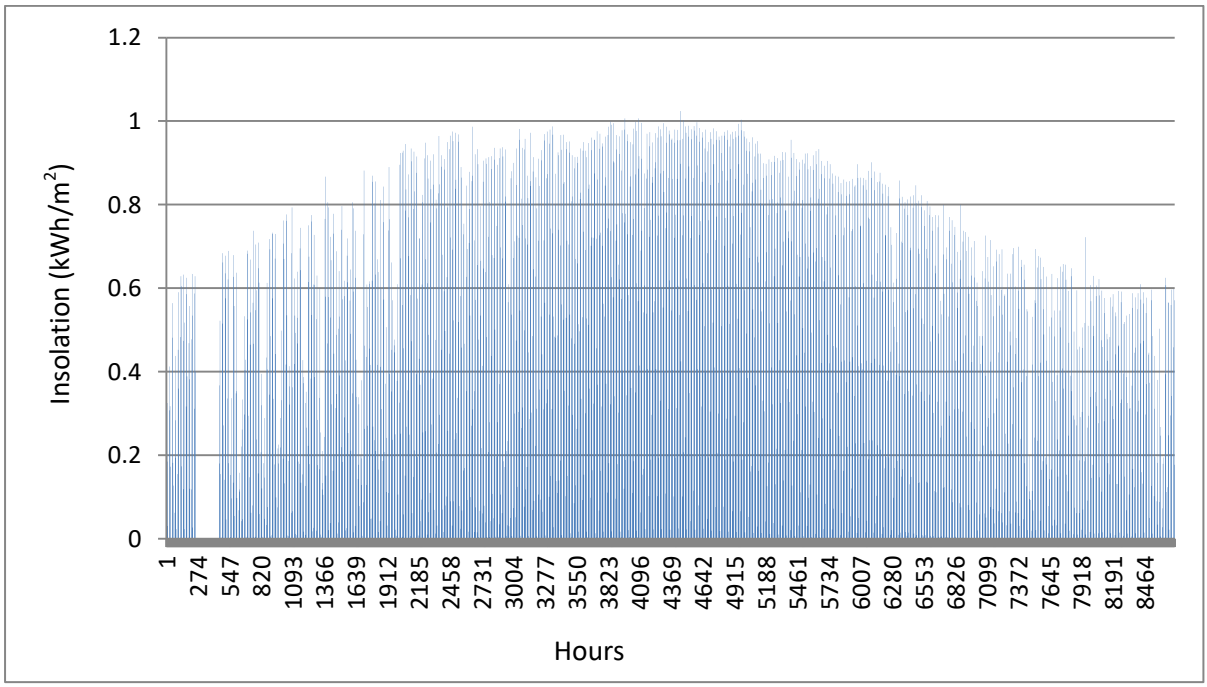

Figure 4.6: Hourly solar insolation (kWh/m^2) for the year 2022.

It’s noted that the data of the solar insolation will be used in calculations since it represents the energy delivered over a specific period, such as daily, monthly, annual, etc., which differs from the POA irradiance, which indicates only the instantaneous readings of sunlight. Although the POA irradiance represents direct, diffuse, and both of them sometimes, this is not the real sunlight that reaches the PV panels. So, the solar insolation will be used to calculate the different techno-economic parameters in this study.

Wind speed values have also been recorded for both the years 2021 and 2022. The hourly wind speed values for 8760 hours per year are represented in Figure 4.7 for the year 2021 and Figure 4.8 for the year 2022. As represented in the figures, it could be seen that the maximum value of wind speed is approximately 7.75 m/s and the average wind speed is around 1.92 m/s for the observed data in the year 2021. While the maximum value of wind speed is approximately 6.67 m/s and the average wind speed is around 1.8 m/s for the observed data in the year 2022,.

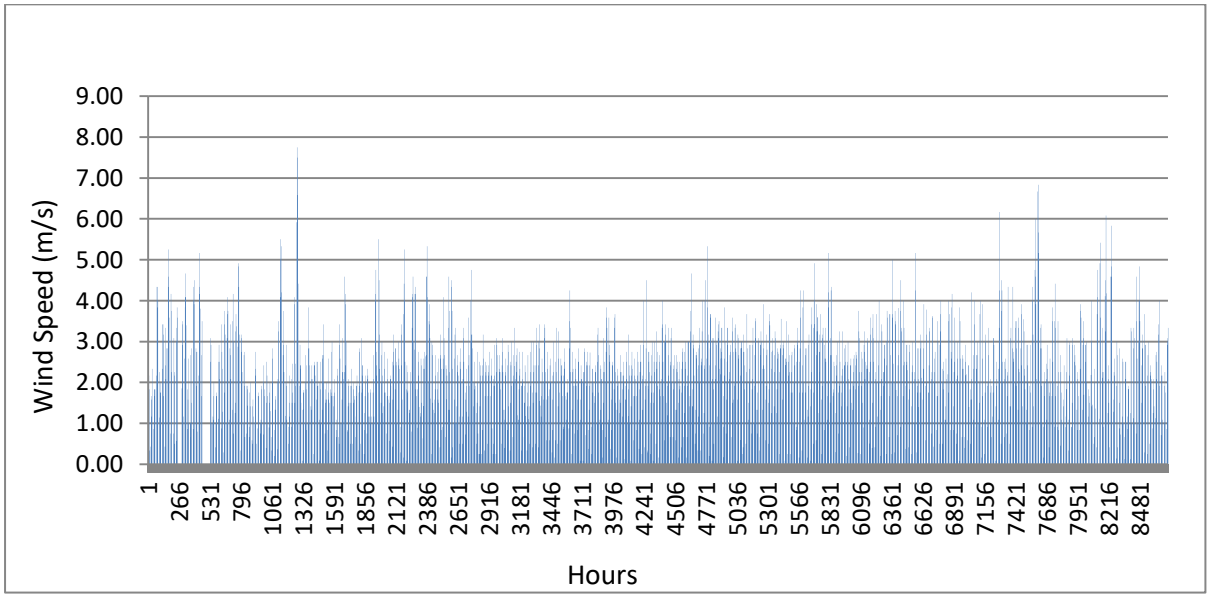

Figure 4.7: wind speed (m/s) for the year 2021.

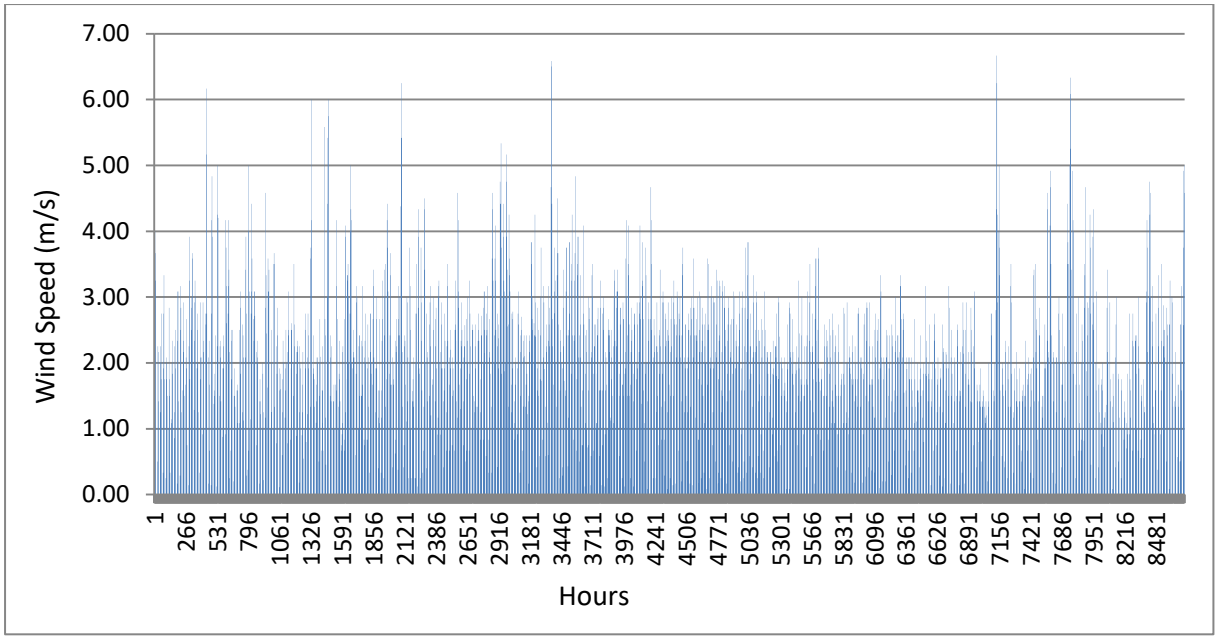

Figure 4.8: wind speed (m /s) for the year 2022.

Daytime ambient temperature values have also been recorded for both the years 2021 and 2022. The hourly ambient temperature values for 8760 hours per year are represented in Figure 4.9 for the year 2021 and Figure 4.10 for the year 2022. As represented in the figures, it could be seen that the maximum recorded value of hourly day ambient temperature is 38.93 C° at 14:00 on July 18th, and the average hourly day ambient temperature is around 22.5 C° for the observed data in the year 2021. While the maximum recorded value of hourly day ambient temperature is 39.16 C° at 13:00 afternoon on August 28th, and the average hourly day ambient temperature is around 21.5 C° for the observed data in the year 2022, It's clearly seen that the average hourly ambient temperature of the year 2022 decreases by 1 °C compared to the year 2021.

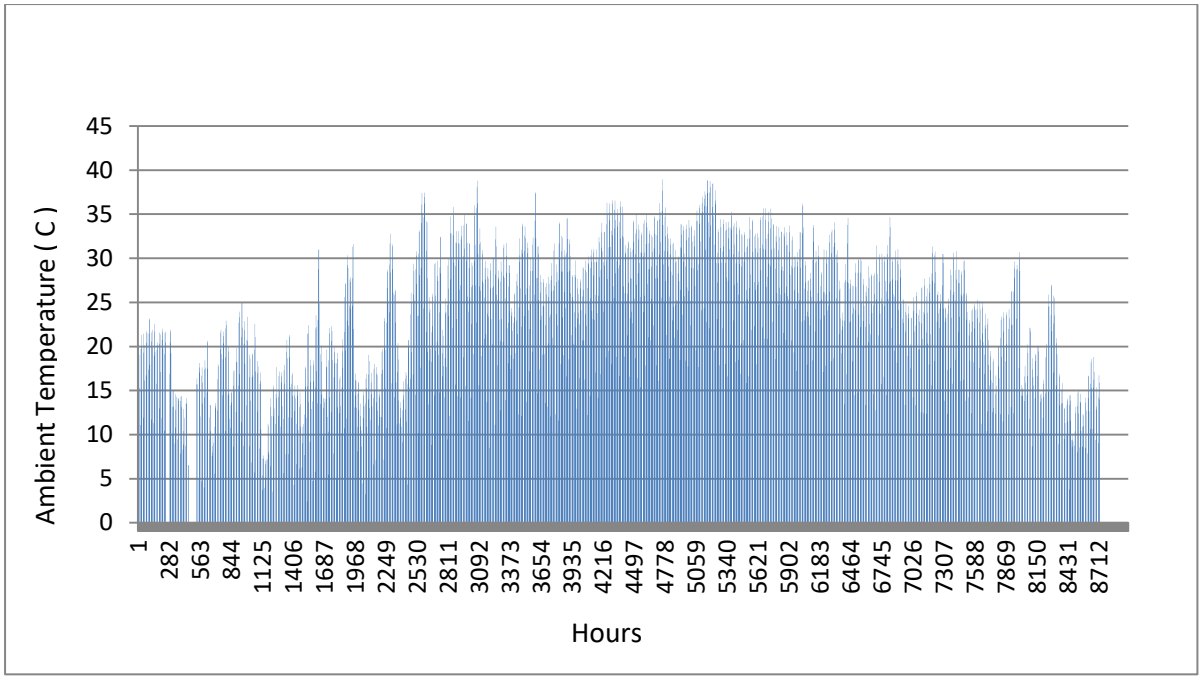

Figure 4.9: Hourly ambient temperature (C°) for the year 2021.

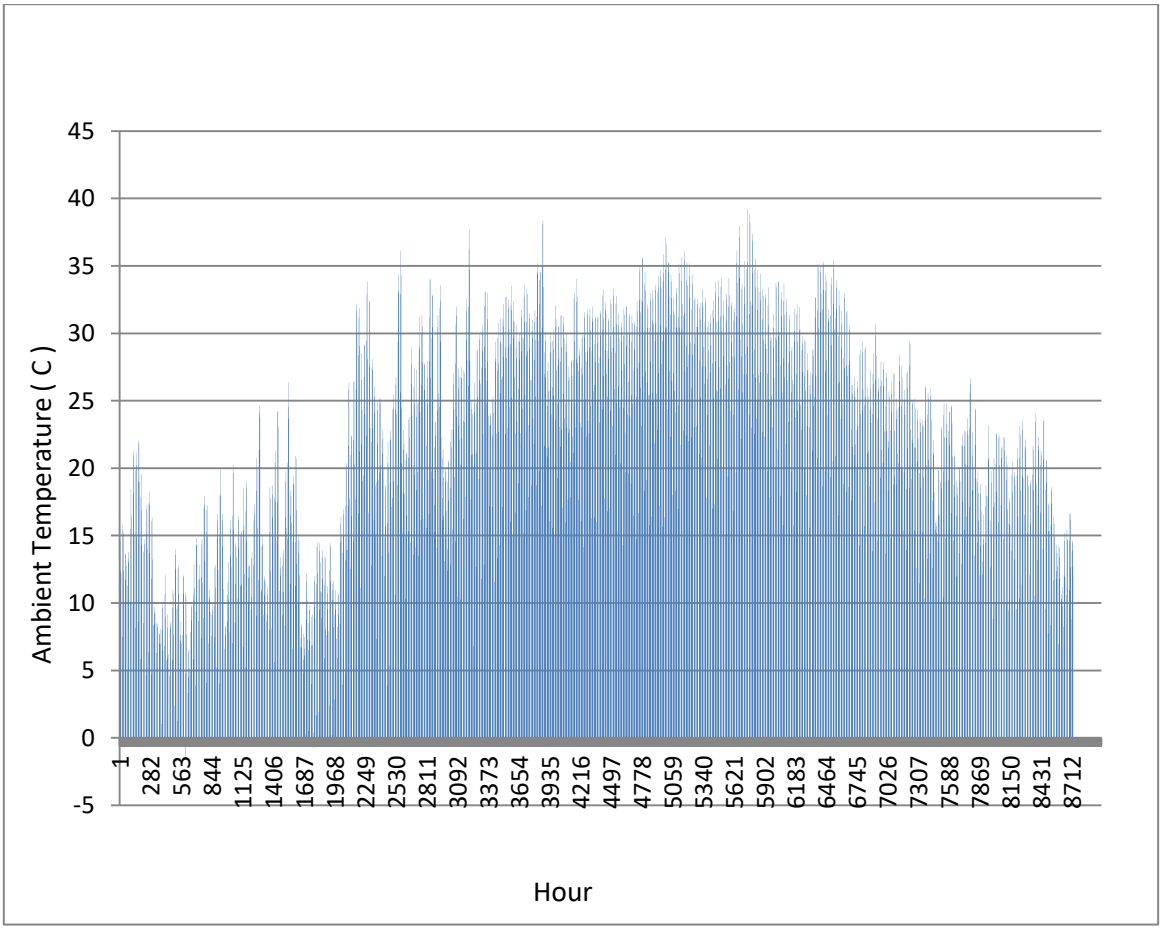

Figure 4.10: Hourly ambient temperature (C°) for the year 2022.

Table 4.1 illustrates the average ambient temperature (C ^{o}), average daily solar insolation (kWh/m^2/day), and average wind speed (m/s) along the months. Those data for the year 2021.

Table 4.1 Average temperature, daily solar Insolation and wind speed for the months of 2021.

Month	Average Ambient Temperature (C ^{o})	Average daily solar Insolation (kWh/m^2/day)	Average Wind speed (m/s)
January	15.09	2.84	2.15
February	14.70	4.12	1.88
March	15.56	5.08	1.66
April	21.78	6.84	1.98
May	25.97	7.75	1.69
June	25.98	8.11	1.67
July	28.68	7.67	2.01
August	29.69	7.11	2.00
September	26.62	6.08	2.05
October	23.91	4.78	1.90
November	21.48	3.81	2.16
December	14.55	2.62	2.03
Average	22	5.57	1.93

Referring to the listed data in Table 4.1 for the year 2021, The average monthly ambient temperature (C^{o}) can be represented in Figure 4.11. Beginning in January, the ambient temperature rises progressively until it reaches its peak in the summer before falling in the autumn until December. The average ambient temperature throughout the year was 22 °C; and the maximum recorded monthly ambient temperature was in August at 29.69 °C.

The average daily solar insolation for each month (kWh/m^2/day) can be represented in Figure 4.12, Beginning in January, the average daily solar isolation rises progressively until it reaches its peak in the summer before falling in the autumn until December. The average solar insolation throughout the year was 5.57 kWh/m^2/day; the lowest daily solar insolation was recorded in December with 2.62 kWh/m^2/day; and the maximum recorded daily solar insolation was in June with 8.11 kWh/m^2/day. The average monthly wind speed (m/s) can be represented in Figure 4.13. The average wind speed along the year was 1.93 m/s; the lowest monthly wind speed was recorded in March with 1.66 m/s; and the maximum recorded monthly wind speed was in November with 2.16 m/s.

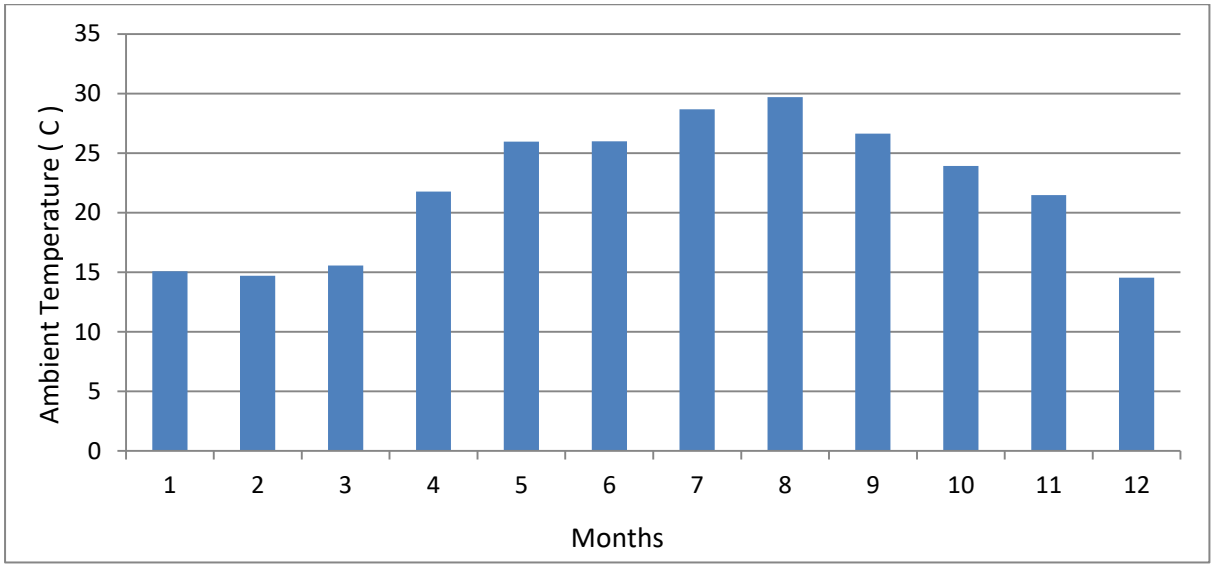

Figure 4.11: Average monthly Ambient Temperature (C^o)for the year 2021.

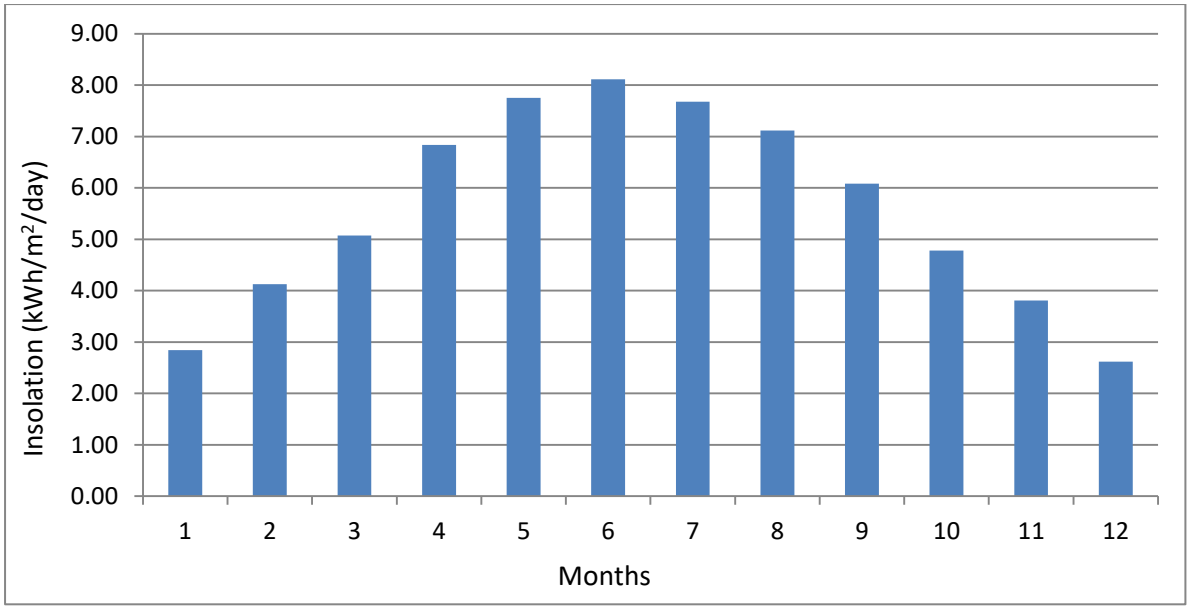

Figure 4.12: Average daily solar Insolation for each month(kWh/m^2/day) for the year 2021.

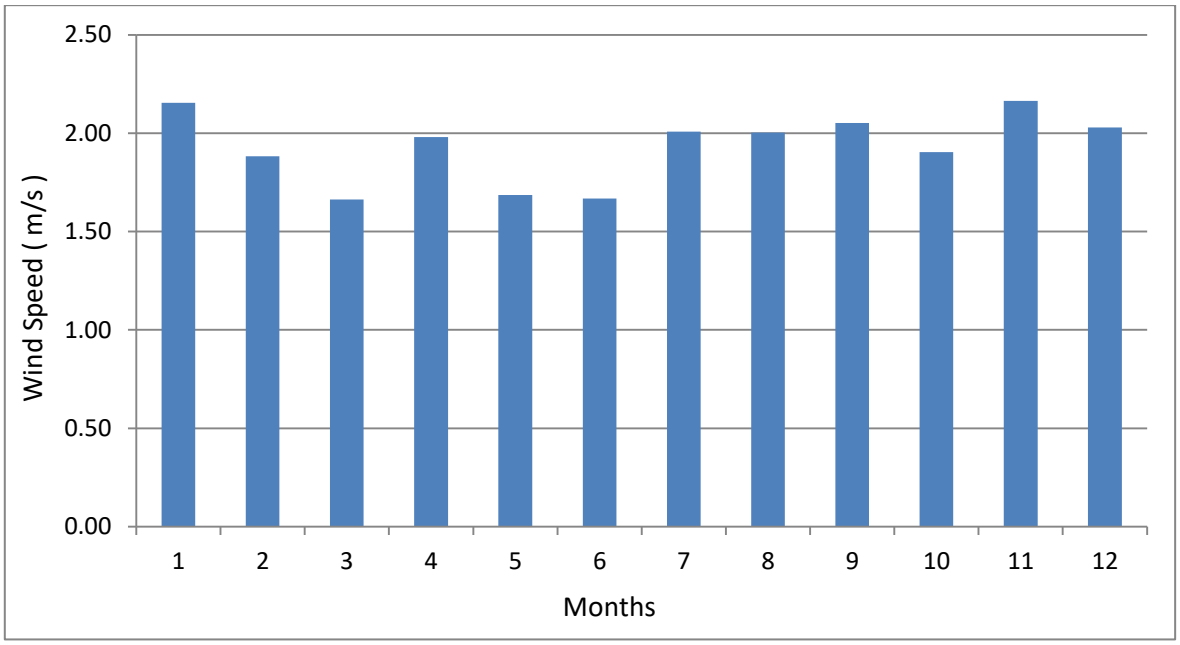

Figure 4.13: Average monthly Wind speed (m/s) for the year 2021.

Table 4.2 illustrates the average ambient temperature (C ^{o}), average daily solar insolation (kWh/m^2/day), and average wind speed (m/s) along the year months. Those data for the year 2022.

Table 4.2 Average temperature, daily solar Insolation and wind speed for the months of 2022.

Month	Average Ambient Temperature (C ^{o})	Average daily solar Insolation (kWh/m^2/day)	Average Wind speed (m/s)
January	10.54	2.29	1.88
February	12.70	3.70	1.80
March	12.30	4.81	1.95
April	22.42	6.68	1.82
May	23.84	7.25	2.21
June	26.44	8.12	1.89
July	27.71	8.16	1.86
August	28.78	7.12	1.57
September	27.66	6.12	1.56
October	23.93	4.63	1.51
November	18.86	3.40	1.84
December	16.30	3.01	1.61
Average	20.95	5.44	1.79

Referring to the listed data in Table 4.2 for the year 2022, The average monthly ambient temperature (C^{o}) can be represented in Figure 4.14. Beginning in January, the ambient temperature rises progressively until it reaches its peak in the summer before falling in the autumn until December. The average ambient temperature throughout the year was 20.95 °C; and the maximum recorded monthly ambient temperature was in August with 28.78 °C.

The average daily solar insolation for each month (kWh/m2/day) can be represented in Figure 4.15. Beginning in January, the average monthly solar insolation rises progressively until it reaches its peak in the summer and then starts decreasing in the autumn until December. The average solar insolation throughout the year was 5.44 kWh/m2/day; the lowest daily solar insolation was recorded in January with 2.29 kWh/m2/day; and the maximum recorded daily

solar insolation was in July with 8.16 kWh/m2/day. The average monthly wind speed (m/s) can be represented in Figure 4.16; the average wind speed along the year was 1.79 m/s; the lowest monthly wind speed was recorded in October with 1.51 m/s; and the maximum recorded monthly wind speed was in May with 2.21 m/s.

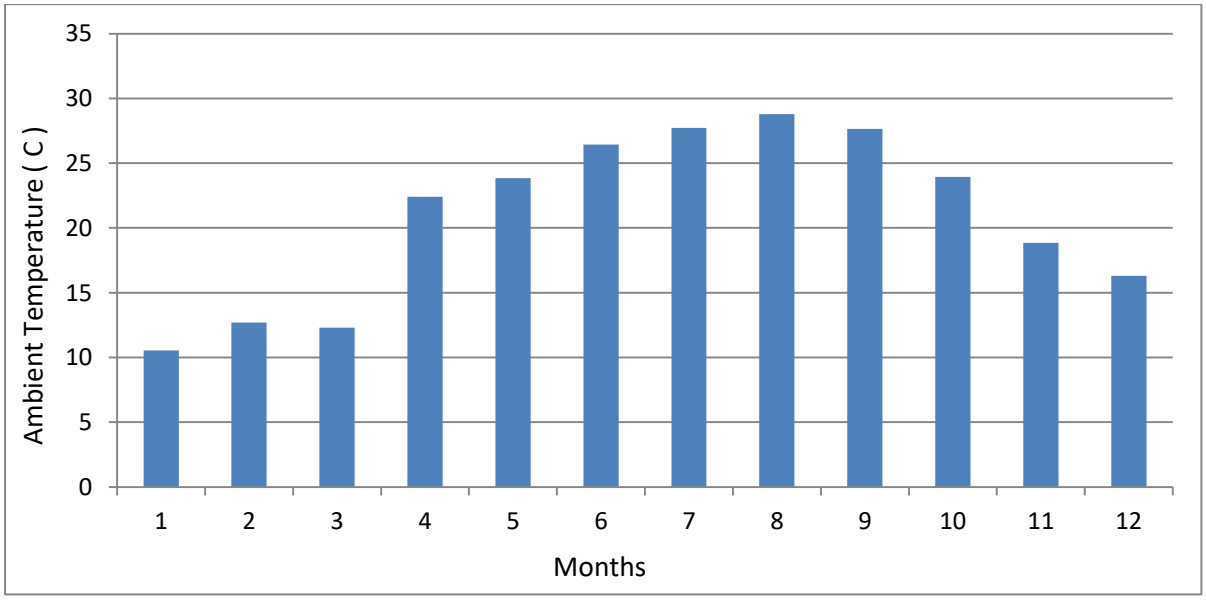

Figure 4.14: Average monthly Ambient Temperature (C^{o})for the year 2022.

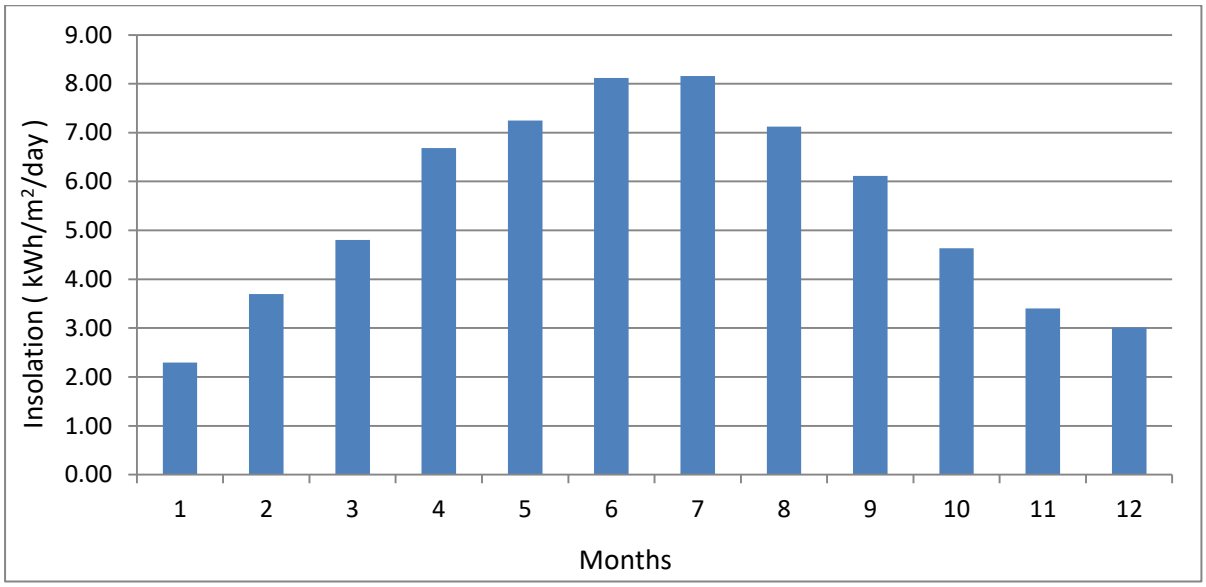

Figure 4.15: Average daily solar Insolation for each month ($kWh/m^2/day$) for the year 2022.

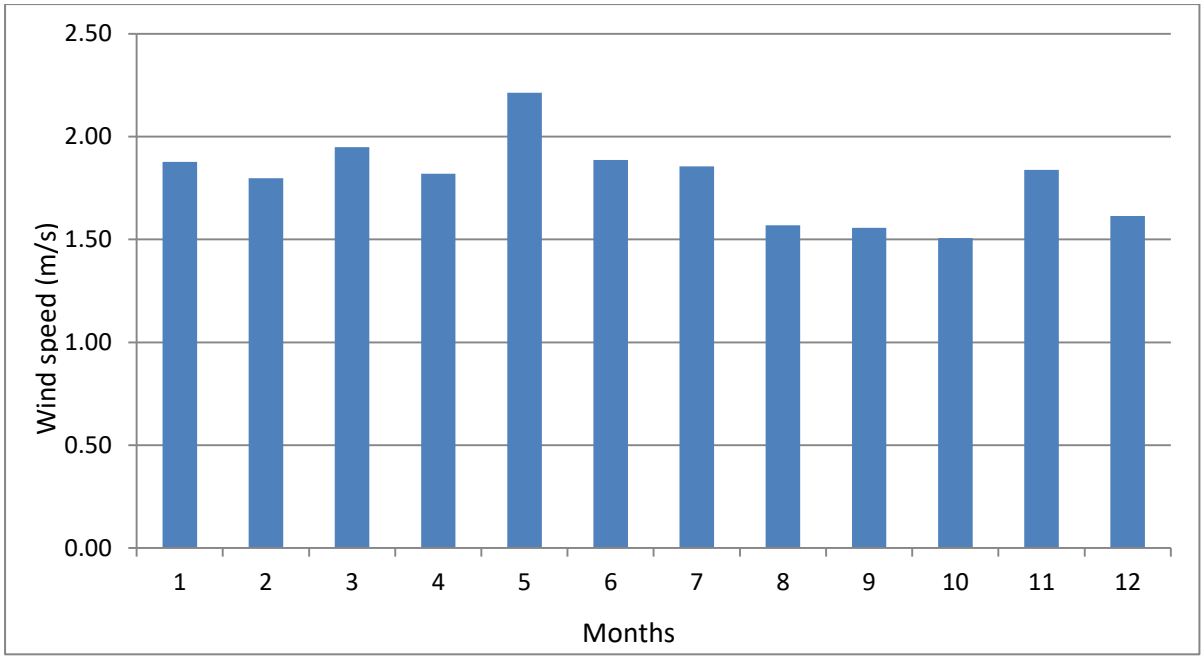

Figure 4.16: Average monthly Wind speed (m/s) for the year 2022.

4.4 PV System Specifications

4.4.1 Specification of PV Modules

The photovoltaic panels used in the plant are 4155 units type (XM72360I+(BI+)) and 150 units type (GCL-M6/72H375) with efficiencies of 18.41% and 19.3%, respectively, and nominal power of 360 Wp and 375 Wp, respectively. The types of modules used for the project are Sunerg XM72360I+ (IB+) and GCL-M6/72H. The modules are monocrystalline.

The parameters of the modules meet all the contemporary requirements for quality and productivity with a good balance of price and quality. The data sheets show that the modules represent good efficiencies (18.41% and 19.3%) and an additional warranty for 0.8% linear annual degradation for over 25 years. The guarantee on product material and workmanship is 10 years. The specifications of the PV panels that are used in this plant are listed in Table 4.3.

Table 4.3: PV panels specifications [89]

Type	XM72360I+(IB+)	GCL-M6l72H
Peak Power (P_{max})	360Wp	375 Wp
Total No. Of Units	4155	150
Module Efficiency	18.41%	19.3%
Open circuit voltage	47.66 V	48 V
Voltage at (P_{max})	39.88 V	39.4 V
Short-circuit current	9.61 A	10.05 A
Current at (P_{max})	9.05 A	9.47 A

4.4.2 Specification of Inverters

The project uses inverters PVS-100/120-TL from ABB (16 pcs). This inverter is very good for large-scale projects because of its easy installation, efficiency of 98.4%, wide temperature range (-25 to +60 °C), and good protection against bad weather conditions. The inverter's field serviceability, high efficiency, Adaptable system design, ease of installation, straightforward commissioning, and approved maintenance requirements all significantly lower the system's overall operating costs. The warranty is 10 years from the date of commissioning, with a 20-year optional upgrade. The used inverters are fitted with the DC and AC boxes, where the DC inputs are equipped with MC4 quick fit inputs, DC switches, DC surge protection, overload fuses, and a DC string monitoring function. However, the AC part is equipped with an AC switch and AC surge protection.

Inverters (PVS-ABB Product Series) that are manufactured by ABB have six independent Maximum Power Point Tracking (MPPT), which improves the system's overall reliability and efficiency by reducing the total number of PV strings per array; it also reduces the shadow effect of shaded strings on the other strings. In addition, the string monitoring function with a preset suitable alarm is included. This enables a fast response to maintenance activities. The specifications of the inverters used in this plant are listed in Table 4.4**.**

Table 4.4: Inverter specification. [90]

Type	PVS-100-TL
No. Independent MPPT	6
MPPT Rated Power	16.67 KVA
Maximum efficiency (η_{max})	98.4%
Weighted efficiency (EURO)	98.2%
Maximum DC input current for each MPPT ($I_{DC,max}$)	36 A
Rated DC input power (P_{DCr})	102 000W
Maximum AC output current ($I_{AC,max}$)	145 A

4.5 Economic data

In order to do the economic analysis, some of data must be collected from power plant operators and other data will be assumed. The data that related to capital investment cost, selling price, selvage cost, replacement cost of components, interest, and other related data have been achieved and they are:

- investment cost of PV power plant equals to $ 1,339,057 preVAT.
- Selvage value equals to $150,000 at the end-of-life cycle.
- Replacement cost of inverter equals to $ 2,800 (10^{th} year).
- The life cycle is 20 years with 7% of interest.
- The selling price assumed to be 9.5 cent / kw preVAT.

4.6 PV Array Distribution

The photovoltaic panels are distributed in 17 rows along the plant, Figure 4.17 shows the layout of the panel arrangement in the project land. The total number of connected PV

modules are 4,305 modules. The project design uses premade mounting structure from Schletter Solar GMBH - Germany. The design has a good quality and can fulfill the durability concerns.

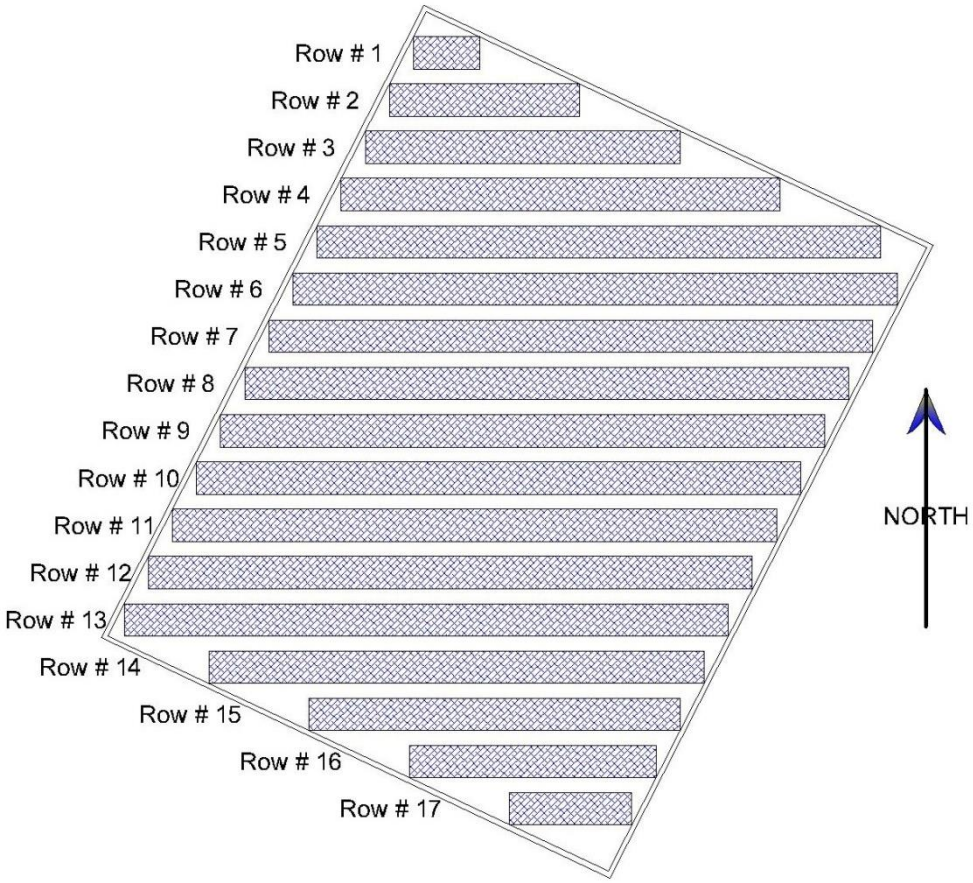

Figure 4.17: Photovoltaic panels arrangement

4.7 PV power plant location optimization

4.7.1 Al Dhahriya grid component

In order to get the most suitable PV power plant location, the grid position with the fewest power losses while maintaining a reasonable voltage profile and voltage harmonic distortion is the ideal place for the power plant. For achieving this goal, Al Dhahriya Single Line Diagram (SLD) have been studied to know the number of transformers, their loads, and their

impedance. As well as the type of used electricity distribution cables, their length, and their impedance.

4.7.1.1 Bus Diagram

Distribution transformers as well as grid cables have been represented in Figure 4.18 which includes the information on transformer numbers and their arrangement in bus diagram. This diagram has been adapted to find the cable path between tow individual transformers that will be used for calculating line's resistance, and reactance, as well as transformer's resistance, reactance, and impedance.

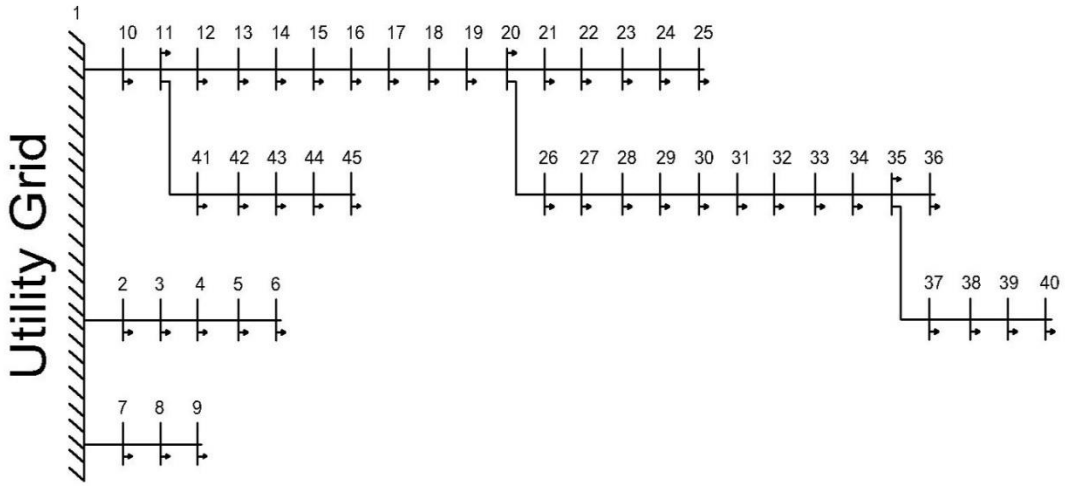

Figure 4.18: Al Dhahriyaa grid bus diagram

4.7.1.2 Distribution Transformers

The electricity grid of Al Dhahriya city consists of 66 distribution transformers, with a rated power of 160 kVA, 250 kVA, 400 kVA, and 630 kVA depending on the connected load. in order to facilitate the grid analyzing, the transformers that located closed to each other's with small distance and negligible cable resistance, have been considered as a one transformer with a rated power equals to sum of the individual rated powers of those transformers. the new generated SLD consists of 44 distribution transformers. Table 4.5 represents those transformers with rated power and their location at Al Dhahriya city.

Table 4.5: Distribution Transformers.

Transformer no.	Location	Rated Power (kVA)	Transformer no.	Location	Rated Power (kVA)
١	Mothalath somara	400	٢٣	Shweekeh	160
2	Almalahi	250	24	Shweekeh 2	160
3	Almuntazah 2	250	25	Haret al shekh	630
4	Anab Alkabera 2	250	26	Aboal homoos	630
5	Anab Alkabera	160	27	Mana'a	630
6	Al gollha	250	28	Jamooq	250
7	Al stad	250	29	Massafi	250
8	Om aldahab	160	30	Mektaa doma	400
9	Al merzab	250	31	Al-khansa school	630
10	Al helal alahmar	400	32	Sa'adeh	630
11	Alsadaqa	400	33	Doma hospital	250
12	Wad Al Gamri	630	34	Domat al wardabat	250
13	Be'er motawe	630	35	Domat al wardabat 2	250
14	Rasmi wahhab	250	36	Al marj 2	250
15	Aqbet el arsha	250	37	Al marj 1	250
16	mothalath elberj	630	38	Kurza	630
17	Al baladiya	400	39	Al jebrini	630
18	Al Deer	630	40	Enab elzaghera	400
19	Bank al eskan	630	41	Al shoqfan	630
20	Al masjed	630	42	Abo hashem	400
21	Al bahaa	160	43	Wad ali	250
22	Al bahaa 2	250	44	Sama'a	250

4.7.1.2.1 Resistance, Reactance, and Impedance for Distribution Transformers

The internal resistance, reactance, and impedance for the 44 distribution transformers have been recorded from the data sheet and reflected as line impedance to be entered as an input to MATLAB in order to calculate the total grid losses. Table 4.6 presents those values.

Table 4.6 Resistance (R), Reactance (X), and Impedance (Z) for Distribution Transformers [91].

Trans-former	Rated Power (KVA)	R %	X %	Z %	Trans-former	Rated Power (KVA)	R %	X %	Z %
2-46	400	1.09	4	4.14	24-68	160	1.23	4	4.19
3-47	250	1.17	4	4.17	25-69	160	1.23	4	4.19
4-48	250	1.17	4	4.17	26-70	630	0.99	4.57	4.68
5-49	250	1.17	4	4.17	27-71	630	0.99	4.57	4.68
6-50	160	1.23	4	4.19	28-72	630	0.99	4.57	4.68
7-51	250	1.17	4	4.17	29-73	250	1.17	4	4.17
8-52	250	1.17	4	4.17	30-74	250	1.17	4	4.17
9-53	160	1.23	4	4.19	31-75	400	1.09	4	4.14
10-54	250	1.17	4	4.17	32-76	630	0.99	4.57	4.68
11-55	400	1.09	4	4.14	33-77	630	0.99	4.57	4.68
12-56	400	1.09	4	4.14	34-78	250	1.17	4	4.17
13-57	630	0.99	4.57	4.68	35-79	250	1.17	4	4.17
14-58	630	0.99	4.57	4.68	36-80	250	1.17	4	4.17
15-59	250	1.17	4	4.17	37-81	250	1.17	4	4.17
16-60	250	1.17	4	4.17	38-82	250	1.17	4	4.17
17-61	630	0.99	4.57	4.68	39-83	630	0.99	4.57	4.68
18-62	400	1.09	4	4.14	40-84	630	0.99	4.57	4.68
19-63	630	0.99	4.57	4.68	41-85	400	1.09	4	4.14
20-64	630	0.99	4.57	4.68	42-86	630	0.99	4.57	4.68
21-65	630	0.99	4.57	4.68	43-87	400	1.09	4	4.14
22-66	160	1.23	4	4.19	44-88	250	1.17	4	4.17
23-67	250	1.17	4	4.17	45-89	250	1.17	4	4.17

4.7.1.3 Distribution Cables

The grid cables that have been used for electricity transmission consists of 4 main types they are: Rabbit cable, Dog cable, Coyote cable, and the 95 mm^2 underground cable. Table 4.7 indicates cables type, length, and their path between each to connected transformers.

Table (4.7): Distribution Cables.

Cable Path	Cable Type	Length (m)	Cable Path	Cable Type	Length (m)
1-2	Underground 95 mm^2	500	23-24	Rabbit	1900
2-3	Rabbit	703	24-25	Underground 95 mm^2	1490
3-4	Rabbit	630	20-26	Underground 95 mm^2	1360
4-5	Rabbit	958	26-27	Underground 95 mm^2	1670
5-6	Rabbit	920	27-28	Underground 95 mm^2	1880
1-7	Rabbit	1880	28-29	Underground 95 mm^2	960
7-8	Coyote	1280	29-30	Underground 95 mm^2	370
8-9	Coyote	465	30-31	Underground 95 mm^2	594
1-10	Dog	629	31-32	Underground 95 mm^2	1540
10-11	Coyote	989	32-33	Underground 95 mm^2	1100
11-12	Rabbit	1000	33-34	Underground 95 mm^2	490
12-13	Underground 95 mm^2	3260	34-35	Underground 95 mm^2	535
13-14	Underground 95 mm^2	50	35-36	Coyote	935
14-15	Rabbit	546	35-37	Underground 95 mm^2	1150
15-16	Underground 95 mm^2	250	37-38	Underground 95 mm^2	825
16-17	Underground 95 mm^2	800	38-39	Rabbit	1315
17-18	Underground 95 mm^2	265	39-40	Underground 95 mm^2	1560
18-19	Underground 95 mm^2	1870	11-41	Rabbit	890
19-20	Underground 95 mm^2	1125	41-42	Underground 95 mm^2	1700
20-21	Underground 95 mm^2	50	42-43	Underground 95 mm^2	975
21-22	Rabbit	1680	43-44	Underground 95 mm^2	804
22-23	Underground 95 mm^2	500	44-45	Underground 95 mm^2	470

4.7.1.3.1 Resistance, and Reactance for Distribution Cables

The resistance, and reactance for each type of used cables in the grid in the unit of Ohms per Kilometre (Ohm / km) have been achieved as indicated in Table 4.8:

Table 4.8 Resistance (R), and Reactance (X), for cable types per unit km [91].

cable type	resistance (ohms / km)	reactance (ohms / km)
Rabbit	0.66	0.297
Dog	0.408	0.276
Coyote	0.267	0.26
Underground 95 mm^2	0.320	0.134

The data listed in Table 4.8 have been used in the calculation of overall resistance, and reactance for the total cable length along each path between two adjacent transformers. Table 4.9 represents cable type, resistance, reactance, and current capacity that will be used in MATLAB analysis.

Table 4.9 Resistance (R), Reactance (X), and current capacity for distribution cables [91].

cable path	cable type	length (km)	resistance (R) (ohms)	reactance (X) (ohms)	capacity winter night (A)	capacity summer noon (A)
1-2	95 mm^2	0.50	0.16	0.07	307	257
2-3	Rabbit	0.70	0.46	0.21	307	257
3-4	Rabbit	0.63	0.42	0.19	307	257
4-5	Rabbit	0.96	0.63	0.28	307	257
5-6	Rabbit	0.92	0.61	0.27	307	257
1-7	Rabbit	1.88	1.24	0.56	581	425
7-8	Coyote	1.28	0.34	0.33	581	425
8-9	Coyote	0.47	0.12	0.12	455	334
1-10	Dog	0.63	0.26	0.17	581	425
10-11	Coyote	0.99	0.26	0.26	307	257
11-12	Rabbit	1.00	0.66	0.30	165	165
12-13	95 mm^2	3.26	1.04	0.44	165	165
13-14	95 mm^2	0.05	0.02	0.01	307	257
14-15	Rabbit	0.55	0.36	0.16	165	165
15-16	95 mm^2	0.25	0.08	0.03	165	165
16-17	95 mm^2	0.80	0.26	0.11	165	165
17-18	95 mm^2	0.27	0.08	0.04	165	165
18-19	95 mm^2	1.87	0.60	0.25	165	165
19-20	95 mm^2	1.13	0.36	0.15	165	165
20-21	95 mm^2	0.05	0.02	0.01	307	257
21-22	Rabbit	1.68	1.11	0.50	165	165
22-23	95 mm^2	0.50	0.16	0.07	307	257
23-24	Rabbit	1.90	1.25	0.56	165	165
24-25	95 mm^2	1.49	0.48	0.20	165	165
20-26	95 mm^2	1.36	0.44	0.18	165	165
26-27	95 mm^2	1.67	0.53	0.22	165	165
27-28	95 mm^2	1.88	0.60	0.25	165	165
28-29	95 mm^2	0.96	0.31	0.13	165	165

29-30	95 mm^2	0.37	0.12	0.05	165	165
30-31	95 mm^2	0.59	0.19	0.08	165	165
31-32	95 mm^2	1.54	0.49	0.21	165	165
32-33	95 mm^2	1.10	0.35	0.15	165	165
33-34	95 mm^2	0.49	0.16	0.07	165	165
34-35	95 mm^2	0.54	0.17	0.07	581	425
35-36	Coyote	0.94	0.25	0.24	165	165
35-37	95 mm^2	1.15	0.37	0.15	165	165
37-38	95 mm^2	0.83	0.26	0.11	165	165
38-39	Rabbit	1.32	0.87	0.39	307	257
39-40	95 mm^2	1.56	0.50	0.21	165	165
11-41	Rabbit	0.89	0.59	0.26	307	257
41-42	95 mm^2	1.70	0.54	0.23	165	165
42-43	95 mm^2	0.98	0.31	0.13	165	165
43-44	95 mm^2	0.80	0.26	0.11	165	165
44-45	95 mm^2	0.47	0.15	0.06	165	165

Chapter 5

Analysis and Discussion of Results

5.1 Overview

As mentioned in the previous chapters, there is an essential need to have a continuous evaluation and assessment of PV systems. This evaluation should keep in touch with any problems that may occur for the system and the proposed solutions. One of the most important measures for this evaluation is the techno-economic assessment, which deals with the technical and economic aspects that are connected to the system or affect its performance.

There are a lot of parameters that could be used for this assessment: economic parameters like net present value, simple payback period, and levelized cost of electricity, as well as technical parameters like system yields, capacity utilization factor, system efficiency, and performance ratio. Also, one of the important measures for PV power plants is the selection of the best connection point to the grid, which can be achieved by applying artificial intelligence techniques. In this study, the PSO method has been applied in order to get the optimum location of the connection point.

In this chapter, the results of the studied aspects are discussed. The analysis of the technical parameters, economic study, and power plant best location have been reviewed, and conclusions and findings are drawn.

5.2 simulation results of PV system:

According to the collected data from the plant, one of the reports that have been done by the PV power plant supervisors is the plant's expected energy analysis. This analysis that was done by the supervisors has been implemented through PVsyst. Software. The data related to location, area, topography of a solar photovoltaic power plant, climate data, and irradiation intensity have been collected and entered into PVsyst. Software in order to perform system

simulation. The entered variables are: Latitude 31.40° N, Longitude 34.98° E, Altitude 537 m, Tilt 20°, Azimuth 0°, Horizon Average Height 6.8°, and proposed no shadings.

According to that report, three kinds of arrays have been defined in this simulation: Sub-array no. 1, which consists of 3780 Si-mono Model_comp XM72/156-360I+ modules with a unit nominal power of 360 Wp, has been arranged in 252 strings in parallel with 15 modules in series for each string. The array's global power is 1361 kWp. Sub-array no. 2, which consists of 375 Si-mono Model_comp XM72/156-360I+ modules with a unit nominal power of 360 Wp, has been arranged in 25 strings in parallel with 15 modules in series for each string. The array global power is 135 kWp. Sub-array no. 3, which consists of 150 Si-mono Model_comp GCL-M6/72H-375 modules with a unit nominal power of 375 Wp, has been arranged in 10 strings in parallel with 15 modules in series for each string. The array's global power is 56.3 kWp. The total array global power of 4305 modules is 1552 kWp, with 8438 m2 of module area and 7372 m2 of cell area. Inverter Model_comp PVS-100-TL P with a nominal power of 100 kW_{AC}, 16 units have been entered with a total nominal power of 1617 kW_{AC}.

The main simulation results indicate that the produced energy is 2,895 MWh/year; Figure 5.1 indicates the expected monthly energy output. The output results from PVsyst. Software related to expected energy has been compared with the actual generated energy that has been taken for a continuous two years of monitoring, as represented in Table 5.1. The obtained data from the site weather station will be used to calculate the values of the techno-economic parameters of the PV power plant, and artificial intelligence will be utilized in order to ensure that the current plant location is optimal for energy generation in Al Dhahriya.

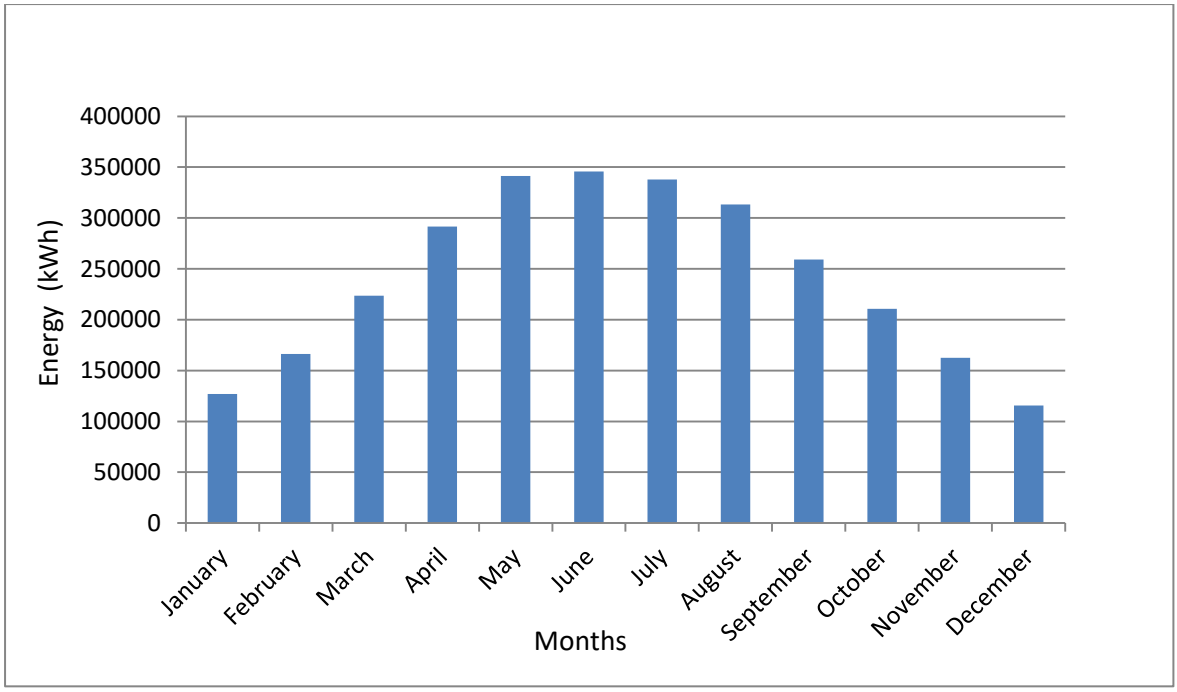

Figure 5.1: monthly energy expected output (kWh).

Table 5.1: monthly measured energy compared with simulated expected output energy.

Capacity: 1,552 kWp		Year 2021	Year 2022
Month	Expected Energy (kWh)	Measured Energy (kWh)	Measured Energy (kWh)
January	127,106.5413	183389.3855	162712.8423
February	166,442.1757	197055.8751	178509.5209
March	223,620.3268	231457.2945	233168.7044
April	291,473.0003	277209.0625	269060.5116
May	341,361.2159	302289.7811	288634.447
June	345,784.2725	303119.2557	297085.6557
July	337,921.8469	293740.4897	313890.5541
August	313,299.8194	284922.104	297485.8443
September	259,274.2415	252532.9417	267025.1751
October	210,639.4901	219435.1971	232371.4229
November	162,664.3661	178288.6876	181543.3724
December	115,532.6684	228604.9548	176552.1714
Total	2,895,119.965	2952045.029	2898040.222

Figure 5.2 represents the monthly measured energy compared with the simulated expected output energy for both years 2021 and 2022 that is indicated in Table 5.1. It could be noticed

that the monthly measured energy output for both years 2021 and 2022 exceeds the proposed energy in the cold climate in the autumn and winter seasons like January, February, March, October, November, and December. While the monthly measured energy output for both years 2021 and 2022 is less than expected in hot climates in spring and summer, like April, May, June, July, and August,.

These results could be explained by the negative effect of the high ambient temperature, which raises the cell temperature, which leads to a decrease in overall module efficiency and a decrease in energy generation. It's also noticed that the measured energy output in December 2021 is too high compared with the same month in 2022 and compared with the expected energy output. This could also be explained depending on the ambient temperature effect; in this case, the average ambient temperature in December 2021 decreases by 1.75 °C compared with the same period in 2022.

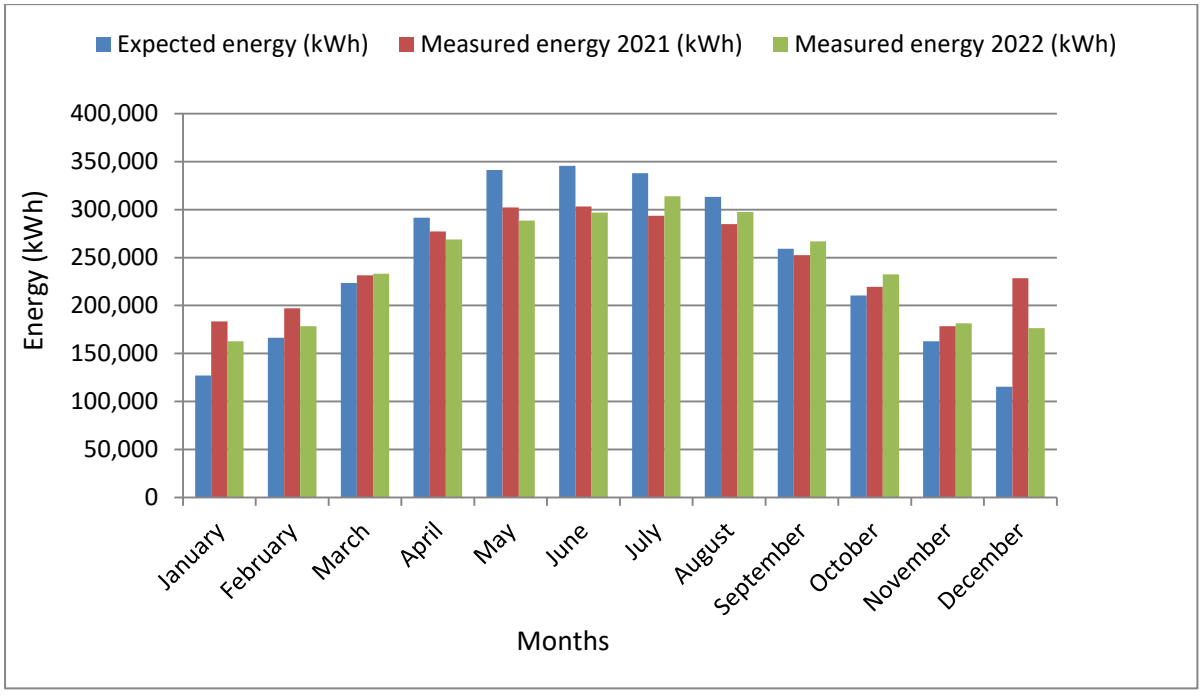

Figure 5.2: monthly expected, and measured energy output. (kWh).

5.3 Techno-economic assessment of the grid connected PV power plant

5.3.1 Technical PV system analysis

5.3.1.1 System yields

The three categories of system yield that show how well the array is actually operating compared to its rated capacity are analyzed in this section. The results are expressed and discussed for the array, final, and reference yields.

In order to find out the array yield (Y_A), equation (1) is applied, which is represented by the ratio of the annual DC energy output from the PV power plant to the rated capacity of PV system power. To calculate the final yield (Y_F), equation (2) is used, which indicates the ratio of the total annual AC energy output from the PV power plant to the rated capacity of PV system power. While equation (3) is used for calculating the reference yield (YR), which is defined as the total in-plan solar insolation H_T divided by the reference irradiance H_R (1 kW/m2),.

Table 5.2 indicates the values of array yield (Y_A), final yield (Y_F), and reference yield (Y_R) for the years 2021 and 2022. After having the required data related to the annual DC energy output, the total annual AC energy output, and the total in-plane solar insolation, taking into consideration the $P_{PV\ rating}$ of 1552 kWp,.

Table 5.2: system yields (2021), (2022).

Year	E_{DC} (kWh)	Y_A (kWh/kWp)	E_{AC} (kWh)	Y_F (kWh/kWp)	H_T (kWh/m2)	Y_R (kWh/kWp)
2021	3,050,044	1,965	2,952,045	1,902	2,038	2,038
2022	2,980,050	1920	2,898,040	1,867	1,989	1,989

It's clearly noted from the above-listed results in Table 5.1 that the total in-plan solar insolation H_T for the year 2021 was higher than what was recorded in the year 2022, which contributed to the overall average ambient temperature that appears in Tables 4.1 and 4.2, which indicates the average ambient temperature in 2021 increased by about 1 °C compared

to 2022. The higher total in plane solar insolation H_T is the higher annual DC energy output and total annual AC energy output, which leads to a higher array yield (Y_A) and a higher final yield (Y_F). So the yields in 2021 are higher than the yields in 2022.

The monthly measured insolation for the years 2021 and 2022 is expressed in Figures 5.3 and 5.4, respectively. The average monthly insolation (kWh/m2), which is represented in Figure 5.3 for the year 2021, Beginning in January, the average monthly insolation rises progressively until it reaches its peak in the summer before falling in the autumn until December. The average insolation throughout the year was around 169.51 kWh/m^2, the lowest monthly insolation was recorded in December with about 81.23 kWh/m^2, and the maximum recorded monthly insolation was in June with around 243.35 kWh/m^2.

The average monthly insolation (kWh/m2), which is represented in Figure 5.4 for the year 2022, Beginning in January, the average monthly insolation rises progressively until it reaches its peak in the summer and then starts decreasing to the autumn until December. The average insolation throughout the year was around 165.70 kWh/m^2, the lowest monthly insolation was recorded in January with about 71.03 kWh/m^2, and the maximum recorded monthly insolation was in July with around 253 kWh/m^2.

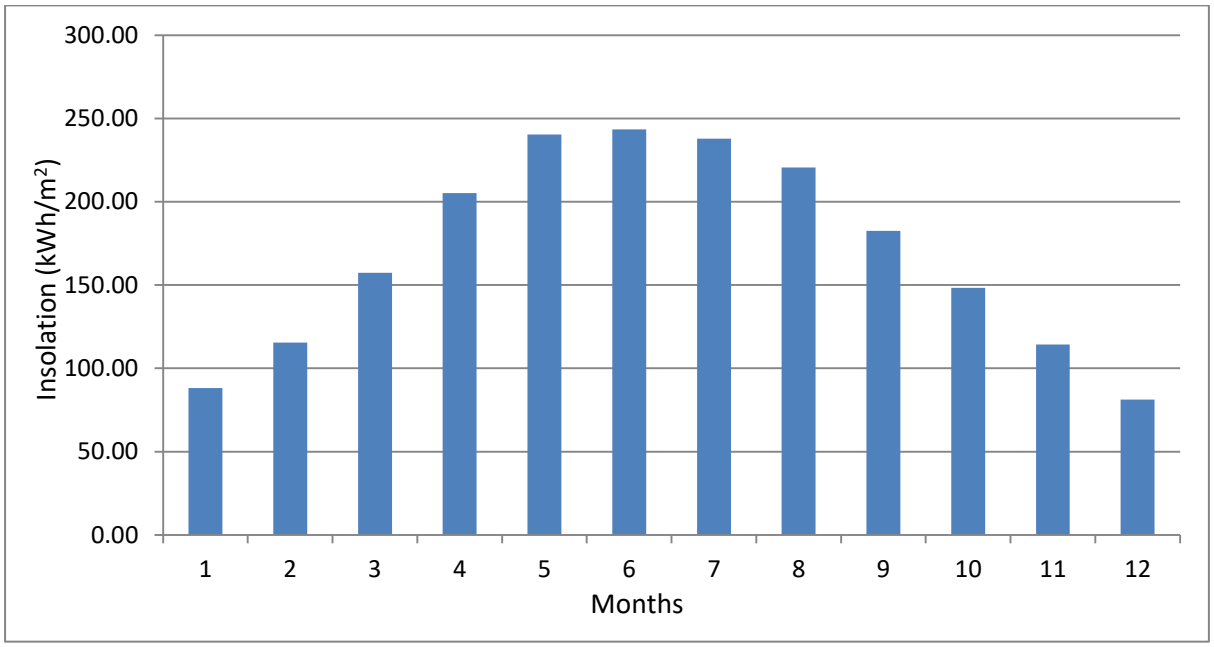

Figure 5.3: Average monthly Insolation (kWh/m^2) for the year 2021.

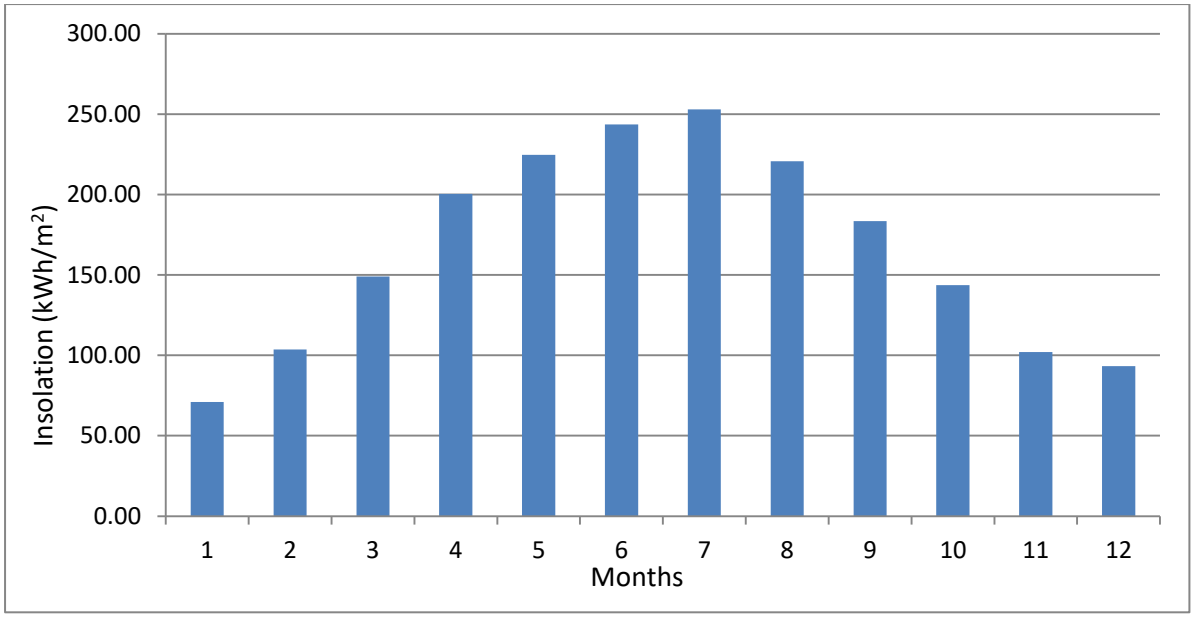

Figure 5.4: Average monthly Insolation (kWh/m^2) for the year 2022.

5.3.1.2 Energy losses

The array capture losses L_C emphasize the array's incapacity to completely exploit the available irradiance by representing losses brought on by array operation. And The energy lost during the inverters' conversion of DC power to AC power is reflected in the system loss, or L_S, which is represented by losses in system components. Both of those losses have been calculated using equations (4) and (5), respectively. Table (5.3) illustrates those results.

Table 5.3: Energy losses 2021, 2022.

Year	Y_A (kWh/kWp)	Y_F (kWh/kWp)	Y_R (kWh/kWp)	L_C (kWh/kWp/ year)	L_S (kWh/kWp/ year)
2021	1,965	1,902	2,038	73	63
2022	1920	1,867	1,989	69	53

Even though the system yields in 2021 are higher than the yields in 2022, it is noted that the energy losses in 2021 are higher than the energy losses in 2022, as indicated in Table 5.2.

5.3.1.3 PV system's efficiencies

The PV array efficiency, system installation efficiency, and inverter efficiency can be achieved by applying equations (6), (7), and (8), respectively. Table 5.4 illustrates the results of those technical parameters for the years 2021 and 2022, after having the required data related to the annual DC energy output, total annual AC energy output, and the total in-plane solar insolation, taking into consideration the total PV module surface area of 8438 m^2.

Table 5.4: PV system's efficiencies 2021, 2022.

Year	E_{DC} (kWh)	E_{AC} (kWh)	H_T (kWh/m2)	η_{PV} (%)	η_{sys} (%)	η_{INV} (%)
2021	3,050,044	2,952,045	2,038	17.7	17.2	96.8
2022	2,980,050	2,898,040	1,989	17.8	17.3	97.3

It's clearly noted from the above-listed results in Table 5.3 that the PV array efficiency, system installation efficiency, and inverter efficiency in the year 2022 are higher than the corresponding percentages in the year 2021. This result could be related to the energy losses since the year 2022 has lower energy losses than the year 2021.

5.3.1.4 Performance ratio

The performance ratio is computed using Equation (9), as the ratio of the PV system's final energy yield (Y_F) to its reference yield (Y_R). Table 5.5 illustrates the results of the average yearly performance ratio for the years 2021 and 2022, after having the required data that relates the final energy yield (Y_F) to its reference yield (Y_R).

Table 5.5: Performance ratio 2021, 2022.

Year	Y_F (kWh/kWp)	Y_R (kWh/kWp)	P_R (%)
2021	1,902	2,038	93
2022	1,867	1,989	94

It's also noted that the performance ratio in 2022 is higher than in 2021. The average performance ratio for both years 2021 and 2022 is represented in Figure 5.5.

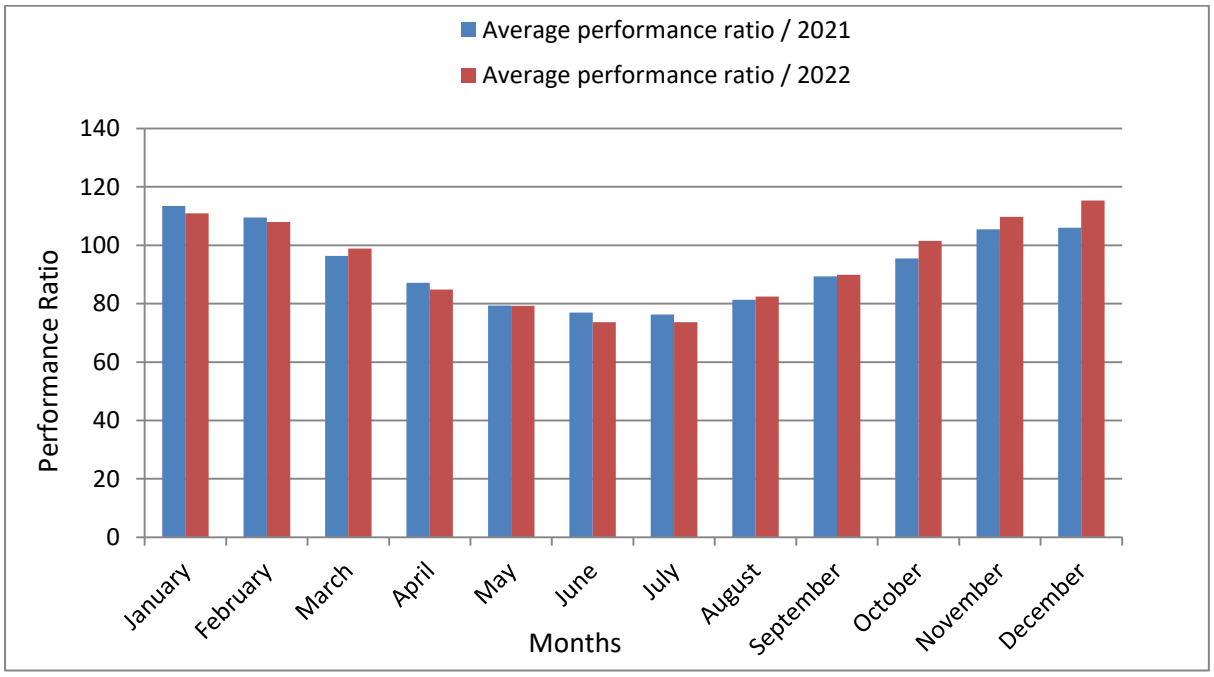

Figure 5.5: average performance ratio, 2021, 2022.

5.3.1.5 Capacity utilization factor

The capacity utilization factor (CUF) is computed according to equation (10), and the results of this technical parameter are listed in Table 5.6 for both years 2021 and 2022. Taking into consideration that the $P_{PV\ rated}$ is 1552 kWp.

Table 5.6: capacity utilization factor (CUF) 2021, 2022.

Year	E_{AC} (kWh)	CUF (%)
2021	2,952,045	21.7
2022	2,898,040	21.3

The overall performance indicators for the PV power plant have been illustrated in Tables 5.7 and 5.8 for both years 2021 and 2022, respectively. The monthly values for measured solar insolation, generated energy, system efficiency, performance ratio, and capacity utilization

factor have been listed as the most important indicators that help in the PV plant technical evaluation.

Table 5.7: performance indicators in 2021.

Month	Solar insolation (kWh/m^2)	Energy output (kWh)	System efficiency η_{sys} (%)	Performance Ratio (%)	Capacity utilization Factor (%)
January	88.05	183389.39	24.3	113	16.2
February	115.48	197055.88	19.9	110	17.4
March	157.35	231457.29	17.4	96	20.4
April	205.11	277209.06	16.0	87	24.5
May	240.24	302289.78	14.9	79	26.7
June	243.35	303119.26	14.8	77	26.8
July	237.88	293740.49	14.6	76	25.9
August	220.55	284922.10	15.3	81	25.1
September	182.46	252532.94	16.4	89	22.3
October	148.2	219435.20	17.5	95	19.4
November	114.2	178288.69	18.5	106	15.7
December	81.23	228604.95	33.3	106	20.2

Referring to the above-listed values, it is noted that the energy output in November is less than the energy output in December, despite the higher solar insolation in November than that recorded in December. This result may be explained by the effect of wind velocity and what may result in dust formation, which decreases the PV panel's energy generation and overall efficiency. It’s noted that the wind velocity in November is higher than the recorded one in December.

Table 5.8: performance indicators in 2022.

Month	Solar insolation (kWh/m^2)	Energy output (kWh)	System efficiency η_{sys} (%)	Performance Ratio (%)	Capacity utilization Factor (%)
January	71.03	162712.84	27.1	111	14.4
February	103.58	178509.52	20.4	108	15.8
March	149	233168.70	18.5	99	20.6
April	200.44	269060.51	15.9	85	23.7
May	224.63	288634.45	15.2	79	25.5
June	243.6	297085.66	14.4	74	26.2
July	253	313890.55	14.7	74	27.7

August	220.77	297485.84	16.0	82	26.3
September	183.49	267025.18	17.2	90	23.6
October	143.6	232371.42	19.2	102	20.5
November	101.96	181543.37	21.1	110	16.0
December	93.29	176552.17	22.4	115	15.6

5.3.1.6 Cell temperature effect

As the ambient temperature increases, the cell temperature also increases. Because when the cell temperature increases, the open-circuit voltage will decrease substantially while the short-circuit current increases only slightly. Thus, perhaps surprisingly, photovoltaics function better on clear, cool days than on hot ones. For crystalline silicon cells, the maximum power available decreases by roughly 0.5%, as V_{OC} decreases by roughly 0.37% and I_{SC} increases by roughly 0.05% with each degree Celsius of temperature increase.

By applying equation (11), the hourly cell temperature has been calculated over the years 2021 and 2022. One of the important parameters that affects PV efficiency is the cell temperature. The amount of generated power is inversely proportional to the cell temperature. The day cell temperature values have also been recorded for both the years 2021 and 2022. The hourly day cell temperature values for 8760 hours per year are represented in Figures 5.6 for the year 2021 and 5.7 for the year 2022.

As represented in the figures, it could be seen that the maximum recorded value of hourly day cell temperature is 60.42 C° at 12:00 noon on July 18th, and the average hourly day cell temperature is around 31 C° for the observed data in the year 2021. While the maximum recorded value of hourly day cell temperature is 62.38 C° at 13:00 afternoon on August 28th, and the average hourly day cell temperature is around 29.6 C° for the observed data in the year 2022, It's clearly seen that the average hourly cell temperature of the year 2022 decreases by 1.4 C° than the year 2021. Despite that, the maximum recorded value of hourly day cell temperature in the year 2022 increases by around 2 C° than the year 2021. This resulted in data affected by ambient weather conditions like wind speed, dust formation, and other conditions affecting the cell temperature behavior.

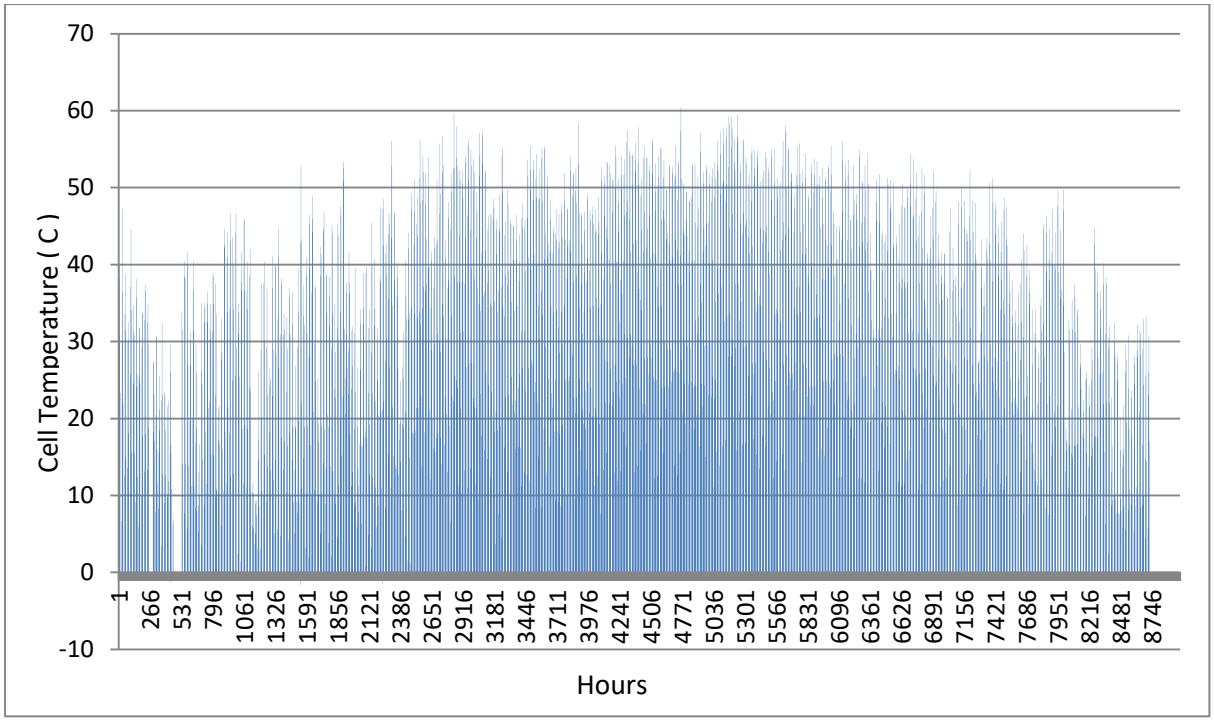

Figure 5.6: Hourly cell temperature (C°) for the year 2021.

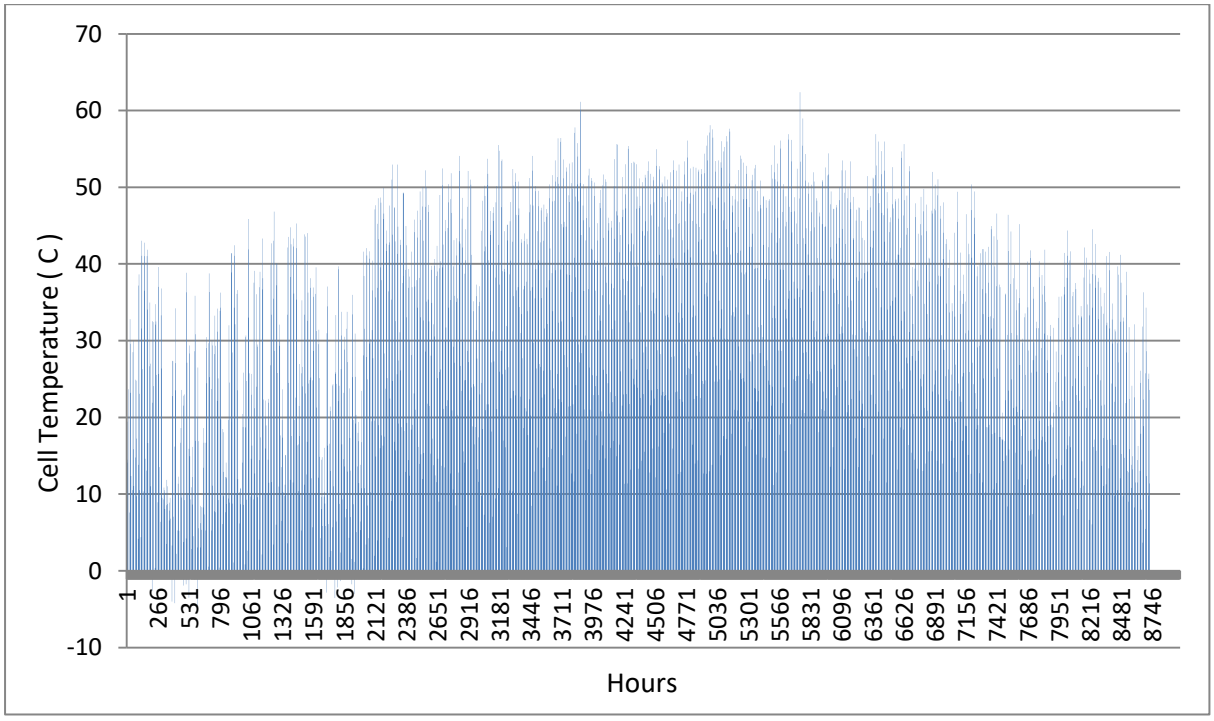

Figure 5.7: Hourly cell temperature (C°) for the year 2022.

In order to study the effect of ambient temperature on energy output, Tables 5.9 and 5.10 illustrate the average ambient temperature (C^o), average cell temperature (C^o), solar

insolation (kWh/m2), and energy output (kWh) along the months. Those data are for the years 2021 and 2022, respectively.

Table 5.9 Average ambient temperature, average cell temperature, solar Insolation and Energy output for the months of 2021.

Month	Average day Ambient Temperature (C ^{o})	Average day cell Temperature (C ^{o})	Solar insolation (kWh/m2)	Energy output (kWh)
January	15.09	21.52	88.05	183389.39
February	14.70	23.01	115.48	197055.88
March	15.56	23.79	157.35	231457.29
April	21.78	30.88	205.11	277209.06
May	25.97	35.03	240.24	302289.78
June	25.98	34.62	243.35	303119.26
July	28.68	37.58	237.88	293740.49
August	29.69	38.96	220.55	284922.10
September	26.62	36.03	182.46	252532.94
October	23.91	32.13	148.2	219435.20
November	21.48	29.08	114.2	178288.69
December	14.55	20.30	81.23	228604.95

From the above table, it could be noticed that the higher the ambient temperature in July and August, the higher the cell temperature overall in those months, which represents an inverse impact on solar insolation as well as energy output.

Table 5.10 Average ambient temperature, average cell temperature, solar Insolation and Energy output for the months of 2022.

Month	Average day Ambient Temperature (C ^{o})	Average day cell Temperature (C ^{o})	Solar insolation (kWh/m2)	Energy output (kWh)
January	10.54	16.98	71.03	162712.84
February	12.70	20.55	103.58	178509.52
March	12.30	19.99	149	233168.70
April	22.42	31.16	200.44	269060.51
May	23.84	32.55	224.63	288634.45
June	26.44	35.65	243.6	297085.66
July	27.71	36.44	253	313890.55
August	28.78	37.41	220.77	297485.84
September	27.66	36.12	183.49	267025.18
October	23.93	31.91	143.6	232371.42
November	18.86	24.94	101.96	181543.37
December	16.30	23.52	93.29	176552.17

From the above table, it could be noticed that the higher the ambient temperature in August, the higher the cell temperature overall over the months, which represents an inverse impact on solar insolation as well as energy output.

5.3.2 Economic PV system analysis

5.3.2.1 Net present value

The net present value will be calculated depending on equation (13), if we know that the investment cost of the PV power plant equals $11,339,057 preVAT, the selvage value equals $150,000 at the end of the life cycle, and the replacement cost of the sixteen inverters equals $444,800 (10th year). The selling price has been assumed to be 9.5 cents per kW preVAT. by multiplying this price with the generated energy in the first year 2021, which leads to a total income of $280,444.275, but this value will not be the same in the future depending on the economic behavior and currency values based on the fundamental rule that says "money now

is more valuable than money later on," which leads to dealing with the concept of net present value. NPV, beginning from the first year of production and celling income, the value of $280,000 will not remain the same value along the project period, so the present value for each year will be calculated as mentioned in equation (12) with an interest rate of 0.07; Table 5.11 represents the present value for each year of the project period over 20 years.

Table 5.11 Present Value of the income for each year of the project period.

year	Present value ($)	year	Present value ($)
2021	261,682	2031	133,026
2022	244,563	2032	124,323
2023	228,563	2033	116,190
2024	213,611	2034	108,589
2025	199,636	2035	101,485
2026	186,576	2036	94,846
2027	174,370	2037	88,641
2028	162,963	2038	82,842
2029	152,301	2039	77,422
2030	142,338	2040	72,357

The values of gross income obtained from sold-generated electricity, which are represented in Table 5.11, will be used to calculate the net income for each year after discounting the annual payment for the loan. When dividing the loan value by the loan period of 20 years, the annual payment for the loan will be $66,953. Table 5.12 indicates the net income for each year.

Table 5.12: Net Income for each year of the project period.

year	Net Income ($)	year	Net Income ($)
2021	194,729	2031	66,073
2022	177,610	2032	57,370
2023	161,610	2033	49,237
2024	146,658	2034	41,636
2025	132,683	2035	34,532
2026	119,623	2036	27,893
2027	107,417	2037	21,688
2028	96,010	2038	15,889
2029	85,348	2039	10,469
2030	30,585	2040	155,404

It is noticed that the year 2030 has a net income of $30,585 generated from the extra payment that will be paid for the replacement of the sixteen inverters, which equals $444,800 at the end of the 10 years of installation. And also, notice that the year 2040 has a net income of $155,404, which was achieved by adding the selvage value, which equals $150,000 at the end-of-life cycle.

The total paid costs for all project's periods are $1,383,857, which include the initial investment cost and the cost of replacing the sixteen inverters. As well, the total income for all project's periods is $3,116,324, including the selvage value. Which means the net income for this project over the next twenty years is $1,732,467, which indicates a good and feasible investment.

5.3.2.2 Simple payback period

A simple payback period will be calculated depending on equation (14), if we know that the investment cost of the PV power plant equals $11,339,057 preVAT and the replacement cost of the sixteen inverters equals $444,800 (10th year). As well, the selling price has been assumed to be 9.5 cents per kW preVAT. By multiplying this price with the generated energy in 2021, the total income will be $280,444.275, and for the year 2022, it will be $275,313.8, which leads to calculating the simple payback period for both years by dividing the total investment cost by the yearly income. The simple payback period is 4.78 years and 4.86 years for the years 2021 and 2022, respectively, depending on the generated energy for each year, as represented in Table 5.13.

Table 5.13: PV system yearly Simple Payback Period

Year	**2021**	**2022**
Total investment coast ($)	1,339,057	1,339,057
Yearly income ($)	280,444.275	275,313.8
Simple payback period (years)	4.78	4.86

As a result, the simple payback period on average is 4.82 years. This indicates that the project is feasible because all project costs will be reimbursed over the first five years of its lifetime, and it will turn a profit throughout the remaining fifteen.

5.4 Plant location optimization utilizing PSO

Finding the PV power plant optimum location with the least amount of power loss combined with a good voltage profile and voltage harmonic distortion is the best way to decrease the power losses in the grid while saving money. Al Dhahriya Single Line Diagram SLD has been examined in order to determine the number of transformers, their loads, and their impedance in order to accomplish this purpose. together with the type, length, and impedance of the power distribution cables that are being used. All the required data has been entered into the MATLAB software in order to achieve this purpose. A set of verified equations no. (15), (16), (17), (18), (19), and (20) that have been delivered based on PSO method theory have been used to determine the real power loss in the grid as well as study the bus voltage profile.

5.4.1 Real power losses evaluation

Utilizing the PSO method principle, the real power losses in Al Dhahriya grid have been studied for five different scenarios. The first scenario is the evaluation of the real power losses in Al Dhahriya grid without any Distribution Generation (DG) plant, in other words, without a PV power plant connected to the grid. This scenario indicates 896 kW of real power losses in the grid.

The second scenario is the evaluation of the real power losses in the Al Dhahriya grid with the current grid situation of one DG plant named Wahaj Al Ghuzlan in its current location. This scenario indicates 857 kW of real power losses in the grid.

The other three scenarios aim to get the minimum real power losses at the grid by assuming connecting one DG, two DGs, and three DGs for scenarios 3, 4, and 5, respectively. In order to get the best values, one hundred iterations have been applied in the MATLAP analysis. Table 5.14 indicates the real power losses in kW for scenarios 3, 4, and 5 for the one hundred iterations. Taking into consideration the initial real power losses in the grid without any DG, the value is 896 kW, and from this value, the iterations will start achieving new values of real power losses depending on the number of assumed DGs.

Table 5.14: Real Power Losses (kW)

Iteration	Real Power Losses (kW)			Iteration	Real Power Losses (kW)		
	Scenario 3 (1 DG)	Scenario 4 (2 DGs)	Scenario 5 (3 DGs)		Scenario 3 (1 DG)	Scenario 4 (2 DGs)	Scenario 5 (3 DGs)
1	706.22	621.46	566.87	51	672.59	543.94	455.97
2	676.15	618.37	566.87	52	672.59	543.94	455.97
3	676.15	612.49	566.87	53	672.59	543.94	455.97
4	676.15	588.94	533.64	54	672.59	543.94	455.97
5	676.15	566.15	531.74	55	672.59	543.94	455.97
6	674.66	566.15	500.86	56	672.59	543.94	455.97
7	674.54	566.15	499.77	57	672.59	543.94	455.97
8	674.54	564.5	499.77	58	672.59	543.94	455.97
9	674.36	562.64	498.15	59	672.59	543.94	455.97
10	674.36	559.16	498.15	60	672.59	543.94	455.97
11	672.69	559.16	498.15	61	672.59	543.94	455.97
12	672.61	553.64	497.68	62	672.59	543.94	455.97
13	672.61	547.14	490.17	63	672.59	543.94	455.97
14	672.61	547.14	489.37	64	672.59	543.94	455.97
15	672.61	547.14	487.77	65	672.59	543.94	455.97
16	672.61	547.11	484.92	66	672.59	543.94	455.97
17	672.61	546.09	484.92	67	672.59	543.94	455.97
18	672.59	545.92	484.92	8	672.59	543.94	455.97
19	672.59	544.87	482.03	69	672.59	543.94	455.97
20	672.59	544.63	482.03	70	672.59	543.94	455.97
21	672.59	543.97	480.4	71	672.59	543.94	455.97
22	672.59	543.97	477.15	72	672.59	543.94	455.97
23	672.59	543.97	473.18	73	672.59	543.94	455.97
24	672.59	543.94	466.49	74	672.59	543.94	455.97
25	672.59	543.94	463.97	75	672.59	543.94	455.97
26	672.59	543.94	461.43	76	672.59	543.94	455.97
27	672.59	543.94	460.76	77	672.59	543.94	455.97
28	672.59	543.94	460.76	78	672.59	543.94	455.97
29	672.59	543.94	460.04	79	672.59	543.94	455.97
30	672.59	543.94	459.12	80	672.59	543.94	455.97
31	672.59	543.94	458.87	81	672.59	543.94	455.97
32	672.59	543.94	457.19	82	672.59	543.94	455.97
33	672.59	543.94	456.79	83	672.59	543.94	455.97
34	672.59	543.94	456.55	84	672.59	543.94	455.97
35	672.59	543.94	456.1	85	672.59	543.94	455.97
36	672.59	543.94	456.01	86	672.59	543.94	455.97
37	672.59	543.94	455.98	87	672.59	543.94	455.97
38	672.59	543.94	455.98	88	672.59	543.94	455.97
39	672.59	543.94	455.98	89	672.59	543.94	455.97
40	672.59	543.94	455.97	90	672.59	543.94	455.97

41	672.59	543.94	455.97	91	672.59	543.94	455.97
42	672.59	543.94	455.97	92	672.59	543.94	455.97
43	672.59	543.94	455.97	93	672.59	543.94	455.97
44	672.59	543.94	455.97	94	672.59	543.94	455.97
45	672.59	543.94	455.97	95	672.59	543.94	455.97
46	672.59	543.94	455.97	96	672.59	543.94	455.97
47	672.59	543.94	455.97	97	672.59	543.94	455.97
48	672.59	543.94	455.97	98	672.59	543.94	455.97
49	672.59	543.94	455.97	99	672.59	543.94	455.97
50	672.59	543.94	455.97	**100**	**672.59**	**543.94**	**455.97**

The final value of real power losses for each scenario has been achieved: 672.59 kW of real power losses for scenario 3 when connecting a 1 DG to the grid, 543.94 kW of real power losses for scenario 4 when connecting a 2 DG to the grid, and 455.97 kW of real power losses for scenario 5 when connecting a 3 DG to the grid. Figure 5.8 indicates the real power losses in kW for scenarios 3, 4, and 5 with the one hundred selected iterations that are illustrated in Table 5.14.

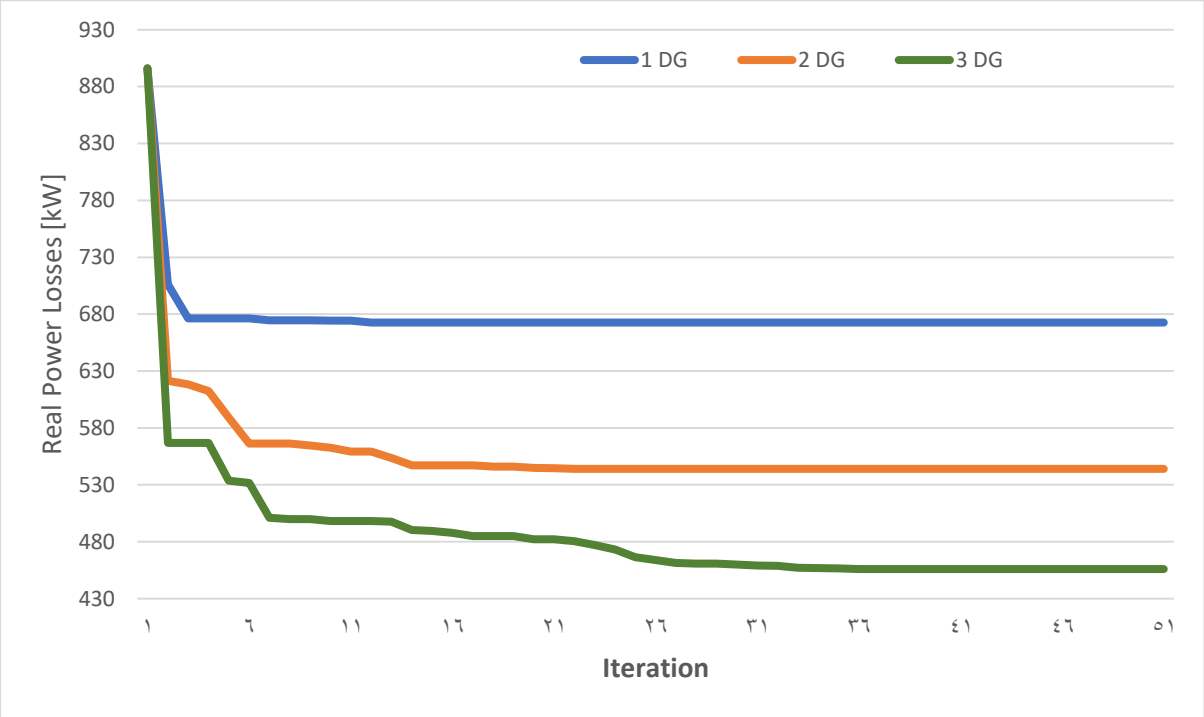

Figure 5.8: Real power losses (kW) for assumed 1 DG, 2 DGs, and 3 DGs.

As seen in Figure 5.8, it's clearly noticed that most of the values of real power losses for the three scenarios have become constant at iteration equals up to 40 iterations, but the values have been taken and studied in the case of applying 100 iterations in order to ensure the final value of real power losses. It is noticeable that while using more DGs, the real power losses

will decrease, which could be explained by the effect of the energy generation that is supplied to the grid from those new DGs, which prevents the current from traveling for long distances in the distribution cables, which leads to less real power losses.

The PSO method analysis through MATLAB hasn't only provided the magnitude of the minimal real power losses in the grid for the studied scenarios, but also the optimal location of the DGs for all scenarios that could be adapted by connecting them to the grid in order to obtain the minimum real power losses. Table 5.15 illustrates the DG's capacity, optimal location, and corresponding real power losses in the grid for the studied scenarios.

Table 5.15: DG's capacity, and location, grid real power losses.

scenario	**No. of DGs**	**Real power losses (kW)**	**DG capacity (MW)**	**Optimal location on bus diagram**	
				Load no.	**Corresponding bus no.**
3	**1 DG**	672.6	2.19	83	39
4	**2 DGs**	544	1.76	77	33
			1.7	83	39
5	**3 DGs**	456	1.49	77	33
			1.46	83	39
			1.5	72	28

Figures 5.9, 5.10, and 5.11 represents the optimal location of DGs (PV power plants) on bus diagram for the scenarios 3, 4, and 5 respectively.

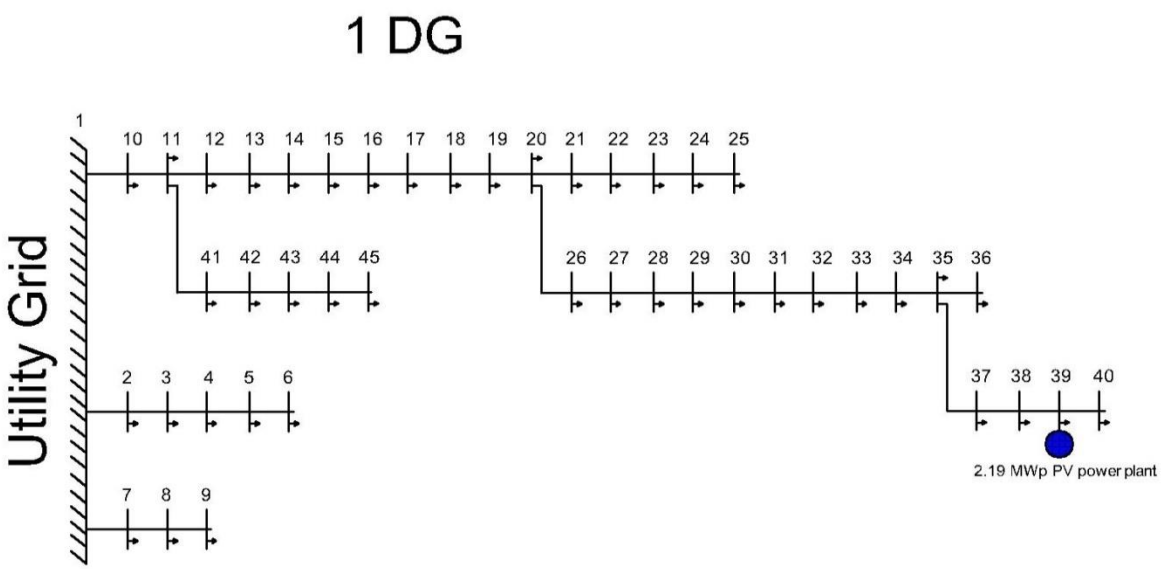

Figure 5.9: Optimal location of PV power plant – scenario 3: 1 DG

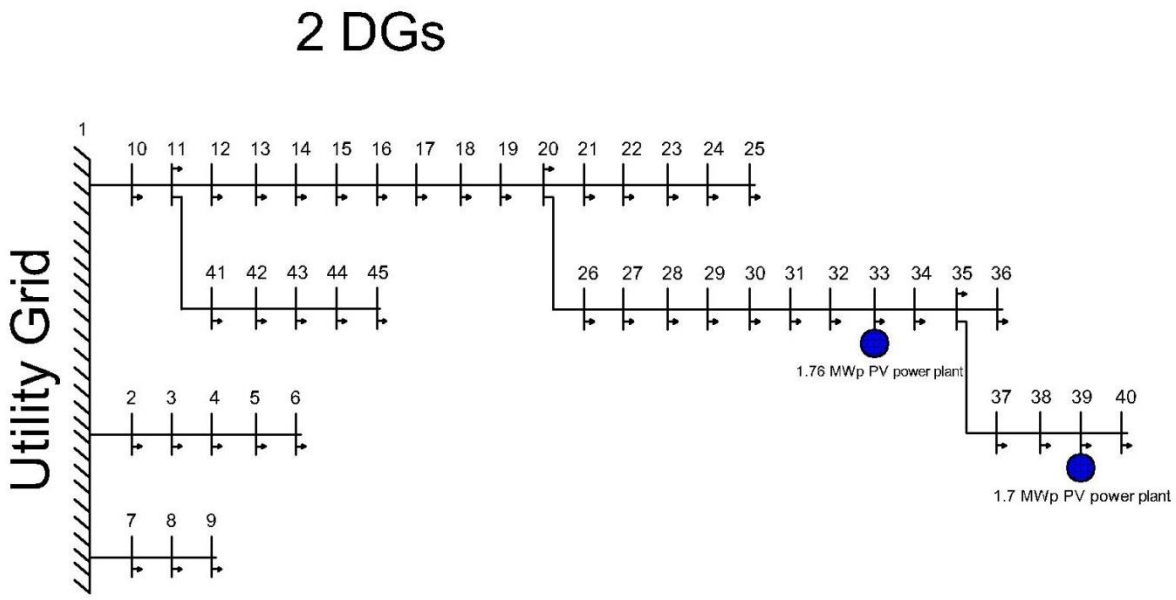

Figure 5.10: Optimal location of PV power plants – scenario 4: 2 DGs

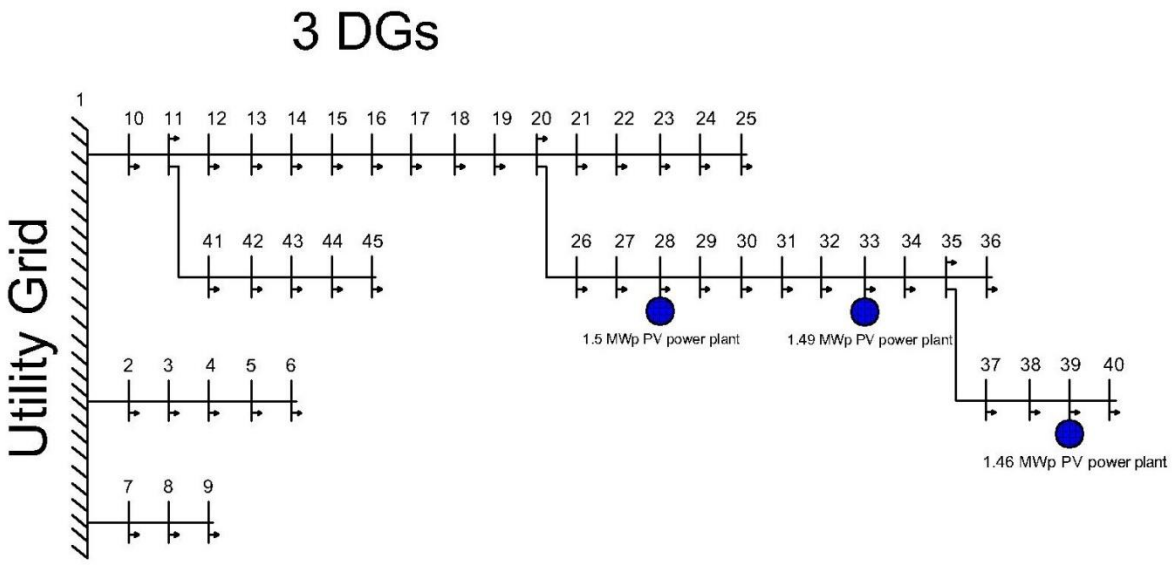

Figure 5.11: Optimal location of PV power plants – scenario 5: 3 DGs

As represented in Figures 5.9, 5.10, and 5.11, it appears that the optimal locations for all the proposed DGs for all scenarios are located at the furthest points from the main electricity feeding point in the grid. This is a logic result since the furthest load from the feeding point is the higher real power losses contributed with the longest paths that the current flows, which could be minimized by installing those DGs mostly near those furthest loads.

When studying scenario 2, which represents the current grid situation that is connected to one DG plant with a 1.5 MW capacity named Wahaj Al Ghuzlan in its current location at load no. 67, which corresponds to bus no. 23 as represented in Figure 5.12, this scenario indicates 857 kW of real power losses in the grid. By comparing this value with scenario 3, which also proposed one DG but in a different location with 672.6 kW of real power loss, it is seen that there is a saving in real power losses of about 180 kW in scenario 3 compared to what was achieved at the current location of the Wahaj Al Ghuzlan power plant. That means the current PV power plant location is not optimal when talking about the real power losses.

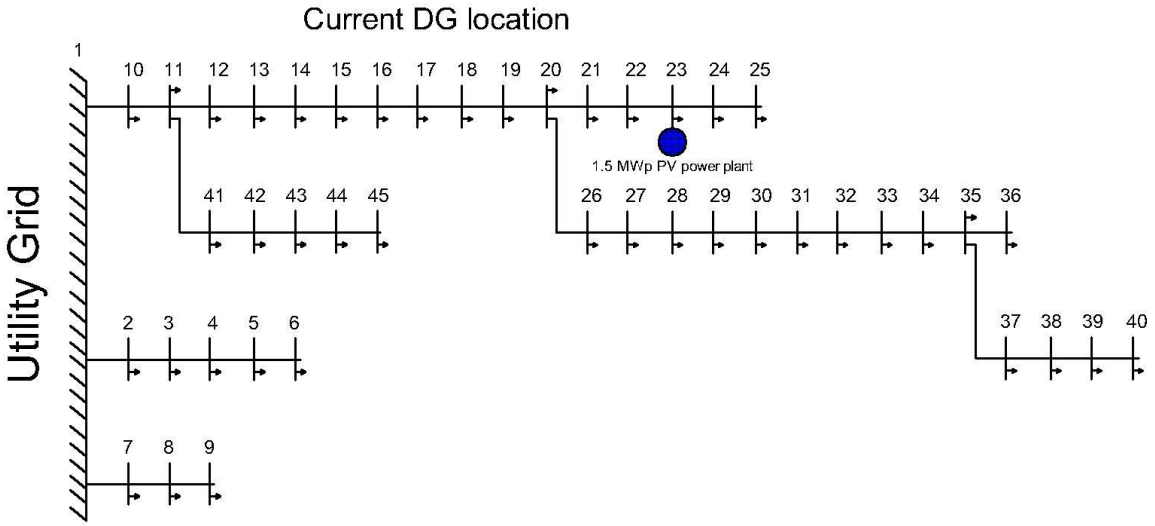

Figure 5.12: current location of Wahaj Al Ghuzlan PV power plants

In order to ensure the ability to apply the suggested scenarios, the location maps of the proposed new DGs have been achieved. Figures 5.13, 5.14, and 5.15 represent the locations of the buses: bus no. 28 (Jamooq), bus no. 33 (Doma Hospital), and bus no. 39 (Al Jebrini), respectively. It is clearly evident that all the suggested DG locations are appropriate for installing the new DGs due to the availability of the wide lands and suitable topography. Although bus 39 (Al Jebrini) is the most appropriate location for installing new DGs because of the availability of large areas without buildings and the furthest bus on the grid from the studied scenarios, which leads to minimal power losses,.

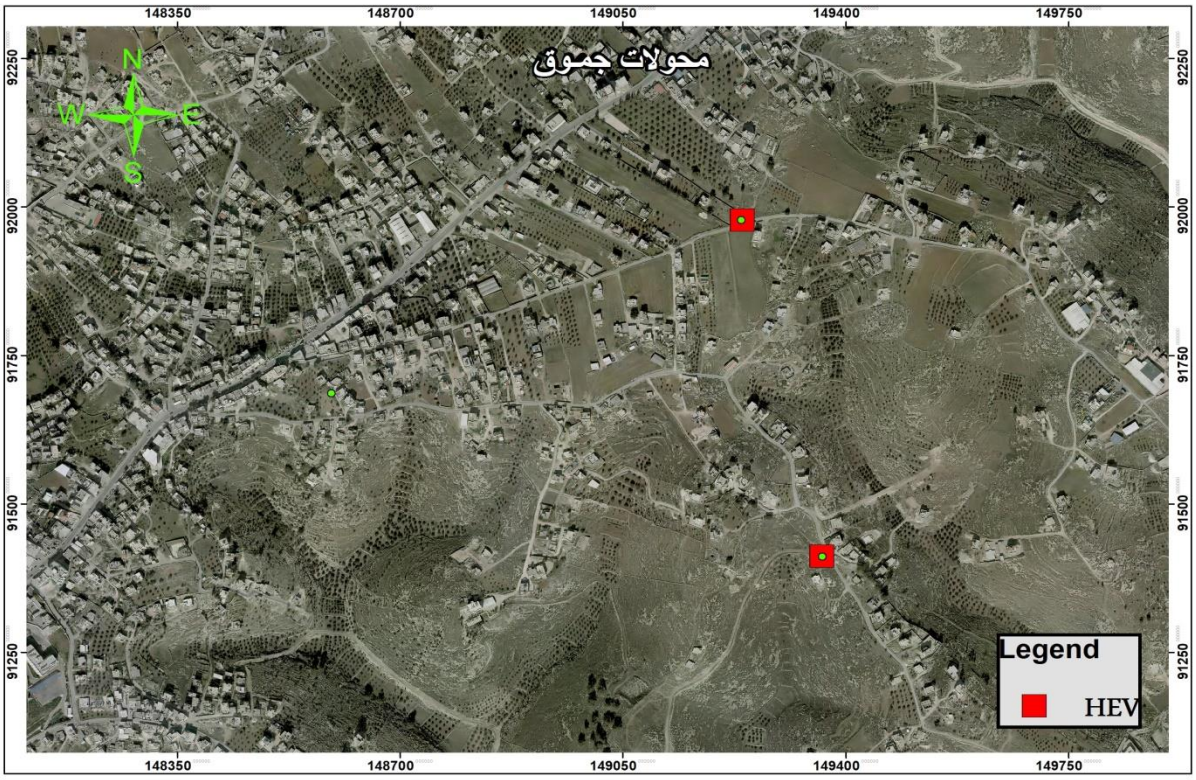

Figure 5.13: Bus 28 (Jamooq) site location.

Figure 5.14: Bus 33(Doma Hospital) site location.

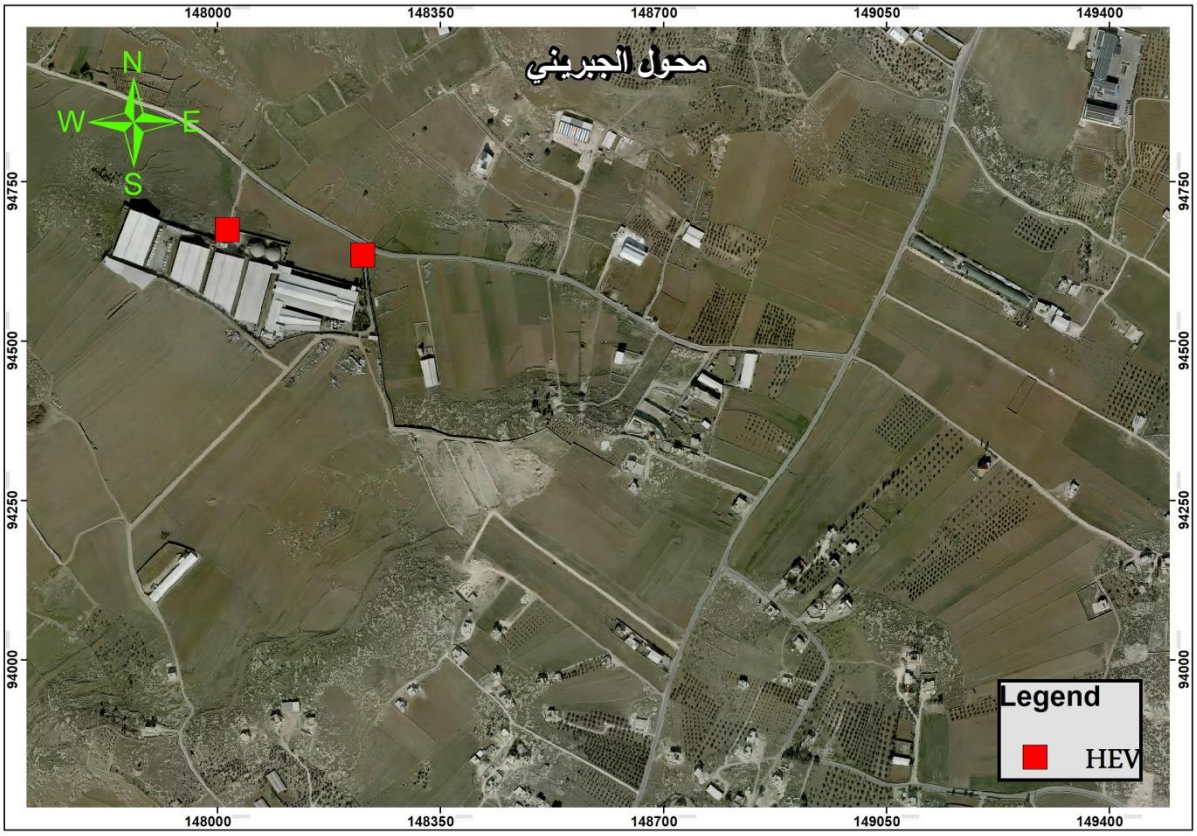

Figure 5.15: Bus 39 (Al Jebrini) site location.

Since the financial impact of real power losses is valuable, it should be taken into consideration in order to minimize these losses to the minimum level. Table 5.16 illustrates the financial side of real power losses, taking into account the local price of electricity at $0.17 per kWh.

Table 5.16 financial losses associated with grid real power losses.

scenario	No. of DGs	Real power losses (kW)	Energy losses (kWh) per year	Financial losses ($ / Year)
1	**without**	896	7,848,960	1,334,323
2	**Current situation 1DG**	857	7,507,320	1,276,244
3	**1 DG**	672.6	5,891,976	1,001,636

4	**2 DGs**	544	4,765,440	810,125
5	**3 DGs**	456	3,994,560	679,075

Referring to the calculated values of the financial losses associated with real power losses in the grid listed in Table 5.16, it is possible to notice the positive impact of the optimal location of DG on minimizing the financial losses related to real power losses.

5.4.2 Voltage profile

Installing a new PV power plant has not only affected the real power losses, but it has also contributed to the improvement of the voltage profile along the electricity grid. In this study, the voltage profile of the grid buses has been studied for the proposed new four scenarios. Table 5.17 indicates the voltage profile per unit (PU) voltage along grid buses for scenarios 2, 3, 4, and 5.

Table 5.17: Bus voltage profile.

Bus no.	Voltage profile (PU)				Bus no.	Voltage profile (PU)			
	Scenario 2 without (DG)	Scenario 3 (1 DG)	Scenario 4 (2 DGs)	Scenario 5 (3 DGs)		Scenario 2 without (DG)	Scenario 3 (1 DG)	Scenario 4 (2 DGs)	Scenario 5 (3 DGs)
1	1	1	1	1	46	0.97	0.97	0.97	0.97
2	1	1	1	1	47	0.97	0.97	0.97	0.97
3	1	1	1	1	48	0.97	0.97	0.97	0.97
4	1	1	1	1	49	0.97	0.97	0.97	0.97
5	1	1	1	1	50	0.97	0.97	0.97	0.97
6	1	1	1	1	51	0.97	0.97	0.97	0.97
7	1	1	1	1	52	0.97	0.97	0.97	0.97
8	1	1	1	1	53	0.97	0.97	0.97	0.97
9	1	1	1	1	54	0.97	0.97	0.97	0.97
10	1	1	1	1	55	0.96	0.96	0.96	0.96

11	0.99	0.99	0.99	0.99	56	0.95	0.95	0.95	0.96
12	0.98	0.98	0.99	0.99	57	0.93	0.94	0.94	0.95
13	0.97	0.97	0.98	0.98	58	0.93	0.94	0.94	0.95
14	0.97	0.97	0.98	0.98	59	0.93	0.94	0.94	0.94
15	0.96	0.97	0.97	0.98	60	0.93	0.94	0.94	0.94
16	0.96	0.97	0.97	0.98	61	0.92	0.93	0.94	0.94
17	0.96	0.97	0.97	0.98	62	0.93	0.93	0.94	0.94
18	0.96	0.97	0.97	0.97	63	0.92	0.93	0.93	0.94
19	0.95	0.96	0.97	0.97	64	0.91	0.92	0.93	0.94
20	0.95	0.96	0.97	0.97	65	0.91	0.92	0.93	0.94
21	0.95	0.96	0.97	0.97	66	0.91	0.92	0.93	0.94
22	0.95	0.96	0.96	0.97	67	0.91	0.93	0.93	0.94
23	0.95	0.96	0.96	0.97	68	0.91	0.92	0.93	0.94
24	0.95	0.96	0.96	0.97	69	0.91	0.92	0.93	0.94
25	0.95	0.96	0.96	0.97	70	0.91	0.92	0.93	0.93
26	0.95	0.96	0.96	0.97	71	0.91	0.92	0.93	0.93
27	0.94	0.95	0.96	0.97	72	0.9	0.92	0.93	1
28	0.94	0.95	0.96	0.97	73	0.9	0.92	0.93	0.94
29	0.94	0.95	0.96	0.97	74	0.9	0.92	0.93	0.93
30	0.94	0.95	0.96	0.97	75	0.9	0.92	0.93	0.94
31	0.94	0.95	0.96	0.97	76	0.9	0.92	0.93	0.93
32	0.93	0.95	0.96	0.97	77	0.9	0.91	1	1
33	0.93	0.95	0.96	0.97	78	0.9	0.92	0.93	0.93
34	0.93	0.95	0.96	0.97	79	0.9	0.92	0.93	0.93
35	0.93	0.95	0.96	0.97	80	0.9	0.92	0.93	0.93
36	0.93	0.95	0.96	0.97	81	0.9	0.92	0.93	0.93
37	0.93	0.95	0.96	0.97	82	0.9	0.92	0.93	0.93
38	0.93	0.95	0.96	0.97	83	0.89	0.99	1	1
39	0.93	0.95	0.96	0.97	84	0.89	0.92	0.93	0.93
40	0.93	0.95	0.96	0.97	85	0.96	0.96	0.96	0.96
41	0.99	0.99	0.99	0.99	86	0.95	0.96	0.96	0.96
42	0.99	0.99	0.99	0.99	87	0.96	0.96	0.96	0.96
43	0.99	0.99	0.99	0.99	88	0.96	0.96	0.96	0.96
44	0.99	0.99	0.99	0.99	89	0.96	0.96	0.96	0.96
45	0.99	0.99	0.99	0.99	**Min**	**0.89**	**0.91**	**0.93**	**0.93**

Referring to the illustrated values of bus per unit voltage in Table 5.17, it is evident that the bus voltage profile has been improved; the minimum per unit voltage profile was 0.89 for the

scenario without DG; when installing a 1DG, the per unit voltage profile became 0.91; and when installing 2DGs or 3DGs, the per unit voltage profile became 0.93, which indicates a considerable voltage profile improvement. Figure 5.16 represents the voltage profile improvement of the studied scenarios for all grid buses.

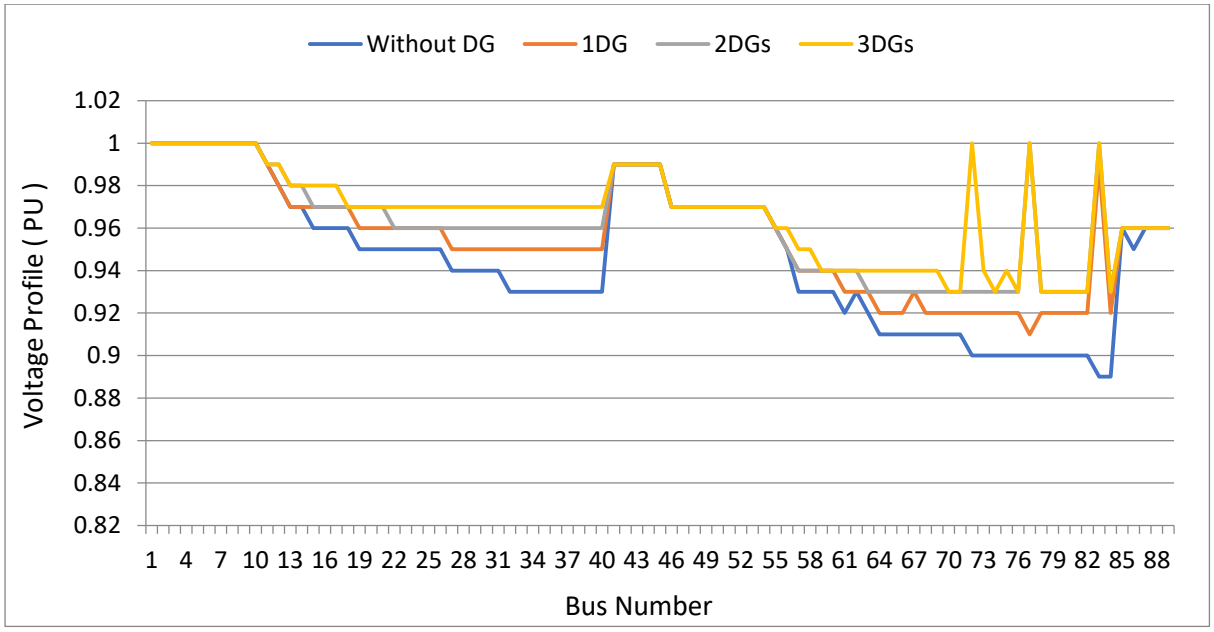

Figure 5.16: Bus voltage profile (PU)

Chapter 6

Conclusion and Remarks

6.1 Summary

Determine the viability and feasibility of such renewable energy projects; one of the most important steps is the techno-economic assessment of a solar power plant. Stakeholders can make educated decisions that significantly affect energy generation, environmental sustainability, and financial returns by carefully analyzing the technical and economic elements of the building and operation of these facilities.

Thorough techno-economic analysis aids in identifying possible obstacles, improving project design, and guaranteeing that photovoltaic power plants contribute significantly to the shift towards a cleaner, more sustainable energy future. These evaluations must be given top priority by legislators and private investors in order to support solar energy's continuous expansion and to help create a more sustainable and economically viable energy landscape.

In this study, in the case of the techno-economic assessment of the photovoltaic power plant, the data related to the climate and the circumstances surrounding two years of continuous readings have been achieved on the basis of hourly readings; those data have been analyzed on the basis of daily, monthly, and annual data that are required for the techno-economic assessment through a set of specified equations.

A group of technical parameters and other economic parameters have been analyzed, and the measured energy output for both years has been compared with the expected values that have been achieved from the system simulation on the PVsyst software. One of the most important technical parameters is the final yield. When compared to other MENA countries, the studied final energy yields for 2021 and 2022, which are 1902 kWh/kW_p and 1867 kWh/kW_p, respectively, can be deemed reasonable values.

This study highlights the direct effect of the ambient temperature on the cell temperature, which affects energy production in an inverse proportion. According to this study, the simple payback period on average is 4.82 years. This indicates that the project is feasible because all project costs will be reimbursed over the first five years of its lifetime, and it will turn a profit throughout the remaining fifteen.

This study has also discussed the most suitable location of the Wahaj Al Ghuzlan photovoltaic power plant at Al Dhahriya electricity grid on the basis of the least power losses. In order to achieve this goal, the distribution transformer's location, loads, and impedance have been collected, as well as the type, length, resistance, and reactance of the distribution cables. The obtained data, along with the transformer locations that appear on the single-line diagram, have been entered into the MATLAB software in order to indicate the most appropriate PV power plant location depending on a set of equations. The analysis process indicates that the optimal locations for all the proposed DGs for all scenarios are located at the furthest points from the main electricity feeding point in the grid. When connecting a 1 DG, the optimal location of the PV plant on the bus diagram is on bus no. 39, and in the connection of 2 DGs, the optimal locations are on bus 39 and bus 33, while in the connection of 3 DGs, the optimal locations for those PV power plants are on bus 39, bus 33, and bus 28. Those locations are associated with the minimum real power losses in the grid as well as the most improved voltage profile.

It's concluded that the PSO method is an effective principle for the assessment of the studied aspects since it provides an accurate result. The optimal location of the studied PV power plant has been achieved within a few iterations, which makes PSO a very effective procedure in power system applications. The installation of PV power plants on the electricity grid does not only reduce the dependency on conventional energy resources, but it also reduces the real power losses in the grid, which contributes to the reduction of the financial losses associated with the grid power losses as well as the achievement of an improved grid voltage profile.

6.2 Recommendations

The photovoltaic power plant is a good way to supply electricity and lower the cost of electric energy, as this argument makes clear. This technology also aids in lowering pollution emissions and managing global warming.

Solar energy is not only economical but also ecologically benign. Compared to conventional fossil fuel power plants, solar power plants have comparatively low operating costs once they are up and running. This economic viability may eventually result in decreased energy costs for customers, bringing down the cost of electricity for homes and businesses, which is a promising and feasible investment.

Building photovoltaic power plants encourages energy independence on a number of fronts. Individuals can lessen their dependency on conventional power systems by installing solar panels to produce their own electricity for use in their homes and businesses. Globally speaking, nations can reduce their reliance on imported fossil fuels by boosting solar energy output. Consequently, this improves energy security and lessens susceptibility to changes in the world energy markets.

When investors or decision-makers are studying the connection of new PV power plants to the Al Dhahriya grid, it is recommended that they connect those PV power plants at the optimal locations that have been selected in this study. This will offer low real power losses in the grid and provide an improved voltage profile.

References:

[1] Al-Ghussain L, Samu R, Taylan O, Fahrioglu M. Techno-economic comparative analysis of renewable energy systems: case study in Zimbabwe, n.d. 10.3390/ inventions5030027.

[2] Abdin Z, M´erida W. Hybrid energy systems for off-grid power supply and hydrogen production based on renewable energy: a techno-economic analysis. Energy Convers Manag 2019;196:1068–79. https://doi.org/10.1016/j. enconman.2019.06.068.

[3] Edalati S, Ameri M, Iranmanesh M, Sadeghi Z. Solar photovoltaic power plants in five top oil-producing countries in Middle East: a case study in Iran. Renew Sustain Energy Rev 2017;69:1271–80. https://doi.org/10.1016/j.rser.2016.12.042.

[4] Gielen, D., Boshell, F., Saygin, D., Bazilian, M.D., Wagner, N. and Gorini, R. (2019) The Role of Renewable Energy in the Global Energy Transformation. Energy Strategy Reviews , 24, 38-50. https://doi.org/10.1016/j.esr.2019.01.006

[5] Alsamamra, H., and Shoqier, J. (2020) Assessment of Wind Power Potential at Eastern-Jerusalem, Palestine. Open Journal of Energy Efficiency , 9, 131-149. https://doi.org/10.4236/ojee.2020.94009

[6] Juaidi, A., Montoya, F.G., Ibrik, I.H. and Manzano-Agugliaro, F., 2016. An overview of renewable energy potential in Palestine. *Renewable and Sustainable Energy Reviews, 65*, pp.943-960.

[7] Alsamamra, H., Isaila, I. and Shoqeir, J. (2021) Promoting Energy Efficiency in the Palestinian Municipalities: A Case Study of Al-Dahriya Municipality. Smart Grid and Renewable Energy, 12, 17-29. https://doi.org/10.4236/sgre.2021.122002

[8] Mason, M., & Mor, A. (2009). Renewable energy in the Middle East enhancing security through Regional Cooperation (pp. 71–89). Dordrecht: Springer. Chapter 5: Energy Profile and the Potential of Renewable Energy Sources in Palestine.

[9] Thomason, Richmond, "Logic and Artificial Intelligence", *The Stanford Encyclopedia of Philosophy* (Summer 2020 Edition), Edward N. Zalta (ed.), URL = <https://plato.stanford.edu/archives/sum2020/entries/logic-ai/>.

[10] J. A. Momoh, ‘‘Smart grid design for efficient and flexible power networks operation and control,’’ in Proc. IEEE/PES Power Syst. Conf. Expo., Mar. 2009, pp. 1–8.

[11] Kuzlu, M., Cali, U., Sharma, V., & Güler, Ö. (2020). Gaining insight into solar photovoltaic power generation forecasting utilizing explainable artificial intelligence tools. *IEEE Access*, *8*, 187814-187823.

[12] Elsheikh, A. H., & Abd Elaziz, M. (2019). Review on applications of particle swarm optimization in solar energy systems. *International Journal of Environmental Science and Technology*, *16*, 1159-1170.

[13] Huda Albisher, Husain Alsamamra. An Overview of Wind Energy Potentials in Palestine. *Journal of Energy and Natural Resources.* Vol. 8, No. 3, 2019, pp. 98-108. doi: 10.11648/j.jenr.20190803.11

[14] González, P., Romero-Cadaval, E., González, E. and Guerrero, M.A., 2011, February. Impact of grid connected photovoltaic system in the power quality of a distribution network. In Doctoral Conference on Computing, Electrical and Industrial Systems (pp. 466-473). Springer, Berlin, Heidelberg.

[15] Swanson RM. Approaching the 29% limit efficiency of silicon solar cells. In: Proceedings of the photovoltaic specialists conference 2005, conference record of the thirty-first IEEE; 2005. p. 889–94.

[16] Steven Bushong. Advantages and disadvantages of a solar tracker system. Sol Power World 2016.

[17] Muneer T, Asif M. Generation and transmission prospects for solar electricity: UK and global markets. Energy Convers Manag 2003;44:35–52.

[18] Jayakumar, P. (2009) Resource Assessment Handbook. Asia and Pacific Center for Transfer of Technology of the United Nations, Economic and Social Commission

for Asia and the Pacific (ESCAP).

[19] Photovoltaic Effect. Mrsolar.com. Retrieved 12 December 2010. ⟨https://www. scribd.com/document/251085129/Photovoltaics⟩.

[20] Afzaal Mohammad, O'Brien Paul. Recent developments in II–VI and III–VI semiconductors and their applications in solar cells. J Mater Chem 2006:17.

[21] Ibrik, I.H. and Mahmoud, M.M. (2005) Energy Efficiency Improvement Procedures and Audit Results of Electrical, Thermal and Solar Applications in Palestine. Energy Policy , 33, 651-658. https://doi.org/10.1016/j.enpol.2003.09.008

[22] Omar, M. A., & Mahmoud, M. M. (2018). Grid connected PV-home systems in Palestine: A review on technical performance, effects and economic feasibility. *Renewable and Sustainable Energy Reviews*, *82*, 2490-2497.

[23] Oloya, I. T., Gutu, T. J., & Adaramola, M. S. (2021). Techno-economic assessment of 10 MW centralised grid-tied solar photovoltaic system in Uganda. Case Studies in Thermal Engineering, 25, 100928.

[24] Akpahou, R., Odoi-Yorke, F., & Osei, L. K. (2023). Techno-economic analysis of a utility-scale grid-tied solar photovoltaic system in Benin republic. *Cleaner Engineering and Technology*, *13*, 100633.

[25] Ahmed, N., Khan, A. N., Ahmed, N., Aslam, A., Imran, K., Sajid, M. B., & Waqas, A. (2021). Techno-economic potential assessment of mega scale grid-connected PV power plant in five climate zones of Pakistan. Energy Conversion and Management, 237, 114097.

[26] Pillai, G., & Naser, H. A. Y. (2018). Techno-economic potential of largescale photovoltaics in Bahrain. Sustainable Energy Technologies and Assessments, 27, 40-45.

[27] Manoj Kumar, N., Sudhakar, K., & Samykano, M. (2019). Techno-economic analysis of 1 MWp grid connected solar PV plant in Malaysia. International Journal of Ambient Energy, 40(4), 434-443.

[28] Li, C., Zhou, D., & Zheng, Y. (2018). Techno-economic comparative study of grid-connected PV power systems in five climate zones, China. Energy, 165, 1352-1369.

[29] Imam, A. A., & Al-Turki, Y. A. (2019). Techno-economic feasibility assessment of grid-connected PV systems for residential buildings in Saudi Arabia—A case study. Sustainability, 12(1), 262.

[30] Duman, A. C., & Güler, Ö. (2020). Economic analysis of grid-connected residential rooftop PV systems in Turkey. *Renewable Energy*, *148*, 697-711.

[31] Li, T., Roskilly, A. P., & Wang, Y. (2018). Life cycle sustainability assessment of grid-connected photovoltaic power generation: A case study of Northeast England. Applied Energy, 227, 465-479.

[32] Mukisa, N., Zamora, R., & Lie, T. T. (2019). Feasibility assessment of grid-tied rooftop solar photovoltaic systems for industrial sector application in Uganda. Sustainable Energy Technologies and Assessments, 32, 83-91.

[33] Mohammadi, K., Naderi, M., & Saghafifar, M. (2018). Economic feasibility of developing grid-connected photovoltaic plants in the southern coast of Iran. Energy, 156, 17-31.

[34] Cui, Y., Zhu, J., Meng, F., Zoras, S., McKechnie, J., & Chu, J. (2020). Energy assessment and economic sensitivity analysis of a grid-connected photovoltaic system. Renewable Energy, 150, 101-115.

[35] Ibrik, I. H. (2020). Techno-economic assessment of on-grid solar PV system in Palestine. Cogent Engineering, 7(1), 1727131.

[36] Mongkoldhumrongkul, K. (2023). Techno-economic analysis of photovoltaic rooftop system on car parking area in Rayong, Thailand. *Energy Reports*, *9*, 202-212.

[37] Khamharnphol, R., Kamdar, I., Waewsak, J., Chiwamongkhonkarn, S., Khunpetch, S., Kongruang, C., & Gagnon, Y. (2023). Techno-Economic Assessment of a 100 kWp Solar Rooftop PV System for Five Hospitals in Central Southern Thailand. *International Journal of Renewable Energy Development*, *12*(1).

[38] Eiva, U. R. J., Fahim, T. M., Islam, S. S., & Ullah, M. A. (2023). Design, performance, and techno-economic analysis of a rooftop grid-tied PV system for a remotely located building. *IET Renewable Power Generation*.

[39] Zhu, X., Lv, Y., Bi, J., Jiang, M., Su, Y., & Du, T. (2023). Techno-Economic Analysis of Rooftop Photovoltaic System under Different Scenarios in China University Campuses. *Energies*, *16*(7), 3123.

[40] Mellit, A., & Kalogirou, S. A. (2008). Artificial intelligence techniques for photovoltaic applications: A review. *Progress in energy and combustion science*, *34*(5), 574-632.

[41] Mandal, P., Madhira, S. T. S., Meng, J., & Pineda, R. L. (2012). Forecasting power output of solar photovoltaic system using wavelet transform and artificial intelligence techniques. *Procedia Computer Science*, *12*, 332-337.

[42] Kermadi, M., & Berkouk, E. M. (2017). Artificial intelligence-based maximum power point tracking controllers for Photovoltaic systems: Comparative study. *Renewable and Sustainable Energy Reviews*, *69*, 369-386.

[43] Chen, C., Hu, Y., Karuppiah, M., & Kumar, P. M. (2021). Artificial intelligence on economic evaluation of energy efficiency and renewable energy technologies. *Sustainable Energy Technologies and Assessments*, *47*, 101358.

[44] Shabbir, N., Kütt, L., Raja, H. A., Jawad, M., Allik, A., & Husev, O. (2022). Techno-economic analysis and energy forecasting study of domestic and commercial photovoltaic system installations in Estonia. *Energy*, *253*, 124156.

[45] Shami, T. M., El-Saleh, A. A., Alswaitti, M., Al-Tashi, Q., Summakieh, M. A., & Mirjalili, S. (2022). Particle swarm optimization: A comprehensive survey. *IEEE Access*, *10*, 10031-10061.

[46] Mirjalili, S., Song Dong, J., Lewis, A., & Sadiq, A. S. (2020). Particle swarm optimization: theory, literature review, and application in airfoil design. *Nature-inspired optimizers: theories, literature reviews and applications*, 167-184.

[47] J. Kennedy , R. Eberhart , Particle swarm optimization, in: Proceedings of the IEEE International Conference on Neural Networks, 4, IEEE, 1995, pp. 1942–1948 .

[48] R. Eberhart , J. Kennedy , A new optimizer using particle swarm theory, in: MHS’95. Proceedings of the Sixth International Symposium on Micro Machine and Human Science, Ieee, 1995, pp. 39–43 .

[49] Elsheikh, A. H., & Abd Elaziz, M. (2019). Review on applications of particle swarm optimization in solar energy systems. *International Journal of Environmental Science and Technology*, *16*, 1159-1170.

[50] Ibrahim, A. W., Shafik, M. B., Ding, M., Sarhan, M. A., Fang, Z., Alareqi, A. G., ... & Al-Rassas, A. M. (2020). PV maximum power-point tracking using modified particle swarm optimization under partial shading conditions. *Chinese Journal of Electrical Engineering*, *6*(4), 106-121.

[51] Abu-Hamdeh, N. H., & Alnefaie, K. A. (2019). Optimal selection and techno-economic analysis of a hybrid power generation system. *Journal of Renewable and Sustainable Energy*, *11*(5), 055902.

[52] Parvin, M., Yousefi, H., & Noorollahi, Y. (2023). Techno-economic optimization of a renewable micro grid using multi-objective particle swarm optimization algorithm. *Energy Conversion and Management*, *277*, 116639.

[53] Ferahtia, S., Rezk, H., Abdelkareem, M. A., & Olabi, A. G. (2022). Optimal techno-economic energy management strategy for building's microgrids based bald eagle search optimization algorithm. *Applied Energy*, *306*, 118069.

[54] K. Kurundkar, G. Karve and G. A. Vaidya, "Techno-Economic Analysis and Optimal Sizing of Stand-alone Hybrid AC-DC Microgrid by Nature inspired Firefly algorithm and Particle Swarm Optimization," *2021 International Conference on Intelligent Technologies (CONIT)*, Hubli, India, 2021, pp. 1-6, doi: 10.1109/CONIT51480.2021.9498511.

[55] Alshareef M, Lin Z, Ma M, Cao W. Accelerated Particle Swarm Optimization for Photovoltaic Maximum Power Point Tracking under Partial Shading Conditions. *Energies*. 2019; 12(4):623. https://doi.org/10.3390/en12040623

[56] P. Reche López, S. García Galán, N. Ruiz Reyes & F. Jurado (2008) A Method for Particle Swarm Optimization and its Application in Location of Biomass Power Plants, International Journal of Green Energy, 5:3, 199-211, DOI: 10.1080/15435070802107165

[57] M. H. Moradi & M. Abedini (2012) A Combination of Genetic Algorithm and Particle Swarm Optimization for Optimal Distributed Generation Location and Sizing in Distribution

Systems with Fuzzy Optimal Theory, International Journal of Green Energy, 9:7, 641-660, DOI: 10.1080/15435075.2011.625590

[58] Yeghikian M, Ahmadi A, Dashti R, Esmaeilion F, Mahmoudan A, Hoseinzadeh S, Garcia DA. Wind Farm Layout Optimization with Different Hub Heights in Manjil Wind Farm Using Particle Swarm Optimization. *Applied Sciences*. 2021; 11(20):9746. https://doi.org/10.3390/app11209746

[59] Gómez, M., López, A., & Jurado, F. (2010). Optimal placement and sizing from standpoint of the investor of photovoltaics grid-connected systems using binary particle swarm optimization. *Applied Energy*, *87*(6), 1911-1918.

[60] Gómez, M., Jurado, F., Díaz, P., & Ruiz-Reyes, N. (2010). Evaluation of a particle swarm optimization based method for optimal location of photovoltaic grid-connected systems. *Electric Power Components and Systems*, *38*(10), 1123-1138.

[61] Bhumkittipich, K., & Phuangpornpitak, W. (2013). Optimal placement and sizing of distributed generation for power loss reduction using particle swarm optimization. *Energy procedia*, *34*, 307-317.

[62] Duong, M. Q., Pham, T. D., Nguyen, T. T., Doan, A. T., & Tran, H. V. (2019). Determination of optimal location and sizing of solar photovoltaic distribution generation units in radial distribution systems. *Energies*, *12*(1), 174.

[63] Kamel, R. M., & Kermanshahi, B. (2009). Optimal size and location of distributed generations for minimizing power losses in a primary distribution network.

[64] Sambaiah, K. S., & Jayabarathi, T. (2021). Optimal reconfiguration and renewable distributed generation allocation in electric distribution systems. *International Journal of Ambient Energy*, *42*(9), 1018-1031.

[65] Rathore, A., & Patidar, N. P. (2021). Optimal sizing and allocation of renewable based distribution generation with gravity energy storage considering stochastic nature using particle swarm optimization in radial distribution network. *Journal of Energy Storage*, *35*, 102282.

[66] Ha, M. P., Nazari-Heris, M., Mohammadi-Ivatloo, B., & Seyedi, H. (2020). A hybrid genetic particle swarm optimization for distributed generation allocation in power distribution networks. *Energy*, *209*, 118218.

[67] Ullah, Z., Wang, S., & Radosavljević, J. (2019). A novel method based on PPSO for optimal placement and sizing of distributed generation. *IEEJ Transactions on Electrical and Electronic Engineering*, *14*(12), 1754-1763.

[68] Haider, W., Hassan, S. J. U., Mehdi, A., Hussain, A., Adjayeng, G. O. M., & Kim, C. H. (2021). Voltage profile enhancement and loss minimization using optimal placement and sizing of distributed generation in reconFigured network. *Machines*, *9*(1), 20.

[69] Samala, R. K., & Kotapuri, M. R. (2020). Optimal allocation of distributed generations using hybrid technique with fuzzy logic controller radial distribution system. *SN Applied Sciences*, *2*(2), 191.

[70] Adepoju, G. A., Aderemi, B. A., Salimon, S. A., & Alabi, O. J. (2023). Optimal Placement and Sizing of Distributed Generation for Power Loss Minimization in Distribution Network using Particle Swarm Optimization Technique. European Journal of Engineering and Technology Research, 8(1), 19-25.

[71] Wanjekeche, T., Ndapuka, A. A., & Mukena, L. N. (2023). Strategic Sizing and Placement of Distributed Generation in Radial Distributed Networks Using Multiobjective PSO. Journal of Energy, 2023.

[72] Salam, I. U., Yousif, M., Numan, M., Zeb, K., & Billah, M. (2023). Optimizing Distributed Generation Placement and Sizing in Distribution Systems: A Multi-Objective Analysis of Power Losses, Reliability, and Operational Constraints. Energies, 16(16), 5907.

[73] Alajmi, B. N., AlHajri, M. F., Ahmed, N. A., Abdelsalam, I., & Marei, M. I. (2023). Multi-objective Optimization of Optimal Placement and Sizing of Distributed Generators in Distribution Networks. IEEJ Transactions on Electrical and Electronic Engineering, 18(6), 817-833.

[74] Rekha, R., & Byalihal, S. C. (2023). Optimal allocation of solar and wind distributed generation using particle swarm optimization technique. International Journal of Electrical and Computer Engineering, 13(1), 229.

[75] http://www.ee.unlv.edu/~eebag/Photovoltaic%20Systems%20II.pdf

[76] Adaramola, M. S., & Vågnes, E. E. (2015). Preliminary assessment of a small-scale rooftop PV-grid tied in Norwegian climatic conditions. *Energy Conversion and Management*, *90*, 458-465.

[77] Sharma, V., & Chandel, S. S. (2013). Performance analysis of a 190 kWp grid interactive solar photovoltaic power plant in India. *Energy*, *55*, 476-485.

[78] Ayompe LM, Duffy A, McCormack SJ, Conlon M. Measured performance of a 1.72 kW rooftop grid connected photovoltaic system in Ireland. Energy Conversion and Management 2011;52:816e25.

[79] Marion B, Adelsten J, Boyel K, Hayden H, Hammon B, Fletcher T, Canada B, Narang D, Kimber A, Michell L, Rich G, Towsend T, Detride A, Kimbler A. Performance parameters for grid-connected PV system. In: Proceeding of the 31st IEEE photovoltaic specialist conference, Lake Buena Vista FL 2005. p. 1601e6.

[80] Wittkopf, S., Valliappan, S., Liu, L., Ang, K. S., & Cheng, S. C. J. (2012). Analytical performance monitoring of a 142.5 kWp grid-connected rooftop BIPV system in Singapore. *Renewable Energy*, *47*, 9-20.

[81] Ibrik, I. H. (2020). Techno-economic assessment of on-grid solar PV system in Palestine. *Cogent Engineering*, *7*(1), 1727131.

[82] Blaesser G. PV system measurements and monitoring the European experience. Sol Energy Mater Sol Cells 1997;47(1–4):167–76.

[83] Decker B, Jahn U. Performance of 170 grid connected PV plants in Northern Germany–Analysis of yields and optimization potentials. Solar Energy 1997;59(4–6):127–33.

[84] Sidi, C. E. B. E., Ndiaye, M. L., El Bah, M., Mbodji, A., Ndiaye, A., & Ndiaye, P. A. (2016). Performance analysis of the first large-scale (15 MWp) grid-connected photovoltaic plant in Mauritania. *Energy conversion and management*, *119*, 411-421.

[85] Brigham, E. F., & Ehrhardt, M. C. (2005). In Financial Management (11th, International Student ed., p. 347). South-Western Cengage Learning.

[86] San Ong, T., & Thum, C. H. (2013). Net present value and payback period for building integrated photovoltaic projects in Malaysia. *International Journal of Academic Research in Business and Social Sciences*, *3*(2), 153.

[87] Zaro, F. (2023). An improved MOPSO technique based optimal location and size of DGs in distribution power grids considering true multi-objectives. *Engineering & Applied Science Research*, *50*(4).

[88] Alsamamra, H., Isaila, I. and Shoqeir, J. (2021) Promoting Energy Efficiency in the Palestinian Municipalities: A Case Study of Al-Dahriya Municipality. Smart Grid and Renewable Energy, 12, 17-29. https://doi.org/10.4236/sgre.2021.122002

[89] PV specifications are provided from manufacturers technical data sheet (Sunerg) – Italy.

[90] Inverter specifications are provided from manufacturers And GCL, www.gclsi.com . technical data sheet www.abb.com/solarinverters , www.abb.com .

[91] transformer's and cable's resistance, reactance, and impedance have been provided from manufacturers technical data sheet existed at Al Dhahriya Municipality and SELCO.

Appendix : PV generation output for each month

Year 2021

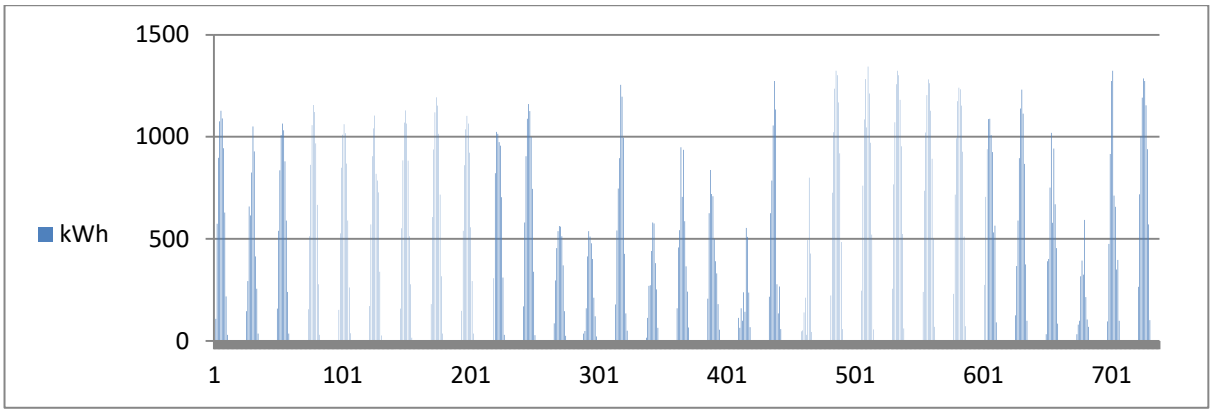

January

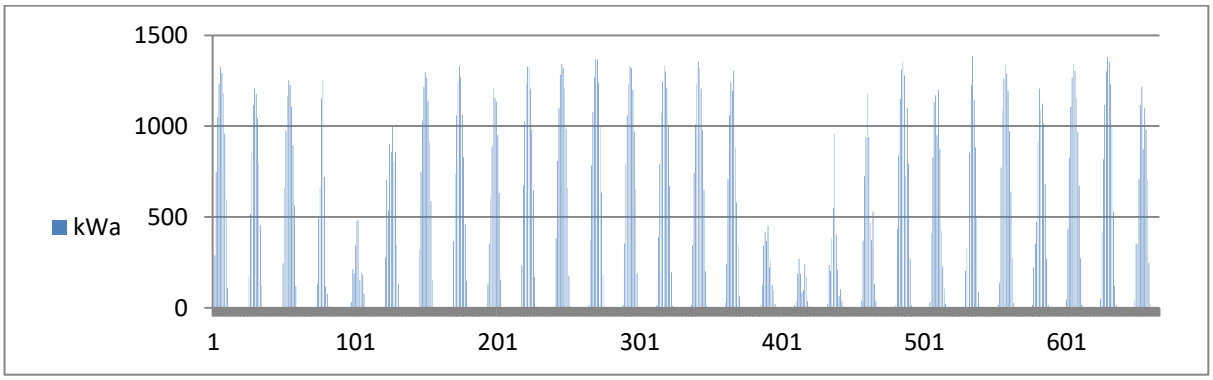

February

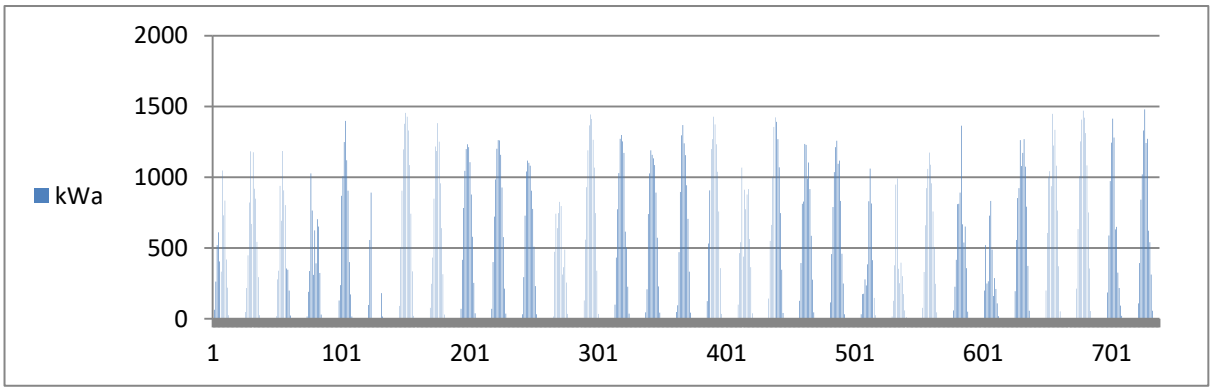

March

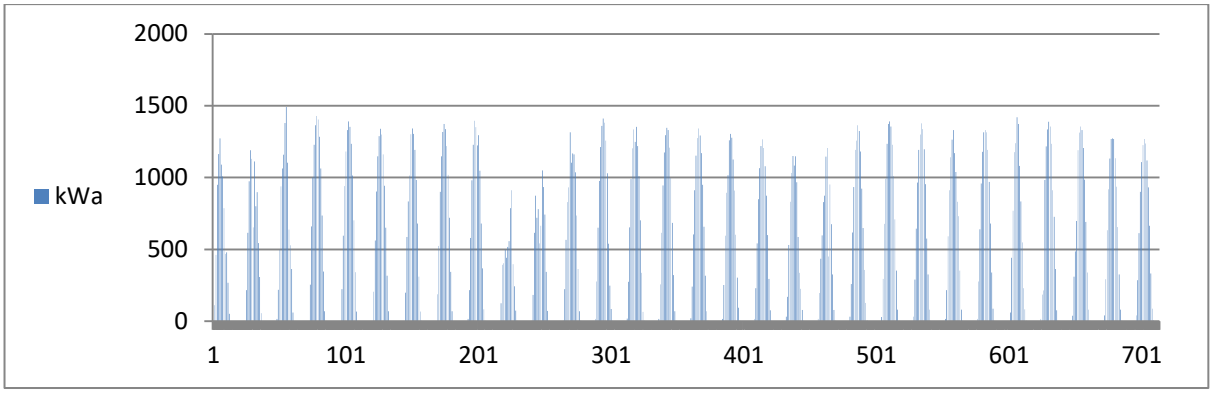

April

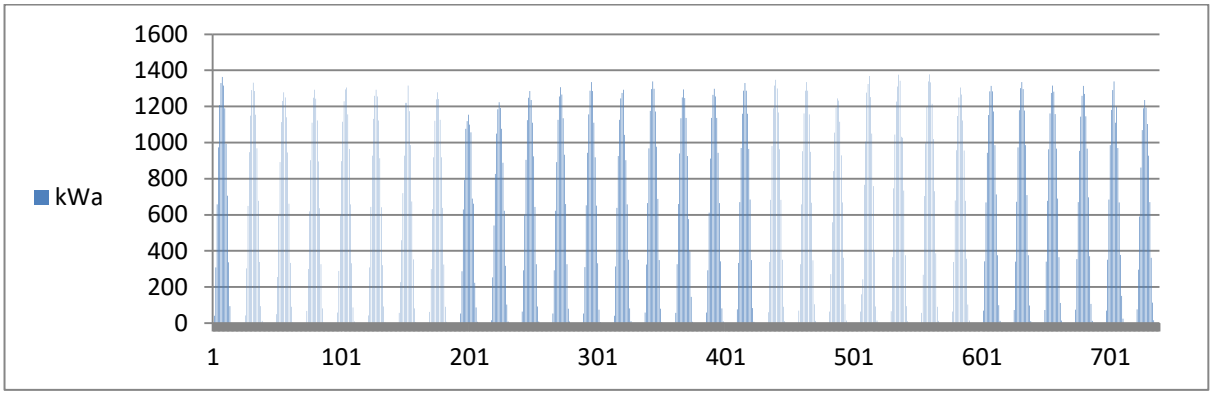

May

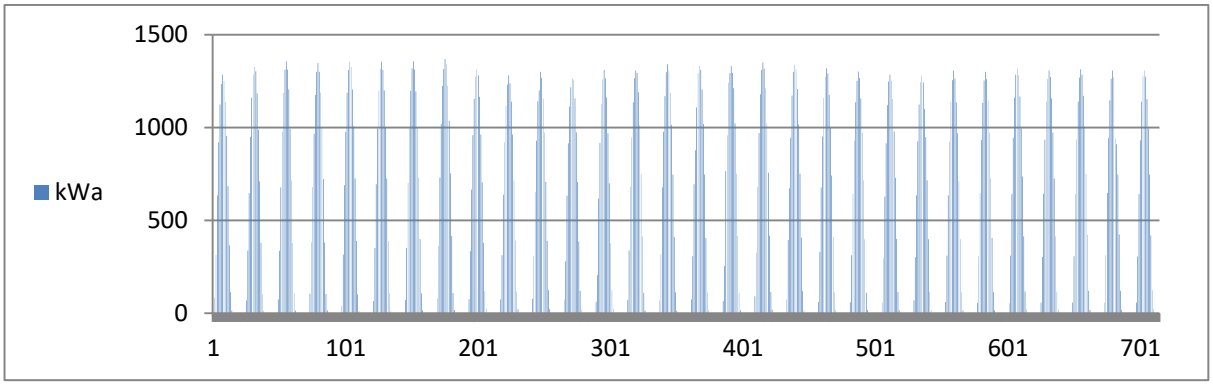

June

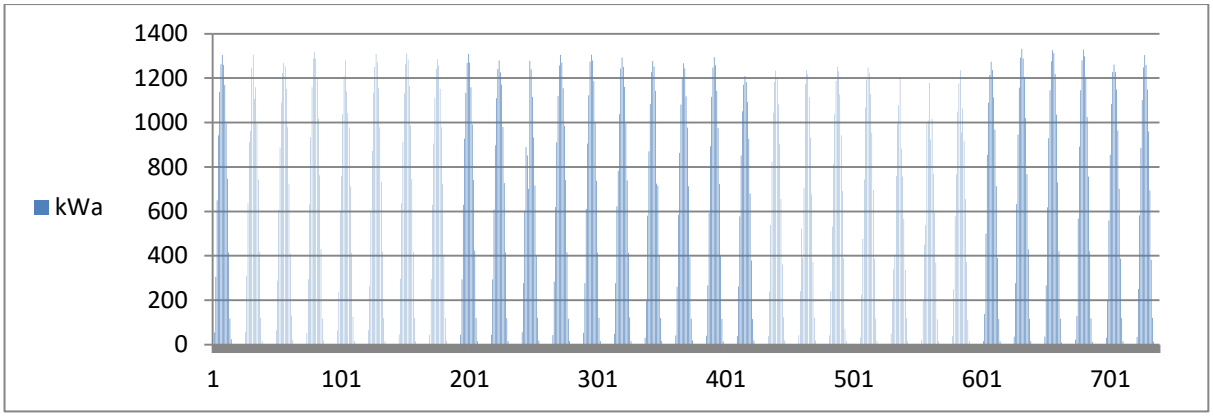

July

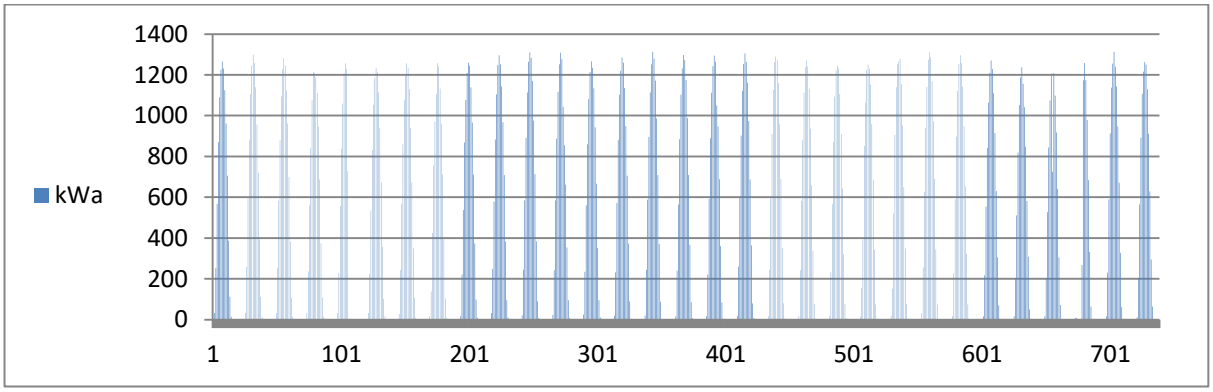

August

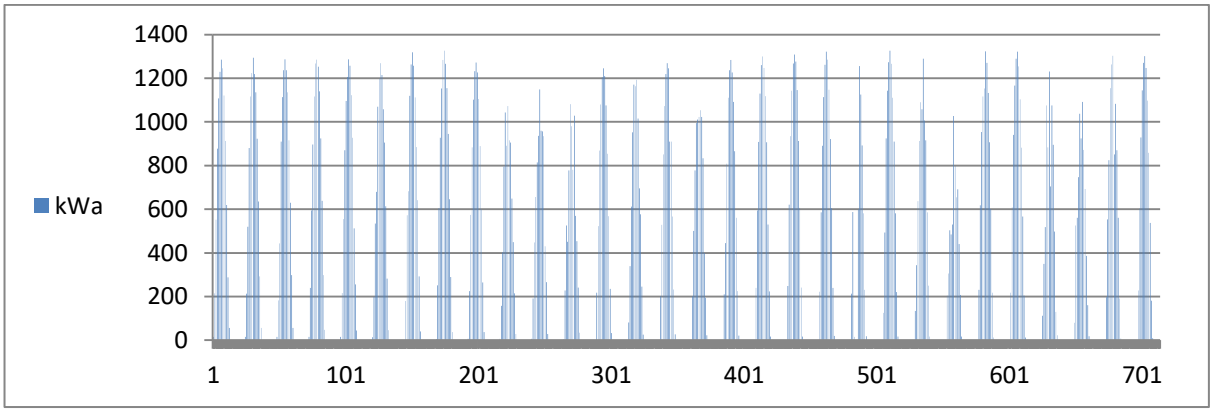

September

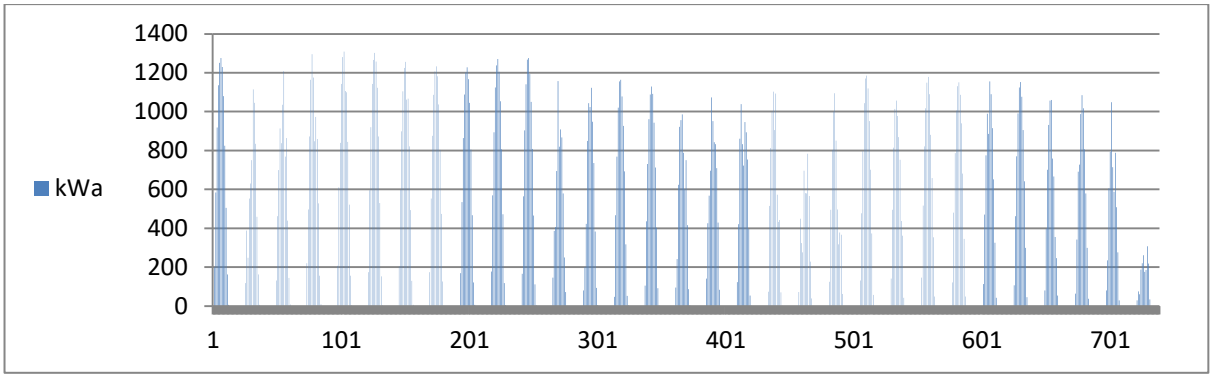

October

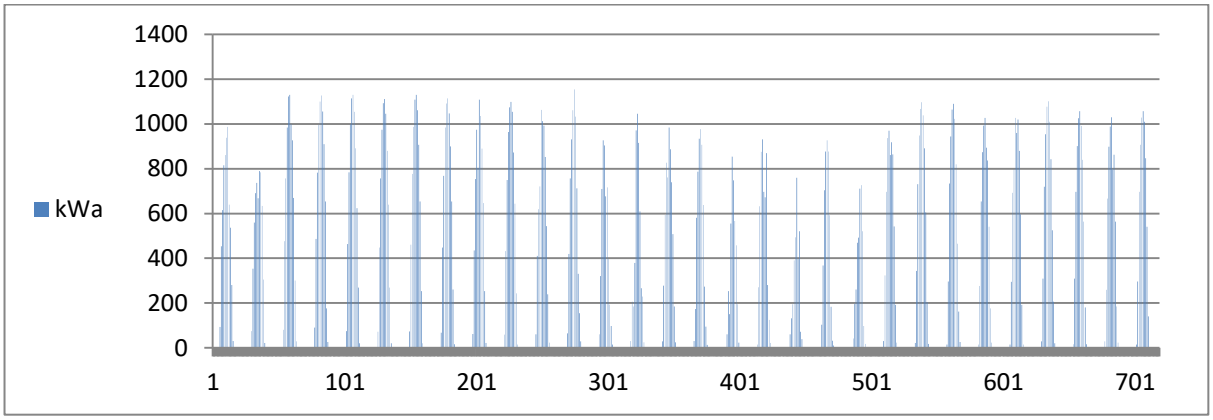

November

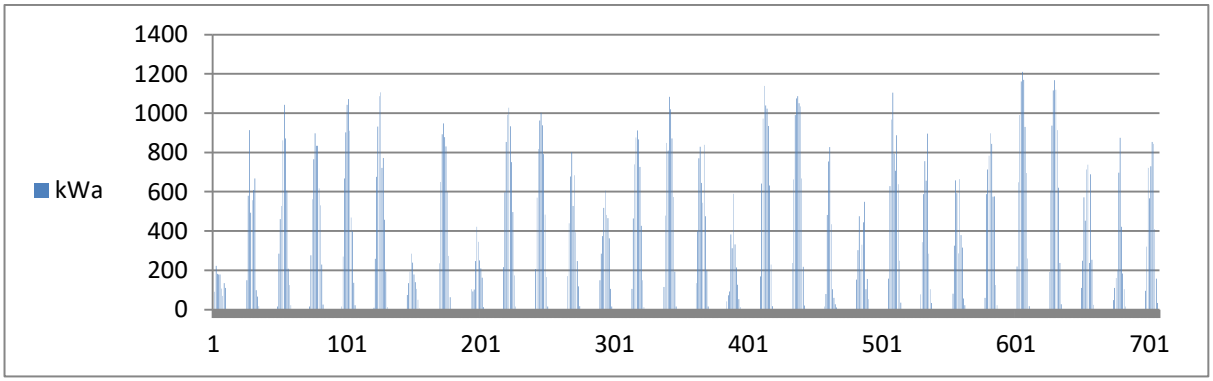

December

Year 2022

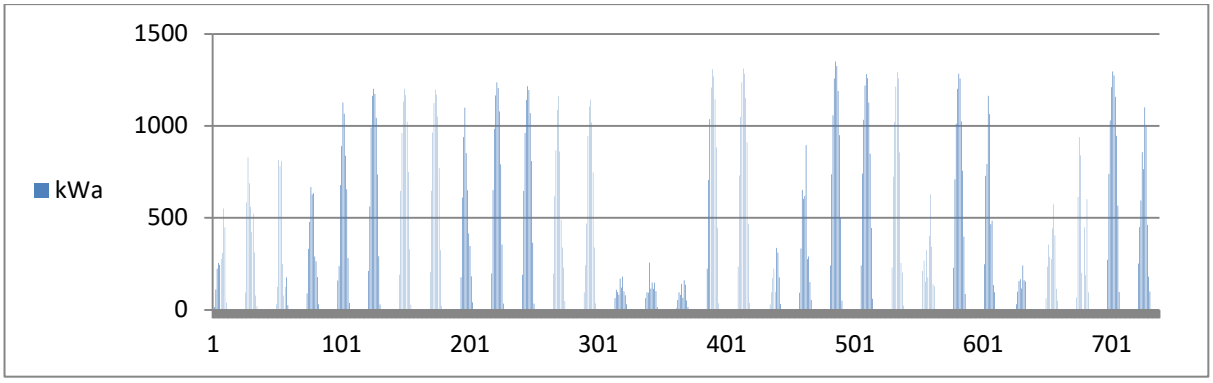

January

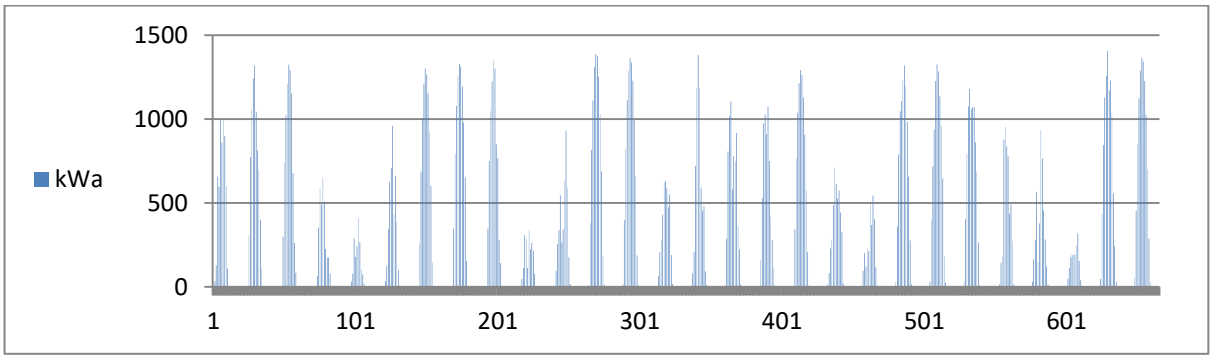

February

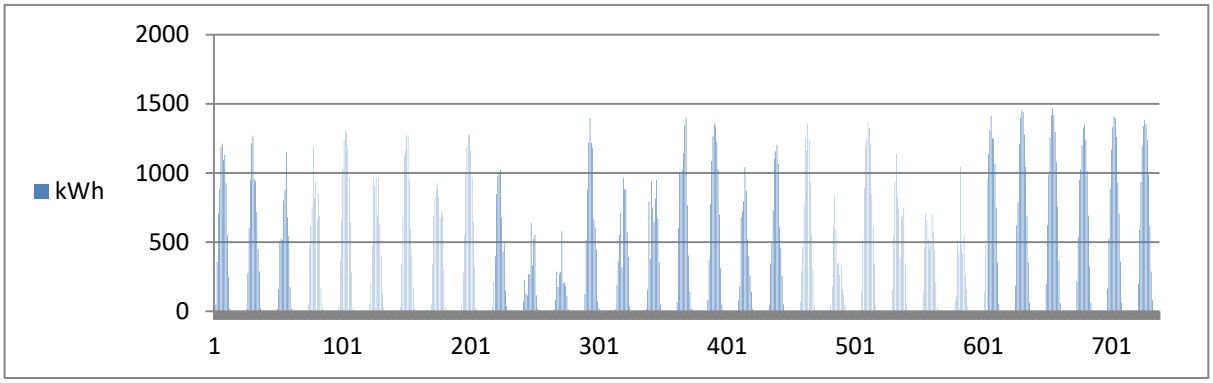

March

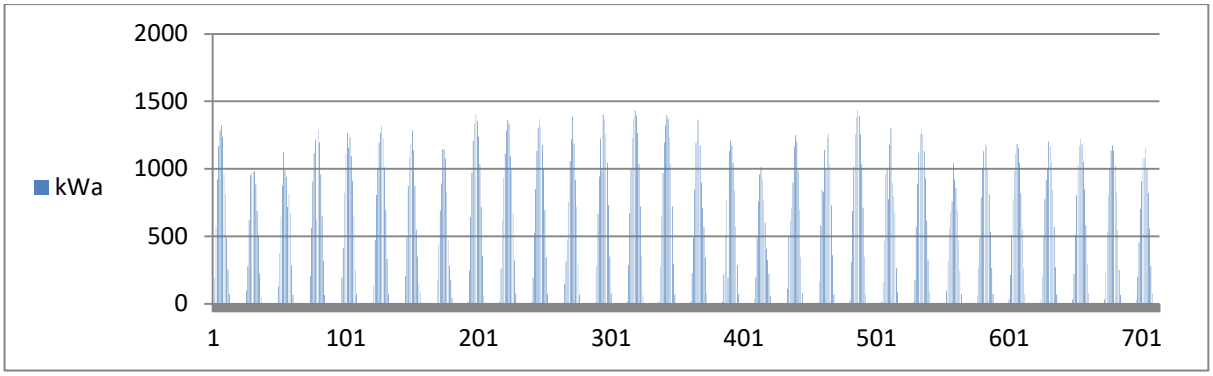

April

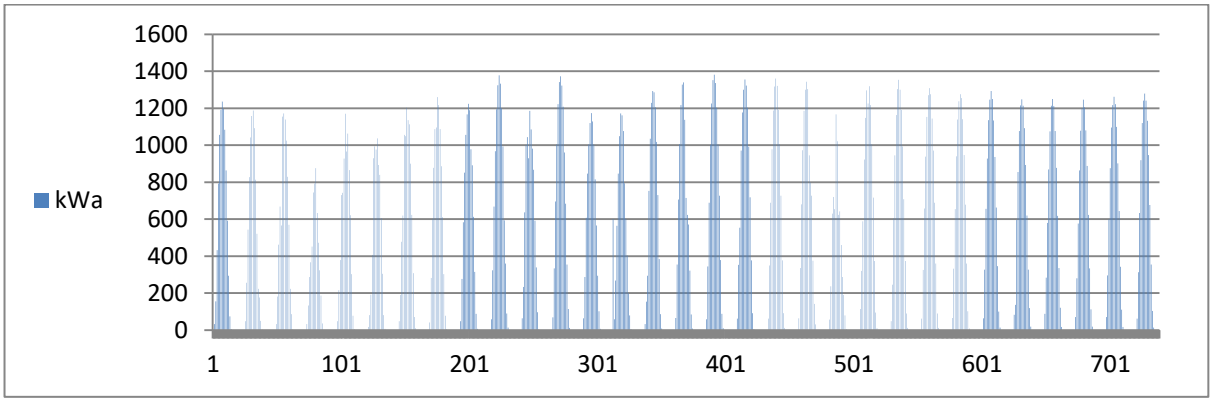

May

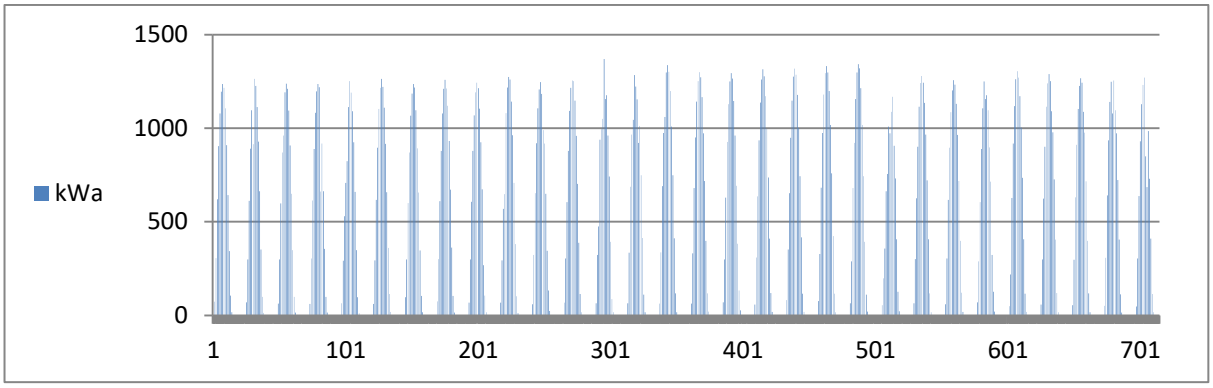

June

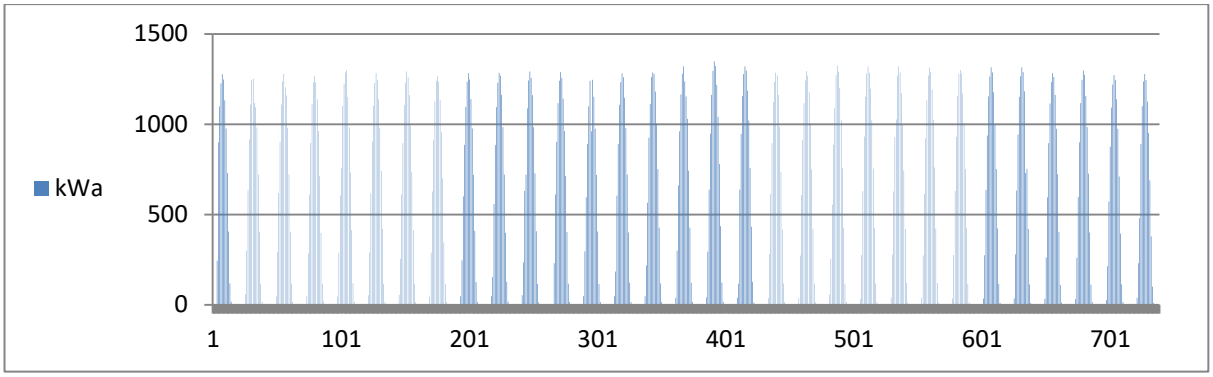

July

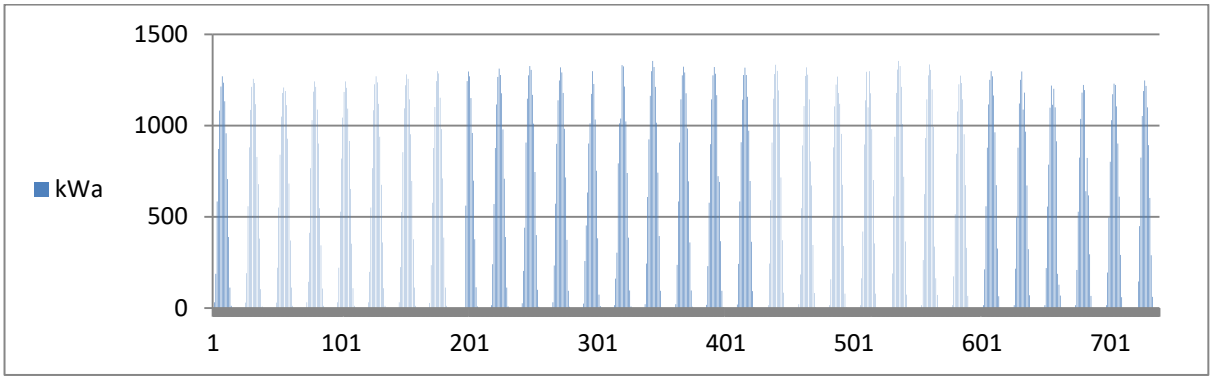

August

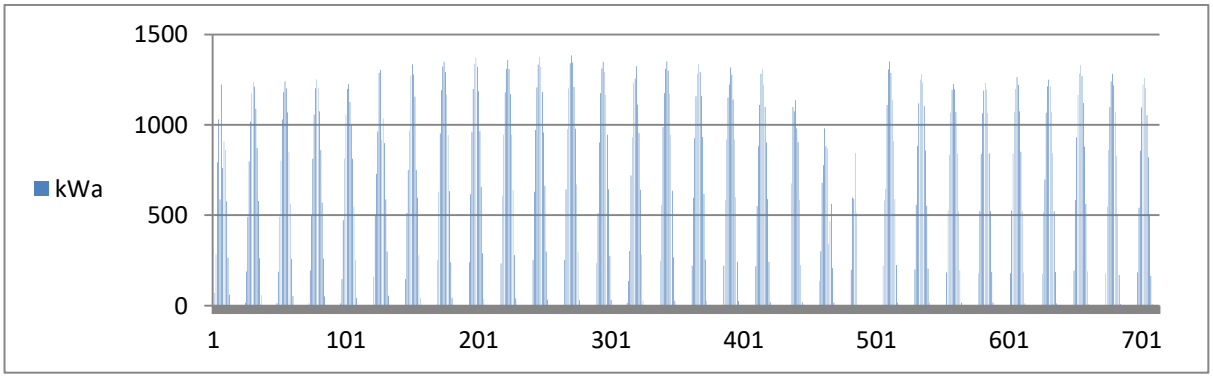

September

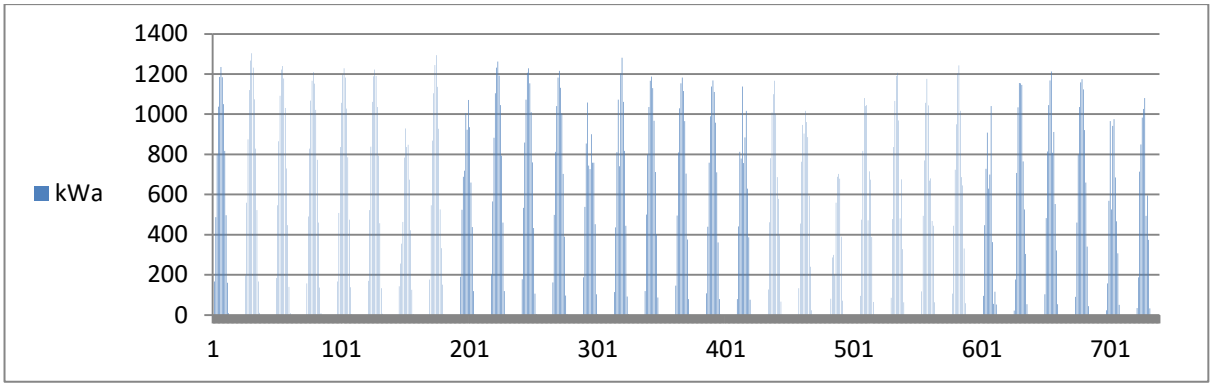

October

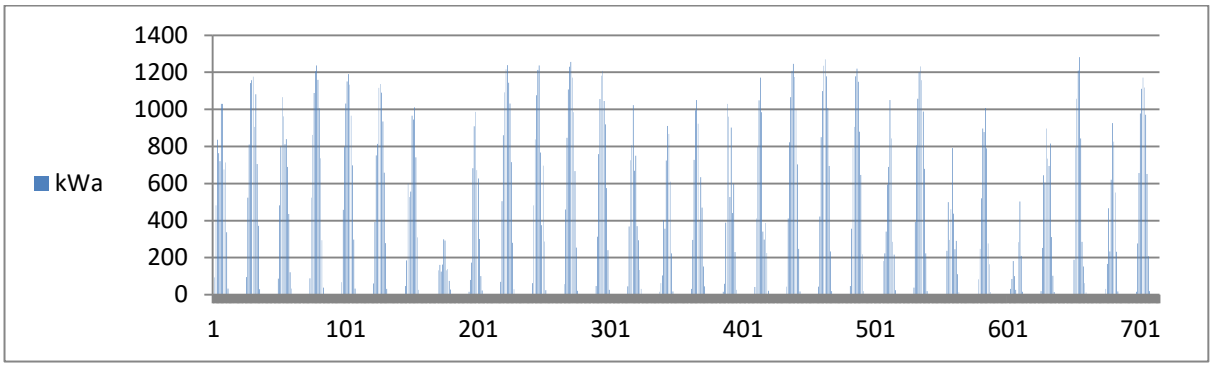

November

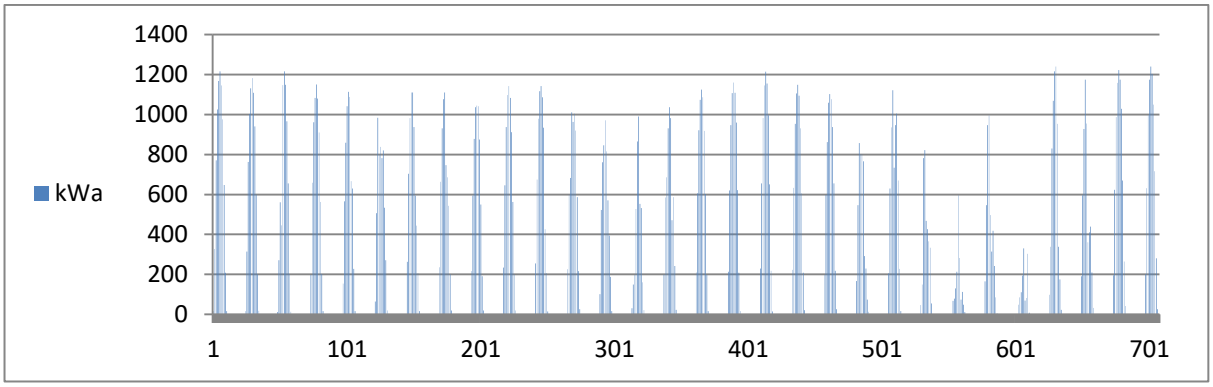

December